2010

Mitotic Exit Control in Budding Yeast: Regulators and Dynamics

Ying Lu

MITOTIC EXIT CONTROL IN BUDDING YEAST: REGULATORS AND DYNAMICS

A Thesis Presented to the Faculty of

The Rockefeller University

in Partial Fulfillment of the Requirements for

the degree of Doctor of Philosophy

by

Ying Lu

June 2010

MITOTIC EXIT CONTROL IN BUDDING YEAST: REGULATORS AND DYNAMICS

Ying Lu, Ph.D.

The Rockefeller University 2010

In budding yeast, the phosphatase Cdc14 is released from nucleolus to promote mitotic exit (ME). Cdc14 release and ME is controlled by mitotic cyclin-Cdk oscillation, the FEAR network including a non-proteolytic function of separase (Esp1), and the Mitotic Exit Network (MEN) indirectly activated by spindle elongation through cohesin cleavage by the proteolytic function of Esp1.

The MEN contributes strongly to ME efficiency. Esp1 contributes to Cdc14 release and ME kinetics mainly through cohesin cleavage: the Esp1 requirement can be largely bypassed if cells are provided Esp1-independent means of separating sister chromatids. In the absence of Esp1 activity we observed only a minor ME delay consistent with a FEAR defect. Esp1 overexpression drives ME in Cdc20-depleted cells arrested in metaphase. We have found that this activity of overexpressed Esp1 depended on spindle integrity and the MEN. Quantitative measure of Cdc14 localization indicates efficient Cdc14 release upon MEN activation; release driven by Esp1 in the absence of microtubules was inefficient and incapable of driving ME.

Reducing mitotic cyclin-Cdk activity is critical for ME, but Cdc14 release and resequestration is not blocked by endogenous undegradable mitotic cyclin Clb2. Using quantitative time-lapse microscopy, we demonstrate an intrinsic oscillatory module controlling Cdc14 localization. This autonomous Cdc14 release oscillator functions at constant cyclin-Cdk levels by titrated introduction of undegradable Clb2, and at cell-cycle-average Clb2 levels given a block of cell cycle progression by actin depolymerization. Using genetic manipulations, we demonstrate that this oscillator can operate in free-running cell cycles even without undegradable Clb2. The Cdc14-Cdh1-Cdc5 negative feedback is the primary mechanism driving this release oscillator. Its mechanism and regulation of its frequency by Clb2-Cdk, suggest the hypothesis that intrinsically autonomous Cdc14 release cycles are locked at once per cell cycle through entrainment by the cyclin-Cdk oscillator. This concept incorporates autonomous cell cycle oscillators previously reported into a coherent cell cycle control by cyclin-Cdk oscillation, therefore, may have broad implications for the structure and evolution of eukaryotic cell cycle.

To All The Scientists

Trying to Understand The Cell Cycle

Acknowledgements

I would like to express my deepest gratitude to Dr. Fred Cross, my mentor, who gave me incessant support, both spiritual and technical, during my stay in his lab, and also allowed me with enough freedom to pursue my interest and to follow my intuition. I also learnt a lot from him about giving presentations and writing scientific papers.

I thank Dr. Eric Siggia, the hard-core physicists in my thesis committee, for having regular discussions with me on even something he is not very interested in, just to help me out of experimental details and focus on the big question.

My other committee members, Dr. Hiro Funabiki, Dr. Mike Rout, Dr. Tarun Kapoor, I thank them for their support to my thesis project, discussion and suggestions on manuscripts.

Dr. Ben Drapkin, who is a former member in Fred's lab, used to have regular conversations with me, and navigate me through the complexity of published information. Almost every discussion with him ended up in my learning something or some interesting experiments.

Dr. Wenying Shou, who is a former member in Stan Leibler's lab, for the first

time let me know that doing biological experiments is not impossible for me.

Dr. Stan Leibler taught me to develop my own personality and characters as a scientist, as well as intellectual independence.

I thank all present and former members in Fred's lab for giving me help and supports.

My mother, my wife Fangliang Shen, and other family members and friends gave me invaluable supports and encouragements during these years.

Table of Contents

List of Figures

List of Tables

List of Abbreviations

ME: Mitotic Exit

PL: Phase-locking

Cdk: Cyclin-dependent-kinase

FEAR: The Cdc14 Early Anaphase Release Network

MEN: The Mitotic Exit Network

SPOC: The spindle positioning checkpoint

SAC: The spindle assembly checkpoint

NOC: Nocodazole

BEN: Benomyl

LAT-B: Latrunculin-B

GEF: Guanine exchange factor

GFP: Green fluorescent protein

YFP: Yellow fluorescent protein

CFP: Cyan fluorescent protein

Chapter 1: Introduction

Mitotic exit (ME) is a transitional stage connecting mitosis to the start of the next cell cycle. In budding yeast *Saccharomyces cerevisiae,* ME refers to a collection of events happening within ~15 minutes from anaphase until rebudding, including spindle disintegration, cytokinesis, mitotic cyclin inactivation, and DNA replication origin licensing. It is important that those events should only happen during ME, and in the right sequence for a normal cell cycle progression. Molecular mechanisms regulating ME involve phosphorylation/dephosphorylation, protein proteolysis, protein localization change, protein complex formation, and gene transcription. A key issue is to understand what commits the cell to exit from mitosis, and how various ME events are controlled efficiently and accurately.

Cyclins and cyclin dependent kinase (Cdk) are at the center of the eukaryotic cell cycle control system (Morgan, 2007). Mitotic cyclin-Cdk activity rises and falls once per cell cycle in all eukaryotes. In budding yeast *S. cerevisiae,* mitotic cyclins (Clb1,2,3,4) are required for mitotic entry (spindle assemble and anaphase), however overexpression of mitotic cyclins prevents ME, resulting in telophase arrest (Surana et al., 1993). If mitotic entry requires high mitotic cyclin-Cdk activity, and ME requires low Cdk activity (King et al., 1994; Murray and Kirschner, 1989), then the oscillation of mitotic cyclin-Cdk activity would render ME dependent on previous

mitotic entry, resulting a ‘ratchet’-like control of mitosis. Ratchet-like control of this nature is most prominently documented in the case of DNA replication, where high cyclin-Cdk simultaneously blocks DNA replication origin reloading, and promotes firing of previously loaded origins; this control yields once-per-cell-cycle replication (Kearsey and Cotterill, 2003). These ideas have been generalized to spindle morphogenesis, function and disassembly, and to mitotic control overall, although the evidence for these other systems is less complete.

In *S. cerevisiae,* the oscillation of mitotic cyclin-Cdk activity is primarily a product of periodic transcription and proteolysis. The anaphase promoting complex (APC), bound to its activator Cdc20 and Cdh1, mediates Clb proteolysis (Visintin et al., 1997; Yeong et al., 2000). Full activation of APC-Cdc20 complex at the metaphase-to-anaphase transition requires phosphorylation of APC subunits by mitotic cyclin-Cdk (Cross, 2003). Active APC-Cdc20 mediates proteolysis of securin Pds1, resulting in activation of separase Esp1 (Cohen-Fix et al., 1996). Esp1 can cleave cohesin subunit Scc1 to promote anaphase (Uhlmann et al., 2000). In *S. cerevisiae,* APC-Cdc20 partially degrades mitotic cyclins (Clb1,2) (Yeong et al., 2000). Further down-regulation of mitotic cyclin-Cdk activity requires APC-Cdh1 and the stoichiometric inhibitor Sic1 (Mendenhall and Hodge, 1998). Phosphorylation of Cdh1 by Cdk prevents its interaction with APC and nuclear accumulation (Shirayama et al., 1998). Cdh1 is dephosphorylated by the phosphatase Cdc14 during ME, and results in complete degradation of mitotic cyclins

(Jaspersen et al., 1999). Sic1 can inhibit Clb-Cdk activity independent of proteolysis . Both transcription and stability of Sic1 is cell cycle regulated (Verma et al., 1997). Sic1 transcription in mitosis is activated primarily by Swi5, which is activated by Cdc14 through dephosphorylation (Toyn et al., 1997; Visintin et al., 1998). Cdc14 also dephosphorylates Sic1 to prevent its proteolysis (Visintin et al., 1998).

Cdc14 is a major phosphatase and a key regulator during ME, and is highly conserved among eukaryotic species. In budding yeast, Cdc14 is essential for cell viability. The activity of Cdc14 is mainly regulated through changing its localization. Cdc14 is sequestered in the nucleolus by the RENT complex (including Net1) during G1, S and G2; this probably sequesters it from most targets, and additionally, Net1 may inhibit Cdc14 enzymatic activity; therefore, Cdc14 is likely inactive through this time (Shou et al., 1999; Visintin et al., 1999). Cdc14 is released from Net1 and the nucleolus into the cytoplasm only during ME (Net1 is constitutively nucleolar). Three major pathways release Cdc14 from nucleolus, including the FEAR network (cdc Fourteen Early Anaphase Release) which is activated by a non-proteolytic function of separase Esp1 at early mitosis to promote a transient release of Cdc14; the MEN (Mitotic Exit Network) which is activated through the Tem1-Cdc15-Dbf2 signal transduction cascade to promote Cdc14 release in later mitosis; in addition, the polo kinase Cdc5 is essential for Cdc14 release, and is required for full activation of FEAR and MEN pathways (Bardin et al., 2000; Stegmeier and Amon, 2004; Stegmeier et al.,

2002; Visintin et al., 2003). Cdc5 can also promote Cdc14 release by phosphorylating Cdc14 and the RENT complex to promote their disassociation (Visintin et al., 2003).

The FEAR network is activated by the non-proteolytic function of Esp1 in early mitosis (Sullivan and Uhlmann, 2003). Esp1 can interact with Cdc55 (PP2A co-factor) to cause Net1 phosphorylation by mitotic cyclin-Cdk to promote a transient release of Cdc14 (Queralt et al., 2006). Besides Esp1, Slk19 and Spo12 are also essential components for the FEAR network (Stegmeier et al., 2002).

The MEN network (also called spindle orientation checkpoint, SPOC) is activated in response to anaphase which pushes the daughter-orientated spindle pole body (SPB) into the bud (Bardin et al., 2000). Then the MEN component Tem1 which localizes at SPB gets close to the bud cortex where Tem1's guanine exchange factor Lte1 sits. This movement of SPB could lead to the activation of Tem1, and leads to a serial activation of Cdc15 and Dbf2/Mob1 complex. Dbf2 can phosphorylate Net1 to promote its disassociation with Cdc14. *BUB2* is essential for SPOC regulation of the MEN; in *bub2Δ* cells, the MEN network is likely near-constitutively active (Fesquet et al., 1999; Pereira et al., 2000).

Cdc14 released by the MEN network induces mitotic cyclin-Cdk inactivation, and directly promotes cytokinesis (Stegmeier and Amon, 2004). Cdc14 released by the

FEAR network can facilitate rDNA segregation, spindle elongation, and nuclear positioning (D'Amours et al., 2004; Higuchi and Uhlmann, 2005; Ross and Cohen-Fix, 2004; Sullivan et al., 2004; Wang et al., 2004). It has also been proposed that the MEN component Cdc15 need to be dephosphorylated by FEAR-released Cdc14 for full activation of the MEN network (Jaspersen and Morgan, 2000; Stegmeier et al., 2002). Cdc14 initially released by the FEAR network may promote MEN activity to induce additional Cdc14 release, and therefore, forms a positive feedback loop to cause rapid release of Cdc14 from nucleolus (Sullivan and Uhlmann, 2003). The non-proteolytic function of Esp1 has been suggested to be essential for ME (Sullivan and Uhlmann, 2003), although the FEAR network components Slk19 and Spo12 are dispensable for the cell cycle. In *slk19Δ* and *spo12Δ* cells, ME is delayed by 10~15 minutes (Stegmeier et al., 2002). Preventing Net1 phosphorylation by mitotic cyclin-Cdk, proposed to be a key FEAR pathway event, also only delays ME by 10-15 min (Azzam et al., 2004).

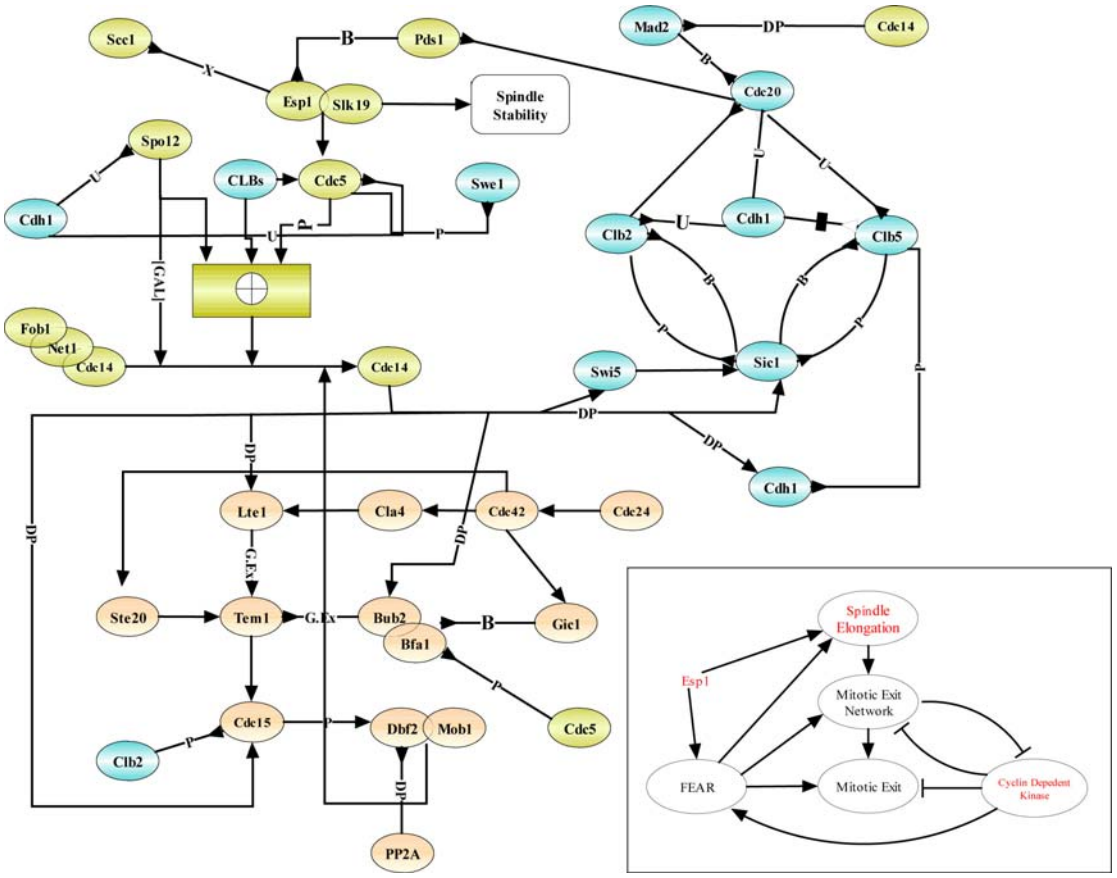

Figure 1.1. **Major proteins and their interactions in mitotic exit control system.** Arrow heads stand for activating interactions; blunt heads stand for inhibitory interactions. Abbreviations: P, phosphorylation; DP, dephosphorylation; U, ubiquitination; X, protein cleavage; [GAL], requiring overexpression from *GAL1* promoter; B, binding; G.Ex, guanine exchange reaction. Green symbols: proteins in the FEAR network; Red symbols: proteins in the MEN network; Blue symbols: proteins involved in regulating cyclin-Cdk activity. Those classifications are not exclusive. The '+' symbol in green stands for logic AND. The inset panel shows modules in mitotic exit and their general interactions.

The networks controlling Cdc14 release and ME are highly interdigitated (Fig. 1.1). Therefore, although many possible interactions have been reported, it is difficult to envisage the dynamical behavior of the system, and a comprehensible model is often complicated by less important interactions due to the lack of its dynamical information. For example, the FEAR and the MEN networks can be activated in many different ways; it is still unclear how those pathways are activated in a normal cell cycle, because the experimental conditions to establish those interactions are generally different. Especially, it is unclear about the role of cyclin-Cdk activity in controlling those pathways. Most proteins involved in the system are potentially Cdk substrates with both positive and negative interactions. It is also unclear whether Cdc14 release alone is sufficient to induce ME, since separase Esp1 and several MEN components have been reported to be directly involved in controlling ME events (Jensen et al., 2001; Jimenez et al., 2005; Tinker-Kulberg and Morgan, 1999).

This thesis is divided into two parts. The first part addresses the question of which signal ultimately leads to ME, and the relative importance of various pathways in this process. The second part tries addresses the question of how Cdc14 release and resequestration is controlled by mitotic cyclin-Cdk activities.

Chapter 2: Materials and Methods

Strains and plasmids

All strains are in the W303 background. Their genotypes are shown in Table 2.1. Strain constructions were carried out by standard tetrad analysis and transformation methods. We used strains containing a *CDC14* allele endogenously tagged with YFP, in order to follow Cdc14 trafficking. This *CDC14-YFP* was previously shown to fully complement, and to be competent for FEAR- and MEN-induced nucleolar exit (Pereira *et al.*, 2002). *GAL1-CLB2kd-GFP* was constructed by C-terminally tagging *GAL1-CLB2kd* construct with GFP, and integrated at URA3 locus. *NET1-mCherry* was constructed by C-terminally tagging the endogenous *NET1* with mCherry. *CDC5pr-GFP-PEST* was first constructed on a plasmid, and inserted at the endogenous *CDC5* locus.

The pYL8 plasmid (*pRS303-GALS-esp1*$_{frag.}$. esp1$_{\text{frag}}$, created by truncating a 2.6kb region from the *ESP1* ORF using SphI) was linearized with BlpI and integrated into the genome to make *esp1::GALS-ESP1*. *ESP1::GALS-ESP1* was made alike, but using plasmid pYL10 which had a full length *ESP1* ORF under the *GALS* promoter. Correct number of integration was confirmed by real time PCR. The construction of *PDS1-mdb esp1::GALS-EPS* (or *ESP1::GALS-ESP1*) strains was the following: A *pds1::LEU2* strain was first transformed with pYL7 (*pRS406-PDS1-mdb*, linearized

with MluI), then the *URA3* marker in the resulting strain was counter-selected on G+FOA plates to obtain Leu- Ura- clones. The structure of the pop-out strain was confirmed by PCR and Southern blot.

Table 2.1. **Strains and Genotypes.** All strains are W303 background. Strains construction is using standard methods.

Strain name	Genotype
2151-7B	*bar1 w303*
YL0931	*cdc20::MET-CDC20-TRP1 ura3::GAL-SIC1-4A-URA3*
YL1721	*cdc20::MET-CDC20-TRP1 ura3::GAL-SIC1-4A-URA3*
2147-3D	*cdc20::LEU2 ade2::GALL-CDC20-ADE2 pds1::URA3*
YL094	*cdc20::MET-CDC20-TRP1 esp1-2td-URA3 GAL-UBR1-HIS3 ura3::GAL-SIC1-4A-URA3 leu2::ESP1C1531A-LEU2*
YL122	*cdc20::MET-CDC20-TRP1 GFP-TUB1-HIS3 MYO1-GFP-KAN ESP1::GALS-ESP1C1531A-URA3*
YL353	*cdc20::MET-CDC20-TRP1 scc1::HIS3 SCC1-TEV-LEU2 GAL-TEV-TRP1 GAL-SIC1-4A-URA3*
353	*cdc20::MET-CDC20-TRP1 scc1::HIS3 SCC1-TEV-LEU2 GAL-TEV-TRP1*
BD96B-4C	*cdc20::MET-CDC20-TRP1 GFP-TUB1-HIS3 MYO1-GFP-KAN*
YL113	*pds1::PDS1-mdb ESP1::GALS-ESP1-TRP1 trp1::LacO-LEU2,TRP1 his3::LacR-GFP-HIS3 MYO1-GFP-KAN*
YL115	*pds1::PDS1-mdb esp1::GALS-ESP1-TRP1 trp1::LacO-LEU2,TRP1 his3::LacR-GFP-HIS3 MYO1-GFP-KAN*
YL018	*pds1::PDS1-mdb ESP1::GALS-ESP1-TRP1*
YL114	*bar1 pds1::PDS1-mdb esp1::GALS-ESP1-TRP1*
YL139	*bar1 pds1::PDS1-mdb-18MYC ESP1::GALS-ESP1-TRP1*
YL049	*bar1 mad2::KAN scc1::HIS3 SCC1-TEV::LEU2 GAL-TEV-TRP1*
YL057	*bar1 mad2::KAN scc1::HIS3 SCC1-TEV::LEU2 GAL-TEV-TRP1 GAL-PDS1-mdb-URA3*
YL044	*bar1 mad2::KAN scc1-73 leu2::GAL-PDS1-mdb-LEU2*
YL0451	*bar1 mad2::KAN leu2::GAL-PDS1-mdb-LEU2*
YL1361	*cdc20::MET-CDC20-TRP1 ESP1::GALS-ESP1-URA3 CDC14-YFP-HIS3 NET1-CFP-KAN MYO1-GFP-KAN*
YL1362	*cdc20::MET-CDC20-TRP1 ESP1::GALS-ESP1-URA3 cdc15-2 CDC14-YFP-HIS3 NET1-CFP-KAN*
YL121	*cdc20::MET-CDC20-TRP1 ESP1::GALS-ESP1-URA3*
YL1451	*cdc20::MET-CDC20-TRP1 trp1::6xGAL-ESP1 CDC14-YFP-HIS3 NET1-CFP-KAN*
YL1452	*cdc20::MET-CDC20-TRP1 CDC14-YFP-HIS3 NET1-CFP-KAN*
ALG611	*bar1 clb2::CLB2,kd trp1::2xGAL-SIC1-TRP1 CDC14-YFP-HIS3 NET1-CFP-KAN MYO1-mCherry-HIS3*
YL165	*cdc20::MET-CDC20-TRP1 cdh1::LEU2 ESP1::GALS-ESP1-URA3 CDC14-YFP-HIS3 NET-CFP-KAN*
YL1701	*net1::HIS3 CDC14-YFP-HIS3 RRN3-LEU2 GALS-ESP1*
YL161	*net1::HIS3 CDC14-YFP-HIS3 RRN3-LEU2 cdc15-2 CLB2-MYC-TRP1*
YL1702	*net1::HIS3 NOP1-DsRed-HIS3 RRN3-LEU2 CDC14-YFP-HIS3*
YL174	*net1::HIS3 CDC14-YFP-HIS3 RRN3-LEU2 ura3::DsRed-NLS-URA3 cdc15-2 CLB2-MYC-TRP1*
YL0932	*cdc20::MET-CDC20-TRP1 trp1::6xGAL-ESP1 ura3::GAL-SIC1-4A*
393	*cdc20::MET-CDC20-TRP1 trp1::6xGAL-ESP1*
YL008	*esp1::GALS-ESP1-TRP1*
YL009	*ESP1::GALS-ESP1-TRP1*
YL0452	*bar1 bub2::HIS3 leu2::GAL-PDS1-mdb-LEU2*
OCF1517.2	*GAL-PDS1-mdb-LEU2*
YL134	*cdc20::MET-CDC20-TRP1 clb5::HIS3 ESP1::GALS-ESP1-URA3*
YL143	*cdc20::MET-CDC20-TRP1 CDC14-TAB6 ESP1::GALS-ESP1-URA3*
YL1461	*cdc20::MET-CDC20-TRP1 trp1::GALS-CDC14-FLAG-TRP1*

Table 2.1 Continued

YL1462	*cdc20::MET-CDC20-TRP1 trp1::GALS-CDC14-FLAG-TRP1 ESP1::GALS-ESP1-URA3*
YL169	*cdc20::MET-CDC20-TRP1 mad2::URA3 ESP1::GALS-ESP1-URA3 MYO1-GFP-KAN*
YL1541	*bar1 net1::HIS3 cdc15-2 RRN3-LEU2*
YL1542	*bar1 net1::HIS3 RRN3-LEU2*
YL1722	*cdc20::MET-CDC20-TRP1 ESP1::GALS-ESP1-URA3 GAL-SIC1-4A-URA3*
YL042	*cdc20::MET-CDC20-TRP1 GAL-PDS1-mdb-18MYC-URA3*
YL043	*cdc20::MET-CDC20-TRP1 GAL-PDS1-18MYC-URA3*
2147-3D	*pds1::URA3 cdc20::LEU2 ade2::GALL-CDC20-ADE2*
YL135	*MET-CDC2-TRP1 GAL-SIC1-4A-URA3 PDS1-18MYC-LEU2*
YL1761	*MET-CDC20-TRP1 ura3::GAL-CLB2kd-URA3 adh1::ADH1pr-GAL4-rMR-URA3 CDC14-YFP-HIS3 NET1-mCherry-HIS3 MYO1-GFP-KanMX*
YL1841	*MET-CDC20-TRP1 ura3::GAL-CLB2kd-GFP-URA3,HIS3 adh1::ADH1pr-GAL4-rMR-URA3 CDC14-YFP-HIS3 NET1-mCherry-HIS3 MYO1-GFP-KanMX*
YL1851	*MET-CDC20-TRP1 ura3::GAL-CLB2kd-URA3 adh1::ADH1pr-GAL4-rMR-URA3 CDC14-YFP-HIS3 NET1-mCherry-HIS3 MYO1-GFP-KanMX CLN2::CLN2pr-GFP-PEST-URA3*
YL1941	*MET-CDC20-TRP1 ura3::GAL-CLB2kd-GFP-URA3,HIS3 adh1::ADH1pr-GAL4-rMR-URA3 CDC14-YFP-HIS3 NET1-mCherry-HIS3 MYO1-GFP-KanMX swi5::KanMX*
YL1971	*ura3::GAL-SIC1-4A-URA3 CDC14-YFP-HIS3 NET1-mCherry-HIS3 MYO1-GFP-KanMX*
YL2061	*MET-CDC20-TRP1 ura3::GAL-CLB2kd-URA3 adh1::ADH1pr-GAL4-rMR-URA3 CDC14-YFP-HIS3 NET1-mCherry-HIS3 MYO1-GFP-KanMX CDC5::CDC5pr-GFP-PEST-TRP1*
YL2091	*MET-CDC20-TRP1 ura3::GAL-CLB2kd-GFP-URA3,HIS3 adh1::ADH1pr-GAL4-rMR-URA3 CDC14-YFP-HIS3 NET1-mCherry-HIS3 MYO1-GFP-KanMX cdh1::LEU2*
YL2201	*MET-CDC20-TRP1 ura3::GAL-CLB2kd-GFP-URA3,HIS3 adh1::ADH1pr-GAL4-rMR-URA3 CDC14-YFP-HIS3 NET1-mCherry-HIS3 MYO1-GFP-KanMX cdc15-2*
YL2211	*MET-CDC20-TRP1 ura3::GAL-CLB2kd-URA3 adh1::ADH1pr-GAL4-rMR-URA3 CDC14-YFP-HIS3 NET1-mCherry-HIS3 MYO1-GFP-KanMX CLB2::CLB2-GFP-HIS3*
YL2221	*MET-CDC20-TRP1 CDC14-YFP-HIS3 NET1-mCherry-HIS3 MYO1-GFP-KanMX bub2::HIS3 cdh1::LEU2*
YL2222	*CDC14-YFP-HIS3 NET1-mCherry-HIS3 MYO1-GFP-KanMX bub2::HIS3*
YL2241	*MET-CDC20-TRP1 ura3::GAL-CLB2kd-URA3 adh1::ADH1pr-GAL4-rMR-URA3 CDC14-YFP-HIS3 NET1-mCherry-HIS3 MYO1-GFP-KanMX CLB2::CLB2pr-GFP-PEST-LEU2*
YL2191	*CDC14-YFP-HIS3 NET1-mCherry-HIS3 MYO1-KanMX cdc5::KanMX ura3::3x(CDC5dB)::URA3*
YL2261	*MET-CDC20-TRP1 CLB2::GAL-CLB2kd-URA3 adh1::ADH1pr-GAL4-rMR-URA3 CDC14-YFP-HIS3 NET1-mCherry-HIS3 MYO1-GFP-KanMX cdc5::KanMX ura3::3x(CDC5dB)::URA3*
YL2271	*CDC14-YFP-HIS3 NET1-mCherry-HIS3 MYO1-KanMX bub2::HIS3 cdc5::GAL-URL-3HA-CDC5-KaxMX*
YL2272	*CDC14-YFP-HIS3 NET1-mCherry-HIS3 MYO1-KanMX cdc5::GAL-URL-3HA-CDC5-KaxMX*
YL2291	*CDC14-YFP-HIS3 NET1-mCherry-HIS3 MYO1-KanMX bub2::HIS3 trp1::2x(GAL-SIC1)::TRP1*
YL1961	*MATa clb1 clb2::GAL-CLB2 clb3::TRP1 clb4::his3::KanMX clb5::KanMX clb6::KanMX swe1::TRP1*
YL1962	*MATa clb1 clb2::GAL-CLB2 clb3::TRP1 clb4::his3::KanMX clb5::KanMX clb6::KanMX swe1::TRP1 cdc14-1*
FC015	*MET-CDC20-TRP1 ura3::GAL-CLB2kd-GFP-URA3,HIS3 adh1::ADH1pr-GAL4-rMR-URA3 CDC14-YFP-HIS3 NET1-mCherry-HIS3 MYO1-GFP-KanMX cdc5-1*
YL2471	*MET-CDC20-TRP1 ura3::GAL-CLB2kd-GFP-URA3,HIS3 adh1::ADH1pr-GAL4-rMR-URA3 CDC14-YFP-HIS3 NET1-mCherry-HIS3 MYO1-GFP-KanMX spo12::KanMX*
YL2491	*CDC14-YFP-HIS3 NET1-mCherry-HIS3 MYO1-GFP-KanMX bub2::HIS3 cdc16-6A::TRP1 cdc23-A-HA*

Table 2.1 Continued

	cdc27-5A::KanMX
YL2501	*CDC14-YFP-HIS3 NET1-mCherry-HIS3 MYO1-GFP-KanMX bub2::HIS3 sic1::HIS3 cdh1::HIS3 ade2::ADE2::GALL-CDC20*
YL2531	*MET-CDC20-TRP1 ura3::GAL-CLB2kd-GFP-URA3,HIS3 adh1::ADH1pr-GAL4-rMR-URA3 CDC14-YFP-HIS3 NET1-mCherry-HIS3 MYO1-GFP-KanMX cdc15-2 bub2::HIS3*
YL2581	*MET-CDC20-TRP1 ura3::GAL-CLB2kd-GFP-URA3,HIS3 adh1::ADH1pr-GAL4-rMR-URA3 CDC14-YFP-HIS3 NET1-mCherry-HIS3 MYO1-GFP-KanMX net1::HIS3 net1-6Cdk-TEV-myc9-TRP1*
YL2051	*MET-CDC20-TRP1 ura3::GAL-CLB2kd-URA3 adh1::ADH1pr-GAL4-rMR-URA3 CDC14-YFP-HIS3 NET1-mCherry-HIS3 MYO1-GFP-KanMX (p)CDC5-GFP-LEU2*

Time course experiments

For alpha factor block, 100nM alpha factor was used. For hydroxyurea (HU) block, 0.16M HU was used. In both cases, cells were washed 3 times by centrifugation and resuspension in fresh media for release. Arresting the *MET3-CDC20* cell in metaphase was done by addition of methionine to culture medium, as described (Uhlmann *et al.*, 2000), and release was done by centrifugation and resuspension in fresh medium lacking methionine. 15μg/ml nocodazole and 10μg/ml benomyl were added to cultures for spindle depolymerization (note: in Figures this is referred to as 'NOC'; we found that adding benomyl as well was important for obtaining a stable block). Protein extraction, immunoblotting and Clb2-associated H1 kinase assay were performed as previously described (Wasch and Cross, 2002). DNA flow cytometry was performed as previously described (Epstein and Cross, 1992). Budding was assessed by microscopic observation. Nuclear content was assessed by examining samples with nuclei stained with propidium iodide by fluorescence microscopy. Growth curve including cell density and mean cell volume was obtained using a Beckman Coulter Z2 Coulter Counter. The final carbon source concentration was, Glucose: 2%, Galactose: 3%, Raffinose: 3%. The *MET-CDC20* block experiment in Figure 3.1 was performed in YEP medium, otherwise in SC medium. The hydroxyurea and alpha factor block and release experiments were performed in SC medium. The alpha factor block and release experiments was performed in YEP medium. The time course experiment in Figure

3.3 was performed in YEP medium. When making a time-lapse movie, only SC medium was used.

Time-lapse and fluorescence microscopy

For time-lapse microscopy, cells were prepared as described in (Bean *et al.*, 2006). We used a Leica DMIRE2 inverted fluorescence microscope equipped with an environmental chamber and objective heater to observe the growth of the yeast cells at various temperatures. Images were acquired every 3 minutes with a Hamamatsu Orca-ER camera. We used custom Visual Basic software integrated with Image-Pro5.0 for microscope control and image acquisition. For still-image fluorescent microscopy, cells were fixed with 4% paraformaldehyde for 10 minutes before microscopy. For DAPI staining, cells were treated briefly with 30% ethanol following the paraformaldehyde fixation step, and stained with 100μg/ml DAPI. For imaging these cells, we used a Zeiss Axioplan2 fluorescent microscope with a Hamamatsu C4742-95 camera. Openlab5.0 was used for microscope control and image acquisition. Three Z-stacks at 0.6 micron intervals were taken for each fluorescent channel and projected onto a single image per channel.

Pulse-expression of *GAL1-CLB2kd(-GFP)* in *MET3-CDC20* blocked cells was described in Drapkin et al. (submitted). After Clb2kd expression, cells were immediately transferred to glucose medium without methionine at 30℃ to take fluorescent pictures every 3 minutes unless otherwise mentioned. To measure the

peak level of endogenous Clb2-GFP, *MET3-CDC20 CLB2-GFP* cells were grown up in glucose medium without methionine, and transferred into glucose medium with methionine to take time-lapse series. Clb2-GFP level at *MET3-CDC20* blocked cells was divided by 2 after background subtraction to be the peak Clb2-GFP in cycling cells; A population average was taken (the two-fold relationship between peak Clb2-GFP in cycling cells and that in *MET3-CDC20* block was established in Drapkin et al. submitted).

Image analysis

Time-lapse movie segmentation and analysis was done using custom software as described in (Charvin *et al.*, 2008). For the analysis of fluorescent microscopy pictures and r value calculation, we designed custom software in the Matlab environment. The Z-stack with the highest signal standard deviation was chosen for r value calculation. r value was calculated by taking the average CDC14-YFP intensity of the brightest 5% pixels within a cell area, and subtracting the average of the dimmest 5% pixels; this value was then divided by a similar value for the NET1-CFP signal.

In Chapter 4, we quantify Cdc14-YFP release by taking the coefficient of variation (CV, standard deviation divided by mean) of Cdc14-YFP pixel intensities inside a cell (mother and bud are treated separately), and divided by the CV of Net1-mCherry. Bud emergence was detected visually; Cytokinesis was detected

using Myo1-GFP (in case Myo1 ring shrinking was slowed down by Clb2kd, we recorded the time when Myo1 ring shrinking was competed.); Nucleolar separation was defined as the initial stretching of Net1-mCherry signals, followed by a full separation in 3~6 minutes. A narrow band-width GFP filter (Chroma, 41020) allows for detection of GFP signals with little intervention from YFP spectrum. Subsequently, the GFP portion was subtracted from original YFP images to restore pure YFP images. Control experiments with single-labeled cells (data not shown) indicate that this method yielded reliable quantifiable images without significant effective bleed-through between channels. Bud-neck regions were always excluded from quantification since Cdc14-YFP can also localize during ME. SPB signaling of Cdc14-YFP was detected by identifying bright YFP pixels whose underlying mCherry signals were low. Those pixels, if scored, were excluded from quantification, but did not cause any difference to our conclusions(Lu and Cross, 2009). In *net1Δ net1-6Cdk* cells in Figure 4.14, Cdc14 release was quantified by taking 3 Z-stacks with 2 micron intervals. And CV(Cdc14-YFP) in the best focused Z-stack was used to qualitatively reflect Cdc14 localization.

Data analysis.

All data analysis was performed using Matlab. Fluorescence time-lapse series were extracted from movies as previously described(Charvin et al., 2008). Smoothing is performed using 3-neighbour averaging method. Because Clb2(kd)-GFP primarily localizes to the nucleus, we took the average GFP intensity of the brightest

10% pixels in a cell and divided it by the square root of the cell area to be the effective Clb2(kd)-GFP concentration (average over the first 5 frames). Clb2kd concentration by this measure correlated best with graded ME delays. Average GFP intensity in a cell was used to measure transcription using promoter-GFP-Pest fusions(Bean et al., 2006).

Simulation of Kuramoto oscillator population with central pace-makers.

Kuramoto oscillator networks containing 100 nodes were generated. The dynamics of the ith node was driven by equation $\frac{d\varphi_i}{dt} = \omega_i + \lambda \sum_j a_{i,j} \sin(\varphi_j - \varphi_i)$, $a_{i,j} \in \{0,1\}$ is the interaction matrix; λ is the coupling strength. Network connections was either completely randomly established or using preferential attachments, and always kept the average in-degree <k_{in}> and out-degree <k_{out}> equal to 2.0 (i.e. on average, each node received 2 interactions and sent out 2 interactions). In preferential attachments(Barabasi and Albert, 1999), a network was grown from a small seed (N=2), and was gradually added nodes and links to it . For each node in the preexisted network, its chance of getting a new connection is in proportion to k^{α} (k is its degree; α is the preferential exponent). Preferential attachment was only applied to out-links. We scanned the coupling strength λ from 0.1 to 3.0 with 100 increments. For each λ, we randomly generated 1000 network connections with randomly chosen intrinsic frequencies $\omega_i \in [-1,1]$ and initial conditions $\varphi^0{}_i \in [-\pi, \pi]$. $R = \frac{1}{N \cdot T} \int_0^T | \sum_{i=1}^{N} e^{i\varphi_i} | dt$ (T=100, N=100) was used as the order parameter

to represent the degree of entrainment. All simulation was programmed in C language with *Numerical Recipe 2.0* package.

The conceptual model of phase-locking.

The kinetics of the peripheral oscillator P and the Cdk oscillator C is governed by simple oscillator equations. The free-running C can affect P's frequency to establish phase-locking. Theirs phases evolve as:

$$d\varphi_C/dt = \omega_C$$
$$d\varphi_P/dt = \omega_P + A * Z(\varphi_P)\sin(\varphi_C)$$

(A: amplitude of C, $Z(\varphi_P)$: P's frequency response function). For simplicity, we assume

$$Z(\varphi_P) = \begin{cases} Z_0 & (\varphi_P \in [0, \frac{5}{7}\pi] + 2k\pi, \quad k = 1,2,3...) \\ 0 & (otherwise) \end{cases}$$

In Figure 4.19B, the frequency of Cdk oscillator $\omega_C = 1.0$ is a constant. Frequencies of the 3 peripheral oscillators ω_P=[0.8 0.3 1.4], which roughly corresponds to budding, SPB duplication and Cdc14 release oscillator. And Z_0=[1.0 7 1.7] respectively. Cdk oscillation amplitude A=1.0. Initial condition $\varphi_C(t=0) = \varphi_P(t=0) = 0$. In Figure 4.20A, let A=0.85, otherwise, identical to Figure 4.19B. Simulation was done using Matlab.

ODE simulation of Cdc5-Cdc14-Cdh1 negative feedback model

Equations:

$$\frac{d[Cdc5]}{dt} = a_{cdc5} * clb2 \Big/ (clb2 + k_{clb2}) - d_{cdc5} * [Cdc5] - [Cdh1][Cdc5] * v_{cdc5} \Big/ ([Cdc5] + k_{cdc5})$$

$$\frac{d[Cdc14]}{dt} = (cdc14T - [Cdc14]) * [Cdc5]^n * v_{cdc14} \Big/ ([Cdc5]^n + k_{cdc14}{}^n) - d_{cdc14} * [Cdc14]$$

$$\frac{d[Cdh1]}{dt} = (cdh1T - [Cdh1]) * [Cdc14] * v_{cdh1p} \Big/ (cdh1T - [Cdh1] + k_{cdh1}) - clb2 * [Cdh1] * v_{cdh1pp} \Big/ (k_{cdh1} + [Cdh1])$$

Parameters

$a_{cdc5} = 1.0$ $k_{clb2} = 1.0$ $d_{cdc5} = 0.15$ $v_{cdc5} = 8.0$ $k_{cdc5} = 0.015$
$cdc14T = 0.2$ $v_{cdc14} = 10$ $k_{cdc14} = 1.0$ $d_{cdc14} = 0.8$ $n = 3$
$cdh1T = 0.5$ $v_{cdh1p} = 1.3$ $v_{cdh1pp} = 0.15$ $k_{cdh1} = 0.6$

Parameter ***clb2*** stands for Clb2kd concentration (/peak). In Figure 4.13E, ***clb2***=1.0; Initial condition=[0 0 0]. Simulation was done using Matlab.

Calculation of Cdc14 release and SPB timing using phase-locking model

Assume a peripheral oscillator P (such as bud emergence, SPB duplication, Cdc14 release…) oscillates at frequency $f_P{}^A$ at a specific locked Clb-Cdk level A (Any such level can be chosen provided it is permissive for oscillations of P). Also assume the Clb-Cdk oscillator C oscillates at a constant frequency f_C (i.e. the frequency of cell cycle). Clb-Cdk activities above or below A could change the instantaneous frequency of P by the amount $\Delta f = Z(\varphi)S_C$, where S_C is Clb-Cdk activity relative to the reference A ($S_C = Clb - A$), and $Z(\varphi)$ is the phase response curve of P to Clb-Cdk activity, and is in general a function of P's phase φ.

According to experiments in Figure 4.10, only the inter-release period (from the end of last release to the beginning of the next) was reduced as Clb2kd level increased, but not the duration of Cdc14 release or release amplitude. This observation will

restrict $Z(\varphi)$ to the following form:

$$Z(\varphi)=\begin{cases} Z_0 & (\varphi<\varphi_0) \\ 0 & (\varphi\geq\varphi_0) \end{cases} ,\varphi\in[0,2\pi)$$

In the unidirectional model, we ignore the feedback from P to C, and assume that Clb-Cdk activity oscillates as a function $0.5*(1+\sin(\boldsymbol{\varphi}+\boldsymbol{\psi}))$, where ψ is the phase difference between P and C. (The simple $\sin(\varphi+\psi)$ function is altered by these arithmetic operations just to avoid biochemically nonsensical 'negative' Clb-Cdk activity, and to keep Clb-Cdk values between 0 and 1, where 1 corresponds to '1X peak' in our experiments; see main text).

To constitute an actual cell-cycle, P and C must oscillate with identical frequency averaging over each cell cycle and a stable phase difference. So we first look for the condition where the original frequency difference $\boldsymbol{f_C}-\boldsymbol{f_P}^{A}$ between C and P is compensated by Clb-Cdk oscillation. i. e. we look for a phase difference ψ satisfying the following equation:

$$\boldsymbol{f_C}-\boldsymbol{f_P}^{A}=<\Delta\boldsymbol{f}>_{\boldsymbol{\varphi}}=\frac{1}{2\boldsymbol{\pi}}\int_0^{2\boldsymbol{\pi}}\boldsymbol{Z}(\boldsymbol{\varphi})(0.5\cdot\sin(\boldsymbol{\varphi}+\boldsymbol{\psi})+0.5-\boldsymbol{A})\boldsymbol{d\varphi}$$

This formulation implies that at any instant, Clb-Cdk can either advance or retard the velocity of P through its cycle, depending on the coincidence of Z_0 with Clb-Cdk above or below A.

The above equation can be solved to yield:

$$\boldsymbol{\psi}=\sin^{-1}\left(\frac{(\boldsymbol{f_C}-\boldsymbol{f_P}^{A}+(\boldsymbol{A}-0.5)<\boldsymbol{Z}(\boldsymbol{\varphi})>_{2\boldsymbol{\pi}})2\boldsymbol{\pi}}{\boldsymbol{Z}_0\sin(\boldsymbol{\varphi}_0/2)}\right)-\boldsymbol{\varphi}_0/2$$

Note: In general, ψ is also a function of φ. To obtain analytical results, we do the integration by approximating ψ to a constant, meaning that the phase of P still progress smoothly. This approximation is exact when $f_C - f_P^A$ and $Z(\varphi)$ are small (Winfree, 1967). Simulations with an ODE model show that with Z_0, f_C and f_P^A in the range of our empirically determined values (see below), Z_0 and $f_C - f_P^A$ are small enough that this approximation is extremely close to the exact value (data not shown).

Different phase-response curves $Z(\varphi)$ will yield different stable solutions for ψ: therefore, oscillators entrained by different $Z(\varphi)$ will cycle at different phases relative to the Clb-Cdk oscillator, potentially ordering cell cycle events.

It's demonstrable that the calculation of ψ is independent of the choice of reference point A. f_P^A is approximately a linearly function of constant Clb2kd levels A below 1.7xPeak (Figure 4.10B). Therefore, we write $f_P^A = k * A + B$. k is the slope of the linear fitting in Figure 4.10B, which is equal to average $Z(\varphi)$ over one cycle ($k = <Z(\varphi)>_{2\pi}$). Then

$$\psi = \sin^{-1}\left(\frac{(f_C - B - 0.5 < Z(\varphi) >_{2\pi})2\pi}{Z_0 \sin(\varphi_0 / 2)}\right) - \varphi_0 / 2, \quad \text{independent of A.}$$

For the convenience of calculation, the Clb-Cdk reference point is set at A=0.5. (MATLAB code for running this and related simulations are available upon request; we have found these simulations very helpful for aiding intuition).

The duration of Cdc14 release is approximately 20 minutes. From Figure 4.10, we estimate the period of the Cdc14 release oscillator at 1X peak Clb2kd at 70 minutes, then we obtain $\varphi_0 = \frac{10}{7}\pi$ (For the Cdc14 oscillator, $\varphi = 0$ corresponds to the completion of Cdc14 resequestration). For the estimation of $< \boldsymbol{Z}(\boldsymbol{\varphi}) >_{2\boldsymbol{\pi}}$ (i.e. the slope of fitting in Figure 4.10B), we use only 'category 3' cells as defined in Figure 4.10B, since only these cells allow an unambiguous interpretation as 'endocycling'. We estimate $Z_0 = \frac{2\pi}{\varphi_0} < Z(\varphi) >_{2\pi}$, and obtain $Z_0 = 0.022 \pm 0.006\,(Peak_{Clb2}{}^{-1} \cdot \min^{-1})$.

When calculating Cdc14 entrainment phase, we took $A = 0.5$ as the reference point of stable Clb-Cdk, so that $\boldsymbol{f_P}^{A}$ is estimated at approximately the average Clb-Cdk activity in a cell cycle When Clb2kd<1X peak, the Cdc14 release oscillator is entrained or partially entrained into cell cycle due to endogenous Clb-Cdk oscillation, because at these low levels of Clb2kd, mitotic exit occurs and endogenous cyclin accumulates to sub-peak levels (data not shown). For this reason, we lack endocycle data at Clb2kd=0.5, and we are obliged to linearly extrapolate the frequency response of Cdc14 release oscillator in Figure 4.10B to 0.5X peak Clb2kd. We obtain $\boldsymbol{f_P}^{A^{-1}} = 95 \pm 15\,(\min.)$. For the frequency of Clb-Cdk cycles in wild-type mother cells, we take $f_C{}^{-1} = 80\,(\min.)$ based on abundant and reliable data for cycling wild-type cells (data not shown). Since $\boldsymbol{f_P}^{A}$ and Z_0 measurements contain substantial uncertainty, we calculate ψ at the average, +/- one standard deviation for each, summarized in the following table, and plotted below together with modeled Clb-Cdk levels (see Figure 4.20C legend):

Z_0 (Peak·min^{-1}) / f_P^{-1} (min.)	0.017	0.0224	0.028
80	-0.71π	-0.71π	-0.71π
95	-0.33π	-0.47π	-0.52π
110	No solution	No solution	-0.30π

(The lack of a solution in two cells of the table is likely due to oversimplifications in the model, such as describing $Z(\varphi)$ as a step function, which results in unrealistically tight boundary conditions).

We next consider the phase-locking between SPB duplication oscillator and Clb-Cdk oscillator. This demonstration can be based only partially on empirical data, because in particular there is no quantitative information on the period of the SPB re-duplication cycle as a function of Clb levels. According to previous studies, there is a licensing period following SPB separation when SPB reduplication is inhibited by high Clb-Cdk activity, but not in other parts of the SPB duplication cycle. Therefore according to our formulation, $Z_0 < 0$ within the licensing period, $Z_0 = 0$ elsewhere. In cycling cells, the licensing period starts from SPB maturation in G2 until the next G1. For a typical cell cycle of 80 minutes (for mother cells), G1 lasts for ~20 minutes; S phase lasts for ~15 minutes. Therefore the licensing period is ~45 minutes, and we have $\varphi_0 = \frac{9}{8}\pi$ ($\varphi = 0$ corresponds to the beginning of the licensing

period, since by convention we set the beginning of the cycle to be the beginning of the part of the cycle affected by Clb2).

While free oscillation of SPB duplication and cell-cycle-regulated transcription have been established, there is insufficient data to obtain empirical estimates of $Z(\varphi)$ and $f_P{}^A$. The fact that SPB duplication is always entrained with cell cycle in wild type cells indicates that $(f_C - f_P{}^A)/Z_0$ should be small, which is easy to obtain with a large Z_0. Consistently, having Clb4 as the only mitotic cyclin completely blocks SPB reduplication (Haase et al., 2001), implying that the frequency of SPB oscillator is sensitive to Clb-Cdk levels, suggesting a large Z_0. Therefore, we could assume $(f_C - f_P{}^A)/Z_0 \sim 0$, and obtain

$\psi = \pi - \frac{\varphi_0}{2} = \frac{7}{16}\pi$ (the $\psi = -\frac{\varphi_0}{2} = -\frac{9}{16}\pi$ solution is dynamically unstable due to $Z_0 < 0$) (Winfree, 1967).

The stable solution restricts SPB duplication and maturation to the rising-phase of Clb-Cdk oscillator, roughly corresponding to G1 → G2, which is physiologically meaningful. (See Figure 4.20 legend)

Proof of linearity for the metric used to quantify Cdc14 release

At Cdc14 fully sequestered state:

$O_0 = N_0 + S_0$: where O is the observed signal, S is the real Cdc14 - YFP signal, and N is noise.

When there is a fraction (1-λ) of Cdc14 released and become a uniform background C

$$O_1 = N_1 + S_1 + C = N_1 + \lambda S_0 + C$$

Assuming that Net1-mCherry is always nucleolar, and when Cdc14 is fully sequestered, Cdc14 totally colocalizes with Net1:

$$r^2 = (\frac{CV(O_1^{Cdc14})}{CV(O_1^{Net1})})^2 = (\frac{CV(O_1^{Cdc14})}{CV(O_0^{Cdc14})})^2 = \frac{Var(O_1^{Cdc14})}{Var(O_0^{Cdc14})} = \frac{\lambda^2 Var(S_0) + Var(N_1)}{Var(S_0) + Var(N_0)}$$

The last step is obtained by assuming no covariance between Cdc14 signal and background noise.

$$\mathrm{cov}(S_0, N_1) = \mathrm{cov}(S_0, N_0) = 0$$

We can see that, even when Cdc14-YFP is completely released, λ=0, *r* is still >0 due to background fluctuations.

The bidirectional phase-locking model

Cdc14 is not a simple peripheral oscillator, since it regulates Clb-Cdk activity (see main text). Therefore, in a full account, it should be necessary to take mutual entrainment into account. The fact that initial Cdc14 release and resequestration occur with normal kinetics at all levels of Clb2kd (main text) suggests, however, that the bidirectionality is not highly important in determining phasing of Cdc14 release relative to peak Clb2.

To construct a bidirectional model, we adopt all basic assumptions in the

unidirectional model; in addition, assume there is also a feedback interaction from a peripheral oscillator P to the Cdk oscillator C. We named the coefficient of the interaction from C to P as $Z_{C->P}(\varphi)$, and the one from P to C as $Z_{P->C}(\varphi+\psi)$, then the steady state condition reads

$< f_P >_\varphi = < f_C >_\varphi \rightarrow f_C + < Z_{P->C}(\varphi+\psi) S_P >_\varphi = f_P + < Z_{C->P}(\varphi) S_C >_\varphi$

Also consider

$$Z_{C->P} = \begin{cases} Z_0 & (\varphi < \varphi_0) \\ 0 & (\varphi \geq \varphi_0) \end{cases}$$

In the case of Cdc14-release oscillator, we can get an analytical solution by assuming whenever there is Cdc14 release in a cell-cycle, there will be activation of Cdh1/Sic1 to inactivate Clb-Cdk, then we have $Z_{P->C}(\varphi+\psi) = \text{constant}$. Therefore

$< Z_{C->P}(\varphi) S_C >_\varphi = f_C - f_P + \frac{1}{2\pi}\int_0^{2\pi} Z_{P->C}(\varphi+\psi) S_P d\varphi = f_C - f_P + \Lambda$, (Λ is a constant)

Then

$$\frac{1}{2\pi}\int_0^{\varphi_0} Z_0(0.5 \cdot \sin(\varphi+\psi) + 0.5 - A) d\varphi = f_C - f_P + \Lambda$$

Solve it to get

$$\psi = \sin^{-1}[(f_C - f_P + \Lambda + (A-0.5) < Z(\varphi) >_{2\pi}) \frac{2\pi}{Z_0 \sin\frac{\varphi_0}{2}}] - \frac{\varphi_0}{2}$$

$\frac{f_C - f_P + \Lambda}{Z_0}$ needs to be determined experimentally.

Due to the unknown parameter Λ, ψ calculated using the bidirectional model can be different from the unidirectional model. But the same general conclusions hold for both models, such as 1. There will be at least one stable phase-locking solution ψ

giving strong enough coupling Z_0; 2. Cell cycle oscillators with different phase-response curve $Z(\varphi)$ could oscillate at different ψ, which may order the cell cycle.

Chapter 3: Mitotic Exit in The Absence of Separase Activity

1. Background information

Mitotic Exit (ME) is a complex set of events encompassing spindle disassembly, cyclin inactivation, cytokinesis and relicensing of replication origins. In budding yeast *Saccharomyces cerevisiae*, the phosphatase Cdc14 is required for ME. A first wave of Cdc14 release has been described in early anaphase, controlled by the separase-induced FEAR (cdc Fourteen Early Anaphase Release) network which includes separase (Esp1), Spo12, Slk19, Cdc5 (Stegmeier et al., 2002). After DNA replication in S phase and kinetochore attachment, activated APC-Cdc20 commits the cell to chromosome segregation in anaphase by inducing the degradation of B-type cyclins and securin Pds1 to promote the onset of anaphase. Pds1 forms a complex with Esp1, serving as its chaperone, and also inhibiting Esp1 proteolytic activity. After Pds1 proteolysis, free Esp1 may down-regulate phosphatase PP2A (Queralt et al., 2006), enhancing Net1 phosphorylation and promoting transient Cdc14 release (the FEAR network mechanism). FEAR-released Cdc14 modulates nuclear movement, rDNA segregation and spindle stability before ME (Azzam et al., 2004). In later anaphase the release status of Cdc14 is maintained by a second mechanism, the Mitotic Exit Network (MEN), which involves Tem1, Cdc15, Dbf2/Mob1 and its inhibitor Bub2/Bfa1. MEN activation may be due to Cdc14-dependent Cdc15 dephosphorylation, spindle-elongation-induced Tem1 activation, or

Polo-kinase-induced Bub2/Bfa1 inactivation (Bardin et al., 2000; Hu et al., 2001; Jaspersen and Morgan, 2000).

Current concepts place separase Esp1 at the center of ME regulation. A non-proteolytic function of Esp1 is considered responsible for early anaphase release of Cdc14, perhaps to promote Cdc15 dephosphorylation to activate MEN. MEN activity can promote additional Cdc14 release, thus forming a potential positive feedback loop, which could eventually release enough Cdc14 to drive ME.

Although these concepts are supported by much experimentation, the ME system is highly complex, with interdigitated control networks making experimental design challenging, and straightforward interpretation sometimes difficult. I attempted a factorial approach (Fisher, 1935) of independently controlling CDK inactivation, the non-proteolytic function of Esp1, and spindle elongation, aiming to achieve a balanced view of the relative contributions of three major regulators in ME. These experiments have led me to a view of ME emphasizing the importance of CDK inactivation and activation of the MEN as the primary drivers. In contrast to the proposal of a protease-independent essential role for Esp1 in ME, my results suggest that the primary contribution of Esp1 in ME is to promote sister chromatid separation, which leads to spindle-elongation-dependent MEN activation.

2. Factorial control of mitotic exit

Complete factorial design of experiments employs systematic combinations of a set of controlling factors. This approach allows determination not only of the contribution of each individual factor but also of interactions between them (Fisher, 1935). It is especially suitable and efficient for studying a complex system like the ME pathway for which I have little quantitative knowledge about the independence of its components.

I chose three factors known to contribute to ME: Esp1 activation, cohesin cleavage and consequent spindle elongation, and CDK inactivation, as control points of the system (Figure 3.1A). CDK inactivation, by degradation of mitotic cyclins such as Clb2, is essential for ME (Wasch and Cross, 2002). Another essential player that has been proposed is the non-proteolytic function of Esp1, which promotes spindle stability and FEAR network activity; however, the FEAR network has been found to be dispensable for ME in most studies (Jensen et al., 2001; Queralt et al., 2006; Stegmeier et al., 2002). My third factor, cohesin cleavage and consequent spindle elongation, activates MEN by promoting interaction of the daughter spindle pole body with the bud cortex (Bardin et al., 2000; Yeh et al., 1995). Spindle elongation also creates the spindle mid-zone, a signaling center for Aurora kinase and the NoCut pathway (Norden et al., 2006).

A critical requirement for my approach is availability of tools to separately and independently manipulate those inputs. Wherever possible, I have used multiple approaches to control each factor. I prevent CDK inactivation in most experiments by blocking APC activation, using *MET3-CDC20* strains incubated in methionine medium. Conversely, I can promote CDK inactivation by over-expressing unphosphorylatable Sic1 from a galactose inducible promoter (*GAL1-SIC1-4A*) (Verma et al., 1997) or in some experiments by relying on the endogenous cyclin degradation system driven by the APC. I control the presence of active Esp1 in most experiments by expressing undegradable Pds1 (Cohen-Fix et al., 1996), either from strong ectopic promoters or expressed from its endogenous locus. I control spindle elongation independently of Esp1 by bypassing the Esp1 requirement for cohesin (Scc1) cleavage, using the TEV-Scc1-TEV-site system of Uhlmann et al. (Sullivan and Uhlmann, 2003; Uhlmann et al., 1999), or the *scc1-73* temperature-sensitive allele (Michaelis et al., 1997). Alternatively, in the presence of Esp1 I independently block spindle elongation using nocodazole, or MEN activation using the *cdc15-2* temperature-sensitive mutation. Independence of these perturbations (that is, altering one input should not indirectly affect the others) is generally expected from the literature, and confirmed in my experiments wherever possible; however, complete independence of input modules can only be reached approximately. Therefore, I have strengthened my conclusions by alternative experimental designs for testing the same effective factor combinations wherever possible.

Figure 3.1. **Combinatorial control of mitotic exit by Cdk inactivation and cohesin cleavage, in the absence of Cdc20.** **A**. Major components and interactions in ME system; arrows: induction; bars: inhibition. Components indicated in red are exterior control points used here to manipulate the system. **B**. Cultures of *MET3-CDC20* strains were first arrested in metaphase at 23°C by incubation in raffinose+methionine medium to deplete Cdc20, then galactose was added to the cultures to induce the expression of *GAL1-TEV* and *GAL1-SIC1-4A* where present. Methionine was kept in the medium throughout to maintain *cdc20* depletion, except for the experiment labeled 'control', which was released into galactose medium lacking methionine to re-induce Cdc20. Strain genotypes: 1. "control", *MET3-CDC20 GAL1-SIC1-4A* (YL1721). 2. "+ +", *MET3-CDC20 scc1Δ SCC1-TEV GAL1-TEV GAL1-SIC1-4A* (YL353). 3. "+ –", *MET3-CDC20 scc1Δ SCC1-TEV GAL1-TEV* (353). 4. "– +", *MET3-CDC20 GAL1-SIC1-4A* (YL1721). 5. "– –", *MET3-CDC20* (BD96b-4C). + +, + –, – + or – – indicate the presence or absence of *GAL1-TEV/SCC1-TEV* and *GAL1-SIC1-4A*. The fraction of large budded cells (excluding rebudded and small budded cells) was calculated from >200 cells at each time point. DNA flow cytometry profiles from the beginning and end of the time course for each sample are shown (complete DNA flow cytometry data in Fig. 3.2), as well as sketches of the cell morphologies at the end of the experiment. Note that the elongated buds are a consequence of rebudding (with or without prior cytokinesis) in the presence of high Sic1 levels (Lew and Reed, 1993), and thus allow unambiguous discrimination between the large round buds found at the beginning of the experiment and the new buds formed after complete or partial mitotic exit.

Figure 3.1

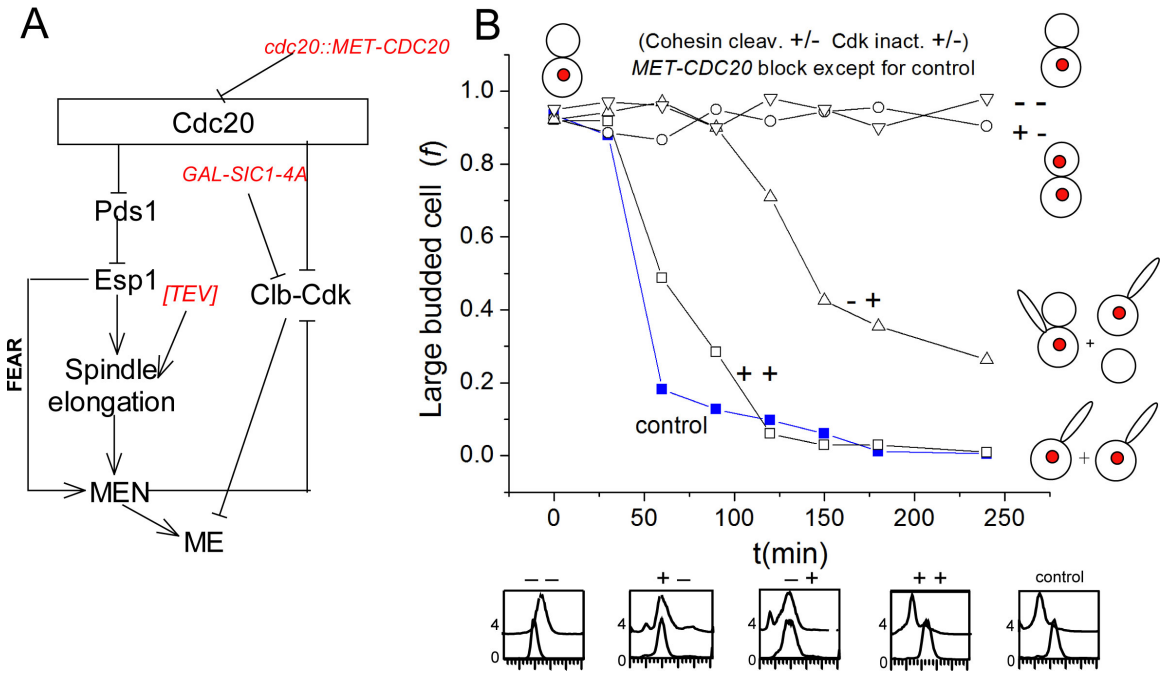
A
cdc20::MET-CDC20
Cdc20
GAL-SIC1-4A
Pds1
Esp1
[TEV]
Clb-Cdk
FEAR
Spindle elongation
MEN
ME
B
(Cohesin cleav. +/- Cdk inact. +/-)
MET-CDC20 block except for control
Large budded cell (f)
1.0
0.8
0.6
0.4
0.2
0.0
0
50
100
150
200
250
t(min)
- -
+ -
- +
+ +
control
– –
+ –
– +
+ +
control
4
0

In the first series of experiments (Figure 3.1B), cells were arrested in metaphase using a methionine-suppressible *MET3-CDC20* construct (Sullivan and Uhlmann, 2003). Cdc20 is an essential activator of the APC, and in its absence cells arrest with high CDK activity due to mitotic cyclin stabilization (Yeong et al., 2000). In addition, the Cdc20 target Pds1 accumulates at high levels, and anaphase is blocked due to Pds1 inhibition of Esp1 (Shirayama et al., 1999); therefore, I assume that Esp1 activity is limited or absent. I then examined if these *cdc20*-blocked cells can carry out mitotic exit, as a function of ectopic regulation of anaphase using the *GAL1-TEV/SCC1-TEV* system (Uhlmann et al., 2000), and of ectopic Clb-Cdk inactivation using *GAL1-SIC1-4A* (Verma et al., 1997). To monitor ME, I employed phase contrast microscopy to detect cell division and budding, and DNA flow cytometry to analyze replication and effective chromosome segregation to daughter cells (implying cytokinesis and cell separation). I were surprised to observe that simultaneously providing ectopic sources of cohesion cleavage and Clb-Cdk inactivation allowed quantitative and rapid mitotic exit, by the assays of cytokinesis, nuclear division and rebudding in the next cell cycle (Figure 3.1B), resulting in the efficient accumulation of 1C budded cells. Of the two factors driving ME in this remarkably effective synthetically driven ME, CDK inactivation is essential, while TEV-mediated cohesin cleavage and consequent spindle elongation is important for efficiency but not absolutely required (Figure 3.1B).

This experiment resembles one published by Sullivan and Uhlmann (2003),

except that in that work, *clb5* deletion was employed for Clb-Cdk inhibition, which is very likely to provide only partial decrease in Clb-Cdk activity (as evidenced by viability of *clb5* cells), while in contrast, *GAL1-SIC1-4A* quantitatively eliminates all Clb-Cdk activity and results in complete inviability (Figure 3.2B).

Strikingly, timing of mitotic exit in the *GAL1-SIC1-4A GAL1-TEV cdc20* cells was similar to that of cells released from the *cdc20* block (Figure 3.1B, + + v.s. control). I assume that Esp1 was effectively inhibited by persistent Pds1 due to the *cdc20* block, since anaphase was completely inhibited without *GAL1-TEV* expression. Therefore, these results suggest that ESP1 does not play a major role in ME besides its function in sister chromatid separation and the resulting spindle elongation.

I further assessed the role of separase in ME in this protocol using a proteolytically inactive mutant $ESP1^{C1531A}$ (Uhlmann et al., 2000). I constructed a *MET3-CDC20* strain that contained the rapidly inactivatable *esp1-2td* allele (Queralt et al., 2006) as well as *GAL1-SIC1-4A* to allow Clb-Cdk inactivation and a copy of $ESP1^{C1531A}$ under control of the endogenous promoter. As expected, release of the *cdc20* block did not lead to anaphase in this strain. Employing the same set of assays for ME, I saw only the same partial mitotic exit phenotype that I could attribute to *GAL1-SIC1-4A* (Figure 3.1), with no detectable contribution from $ESP1^{C1531A}$ (Figure 3.2).

Figure 3.2. **A.** DNA flow cytometry profile for time-courses in Figure 3.1. **B**. *MET-CDC20 6xGAL-ESP1* (393) or *MET-CDC20 6xGAL-ESP1 GAL-SIC1-4A* (YL0932) was arrested in metaphase at 23° by incubation in raffinose+methionine medium to deplete Cdc20. 3% galactose was added to the culture at time zero. Clb2 kinase assay, done as described in Materials and Methods, showed that *GAL-SIC1-4A* induction almost completely eliminated Clb2 kinase activity after 1 hour induction. **C**. *MET-CDC20 esp1-2td GAL-UBR1 ESP1-C1531A GAL-SIC1-4A* (YL094, separase +) was arrested at 25° by depleting Cdc20, followed by temperature shift to 37° to inactivate esp1-2td, and then Cdc20 was reintroduced by transferring to galactose medium lacking methionine. *MET-CDC20 GAL-SIC1-4A* (YL172, separase –) and *MET-CDC20* (BD96B-4C, control) are described in Figure 3.1.

Figure 3.2

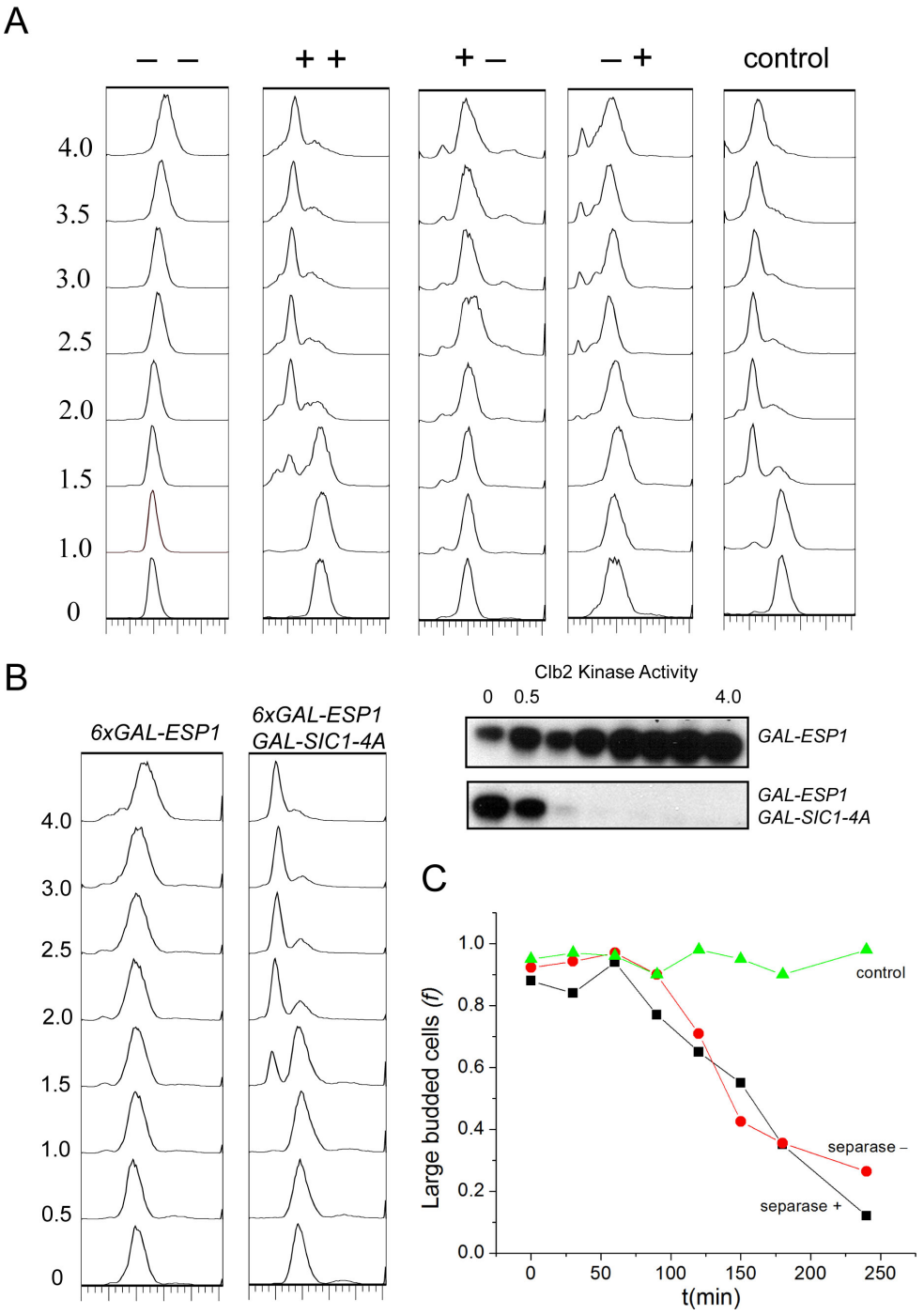
A
– –
+ +
+ –
– +
control
4.0
3.5
3.0
2.5
2.0
1.5
1.0
0
B
6xGAL-ESP1
6xGAL-ESP1
GAL-SIC1-4A
4.0
3.0
2.5
2.0
1.5
1.0
0.5
0
Clb2 Kinase Activity
0 0.5 4.0
GAL-ESP1
GAL-ESP1
GAL-SIC1-4A
C
Large budded cells (f)
1.0
0.8
0.6
0.4
0.2
0.0
0
50
100
150
200
250
t(min)
control
separase –
separase +

3. Endogenous undegradable Pds1 blocks sister-chromatid separation

I wanted to confirm that endogenous levels of Pds1 could effectively block Esp1 activity in the absence of Cdc20-dependent Pds1 degradation, since this was an important assumption in the experiments described above. Inviability of endogenous levels of Pds1-mdb was suggested by failure to recover transformants of *PDS1-mdb* under control of the *PDS1* promoter in low-copy number plasmids (Cohen-Fix et al., 1996), but the reason for the failure to recover these transformants was not elucidated. I constructed a *PDS1-mdb* allele at the endogenous locus, using exact gene replacement. The potential lethality of this allele was overcome by mildly over-expressing Esp1 under a truncated *GAL1* promoter (Mumberg et al., 1994), *GALS-ESP1*. Indeed, this strain is fully viable on galactose media but inviable on glucose (Figure 3.3A), confirming that endogenous levels of undegraded Pds1 were lethal, specifically because of Esp1 sequestration. Pds1-mdb was stable through the cell cycle at endogenous levels, while Pds1-wt was degraded before anaphase as expected (Figure 3.3B). Since Esp1 is a stable protein, transcriptional repression of *GALS-ESP1* by glucose in a *PDS1-mdb* background allows two or more near-normal cell cycles. Subsequently, I observe a gradual increase of unseparated chromosome dots (Bachant et al., 2005) (Figure 3.3C) and a gradual increase of large budded cells with 2C DNA content (Figure 3.4A). These cells were highly delayed in ME, although ultimately most cells underwent aberrant mitosis with generation of

aneuploid or aploid cells (Figure 3.4A). From these results, I conclude that the endogenous level of Pds1 can effectively inhibit Esp1 and block sister-chromatid separation, provided its Cdc20-mediated degradation is blocked.

Figure 3.3. **Endogenous undegradable Pds1 blocks sister-chromatid separation.** **A**. *PDS1-mdb ESP1::GALS-ESP1* (YL018) or a wild-type control were plated by 10x serial dilution on either glucose (D) or galactose (G) plates at 30° to assess viability. **B**. Cultures (*PDS1-mdb-myc ESP1::GALS-ESP1* or control *PDS1-wt-myc*) synchronized by alpha-factor block-release were assayed by Western blotting with anti-Myc antibody. Pgk1 western blot was employed as a loading control. **C**. Endogenous Pds1 is sufficient to block sister-chromatid separation. Glucose was added to galactose-grown mid-log cultures of *PDS1-mdb trp1::LacO LacI-GFP*, containing either *esp1::GALS-ESP1* (YL115, filled bar) or *ESP1::GALS-ESP1* (YL113, hatched bar). Samples were fixed with paraformaldehyde and examined by fluorescence microscopy to score separation of the GFP-labeled chromosome 'dots'. Fraction of large budded cells with unseparated GFP dots (red), with well-separated GFP dots (green) or closely separated GFP dots (blue) are shown. Cell morphologies at the beginning and end of the experiment in the various conditions are diagrammed in the cartoons.

Figure 3.3

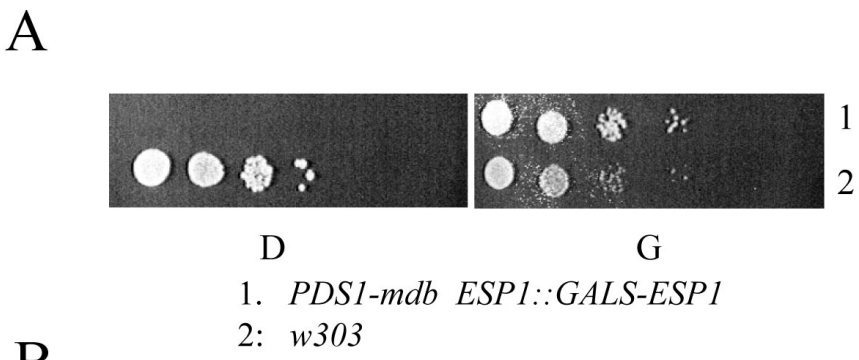
A
1
2
D
G
1. PDS1-mdb ESP1::GALS-ESP1
2: w303
B
t(m) 0 20 40 60 80 100 120 160
anti-Myc
anti-Pgk1
PDS1
anti-Myc
anti-Pgk1
PDS1
-mdb
C
1.0
0.8
0.6
0.4
0.2
0.0
f
0
2
5
t(hr)

Figure 3.4

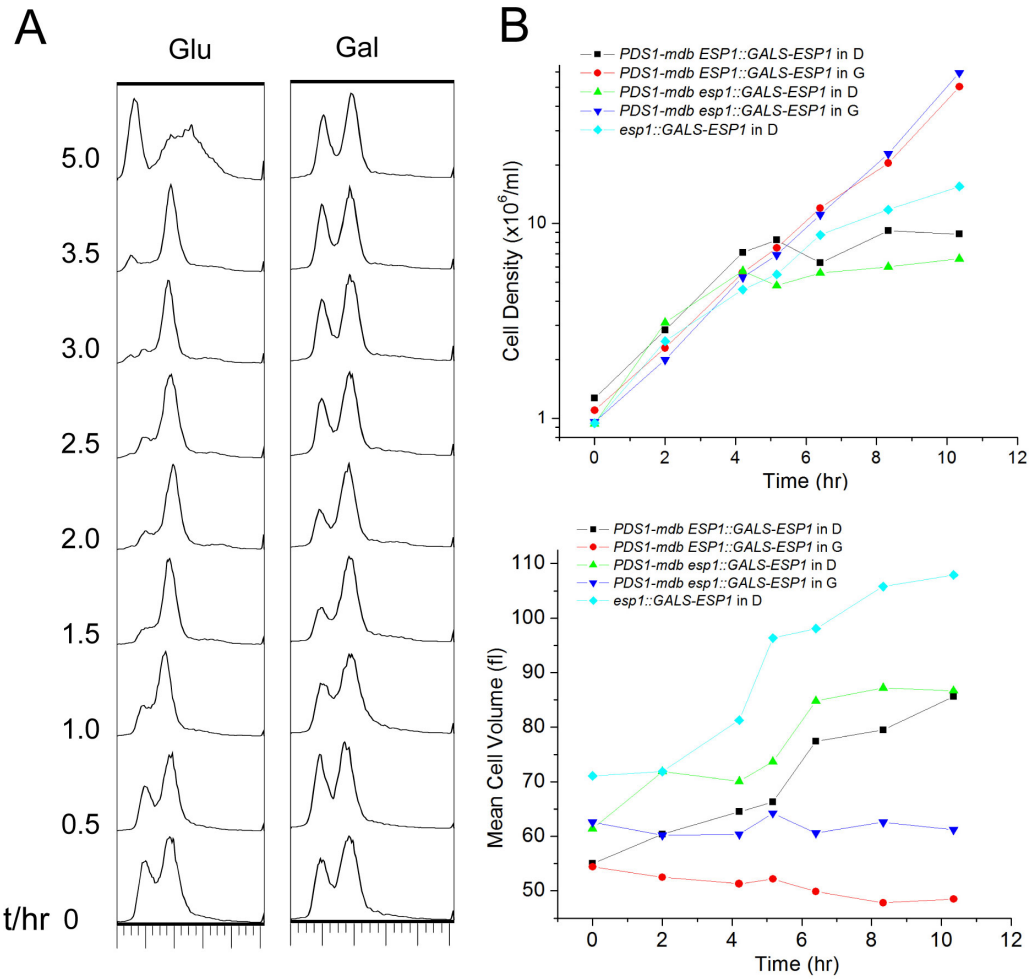

Figure 3.4. **A**. DNA flow cytometry profile: *PDS1-mdb esp1::GALS-ESP1* (YL114) cells were grown to log phase in galactose media, then 2% glucose (Glu) was added at time zero. **B**. Growth curve: *PDS1-mdb esp1::GALS-ESP1* (YL114) and *PDS1-mdb ESP1::GALS-ESP1* (YL018) and *esp1::GALS-ESP1* (YL008) strains growing in glucose or galactose. Cell density and mean cell volume were measured as described in Materials and Methods.

4. Inhibition of Esp1 by overexpression of overexpression of undegradable Pds1 blocks ME via blockage of cohesin cleavage

Overexpression of undegradable Pds1 causes a complete block to anaphase, and a many-hour delay in ME (Cohen-Fix et al., 1996; Queralt et al., 2006; Sullivan and Uhlmann, 2003). Consistently, in my experiments in Figure 3.1, Cdc20 depletion (leading to Pds1 accumulation and Esp1 inhibition), led to a significant delay in ME even when Clb-Cdk inhibition was provided ectopically by *GAL1-SIC1-4A*. However, this delay was efficiently rescued by ectopic cohesin cleavage using *GAL1-TEV* (Figure 3.1B), suggesting that most of the delay was due to failure of cohesin cleavage. I were concerned, though, that I had not achieved complete Esp1 inhibition using endogenous levels of accumulated Pds1. To ensure that I achieved full inactivation of endogenous Esp1, I overexpressed Pds1-mdb from the *GAL1* promoter. I expressed *GAL1-PDS1-mdb* expression for an hour to accumulate abundant Pds1-mdb in *cdc20*-blocked cells, and then released the *cdc20* block by methionine removal. In this protocol, Clb-Cdk inactivation is expected to proceed via the Cdc20-APC system, while Esp1 is sequestered by Pds1-mdb overexpression. I provided an ectopic source of cohesin cleavage using the *GAL1-TEV*/*SCC1-TEV* system. As a control, I carried out the same protocol substituting *GAL1-PDS1(wt)*, expressing the degradable form of Pds1, for *GAL1-PDS1-mdb*. Expression of Pds1-mdb caused no delay in cytokinesis or Clb2 degradation compared to expression

of Pds1-wt, despite persistence of Pds1-mdb but not Pds1-wt, suggesting that Pds1 is not an effective ME inhibitor provided the need for the proteolytic activity of Esp1 is bypassed (Figure 3.5C). While this experiment provides a direct comparison between Pds1-wt and Pds1-mdb at equally overexpressed levels, overexpressed Pds1-wt could delay ME compared to endogenous levels. However, in the remaining experiments I compared overexpressed Pds1-mdb to endogenously expressed Pds1-wt.

Figure 3.5. **Endogenous Esp1 is not necessary for efficient mitotic exit. A**. Artificial cleavage of Scc1 with TEV protease ensures efficient ME in the absence of active Esp1. *mad2Δ* strains were arrested in S phase at 30°C with 0.16M hydroxyurea, and released into galactose with alpha factor. Pds1-mdb and TEV protease were overexpressed from the *GAL1* promoter to inactivate Esp1 and to cleave Scc1-TEV (YL057). Strains lacking *GAL1-TEV* (YL045) *GAL1-PDS1-mdb* (YL049), or both (2151-7B) were used as controls. **B**. Inactivation of cohesin Scc1 restores the efficiency of ME in the absence of active Esp1. *mad2 GAL1-PDS1-mdb* strains, either *scc1-73* (YL044) or *SCC1* (YL045) were arrested by alpha factor at 25°C, then released into the absence of alpha factor either in galactose media to induce undegradable Pds1-mdb or raffinose as a control. Cultures were released at 37°C to inactivate cohesin (*scc1-73*). Alpha factor was reintroduced 1.5 hours post release to cause accumulation of cells in G1 after ME. DNA flow cytometry was used to assess cell cycle progression. **C**. Pds1-mdb doesn't independently block ME in cells provided with ectopic chromosome separation by TEV protease. *GAL1-TEV/SCC1-TEV MET3-CDC20* strains, containing *GAL1-PDS1-wt* (YL042) or *GAL1-PDS1-mdb* (YL043), were arrested at the *cdc20* block by incubation in raffinose plus methionine medium, and then pulsed with galactose plus methionine for an hour. The cultures were then transferred into glucose without methionine to release the *cdc20* block. DNA content was measured by DNA flow cytometry, and Clb2 protein level by Western blot. Even loading was shown by amido-black staining (data not shown).

Figure 3.5

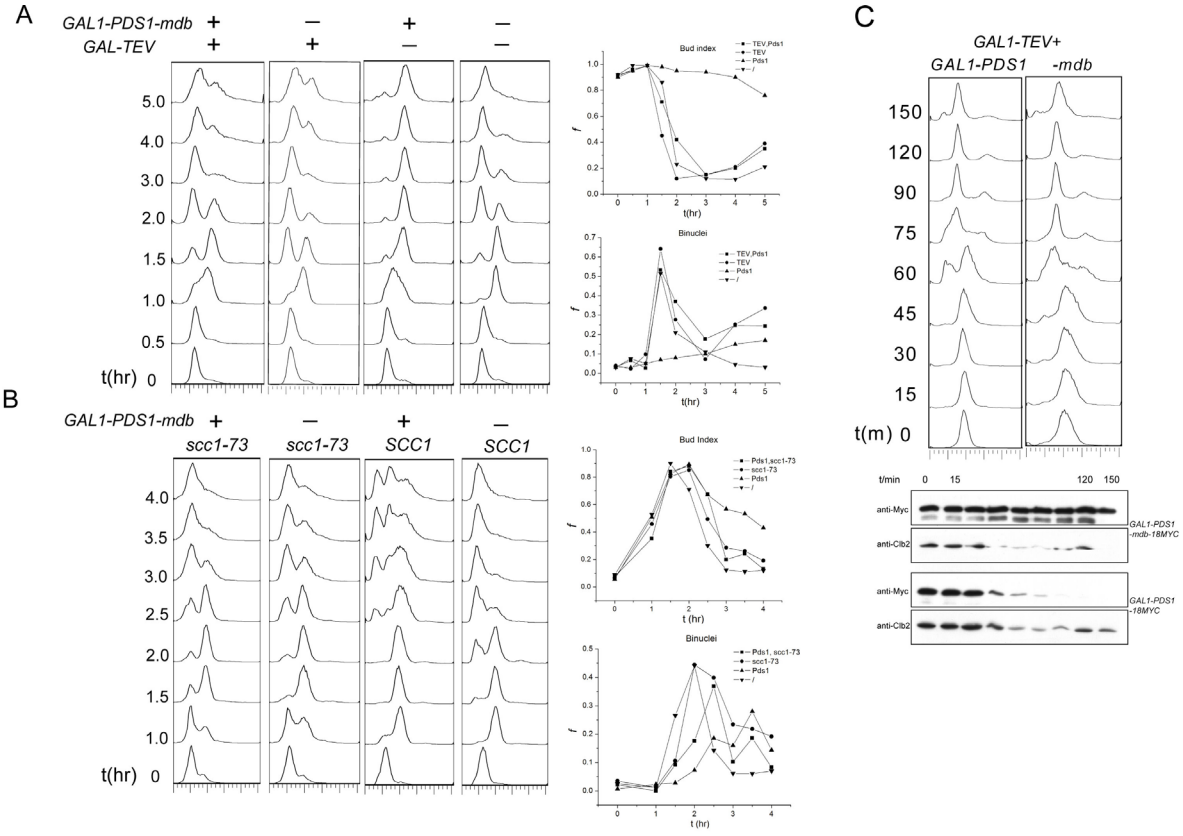
A
GAL1-PDS1-mdb + − + −
GAL-TEV + + − −
5.0
4.0
3.0
2.0
1.5
1.0
0.5
t(hr) 0
Bud index
TEV,Pds1
TEV
Pds1
f
t(hr)
Binuclei
B
GAL1-PDS1-mdb + − + −
scc1-73 scc1-73 SCC1 SCC1
4.0
3.5
3.0
2.5
2.0
1.5
1.0
t(hr) 0
Bud Index
Pds1,scc1-73
scc1-73
Pds1
t (hr)
Binuclei
C
GAL1-TEV+
GAL1-PDS1 -mdb
150
120
90
75
60
45
30
15
t(m) 0
t/min 0 15 120 150
anti-Myc
anti-Clb2
GAL1-PDS1
-mdb-18MYC
GAL1-PDS1
-18MYC

I confirmed and extended this result using S-phase block with hydroxyurea, with the four combinations of presence or absence of *GAL1-PDS1-mdb* and *GAL1-TEV/SCC1-TEV*, all in the presence of wild-type endogenous *PDS1*. Because premature cohesin cleavage can activate the Mad2-dependent spindle checkpoint (Severin *et al.*, 2001), I carried out these experiments in a *mad2Δ* background. In this protocol I allow the endogenous Cdc20-dependent Clb degradation system to eliminate Clb-Cdk activity and endogenous Pds1. As previously reported (Cohen-Fix *et al.*, 1996), Pds1-mdb overexpression blocks mitotic progression, but when chromosome separation is allowed by using *GAL1-TEV/SCC1-TEV* I observed efficient ME, which occurred almost as rapidly as in the *GAL1-TEV/SCC1-TEV* strain lacking *GAL1-PDS1-mdb*, or the wild-type control (Figure 3.5A). The *GAL1-PDS1-mdb GAL1-TEV/SCC1-TEV* strain exhibited a delay of about 20 minutes judging from FACS and bud-count. This delay was consistent with the ME delay in FEAR network mutants (Stegmeier *et al.*, 2002), but much shorter than the >3-hour delay caused by *GAL1-PDS1-mdb* overexpression (Cohen-Fix *et al.*, 1996) (Figure 3.5A). Therefore most of the long delay caused by Esp1 inhibition by Pds1-mdb overexpression is due to failure of cohesin cleavage.

The temperature-sensitive *scc1-73* cohesin allele (Michaelis *et al.*, 1997) allows sister chromatid separation without Esp1 activity at restrictive temperature (Uhlmann *et al.*, 1999). I constructed *mad2Δ* strains that were *scc1-73* or *SCC1*, with or without *GAL1-PDS1-mdb*, synchronized cells in G1 with alpha factor, and expressed

GAL1-PDS1-mdb for one hour before release at 37°C (restrictive temperature for *scc1-73*). *SCC1 GAL1-PDS1-mdb* cells show a lengthy delay before ultimately undergoing aberrant ME with accumulation of aneuploid cells. (Eventual accumulation of aneuploid cells is a consequence of *GAL1-PDS1-mdb* expression at 37°C, where the G2 block is less stable than at 30°C. This may be due to lower expression of *GAL1-PDS1-mdb* at 37°C) (Figure 3.5B). In contrast, *scc1-73 GAL1-PDS1-mdb* cells had indistinguishable ME kinetics compared to *scc1-73* cells lacking *GAL1-PDS1-mdb*, and similar ME kinetics compared to *SCC1* cells lacking *GAL1-PDS1-mdb*. This result confirms that the *GAL1-PDS1-mdb* block to ME can be bypassed by cohesin inactivation. Overall, three independent experiments (Figure 3.5A-C) show that the Esp1 requirement for ME can be largely bypassed by complementing its proteolytic function in Scc1 inactivation. This idea is also suggested by the similar kinetics of ME in *cdc20*-blocked cells with *GAL1-SIC1-4A* and *GAL1-TEV* overexpression to the kinetics of ME upon direct release of the *cdc20* block (Figure 3.1B).

Stegmeier et al. (2002) carried out a similar experiment to the one in Figure 3.5B. Instead of inhibiting Esp1 with *GAL1-PDS1-mdb*, they used the *esp1-1* temperature-sensitive allele, and instead of *scc1-73*, they used the *mcd1-1* temperature-sensitive allele (*MCD1* is the standard name for the cohesin subunit also named *SCC1*). As in my experiment (Figure 3.5A), these strains (with the spindle checkpoint disabled by *MAD1* deletion) were released from an alpha-factor block at

non-permissive temperature. They observed a significant reduction in ME delay by inclusion of *mcd1-1* in the *esp1-1* background, which is qualitatively similar to my findings. Distinct from my findings, they observed that the *esp1-1 mcd1-1* strain exhibited a ~45 minutes delay in ME based on timing of mitotic cyclin (Clb2) degradation compared to the *ESP1 mcd1-1* strain, whereas I observed little delay in ME based on direct examination of cytokinesis comparing the *GAL1-PDS1-mdb* strains that were *SCC1-wt* or *scc1-73*. I do not know if the differences in results between my experiment and the results in Stegmeier et al. (2002) are due to differences between thermal inactivation of *mcd1-1* vs. *scc1-73*, to the use of *esp1-1* vs. *GAL1-PDS1-mdb* to inhibit Esp1 activity, or to the difference in assay for ME. Many previous experiments support the efficacy of *GAL1-PDS1-mdb* in full inhibition of Esp1 (Cohen-Fix et al., 1996; Queralt et al., 2006; Sullivan and Uhlmann, 2003), and the results in Figure 3.5B are consistent with the results in Figure 3.5A using *GAL1-TEV* rather than *scc1/mcd1* mutations to inactivate cohesin. In a recently published similar experiment (Visintin *et al.*, 2008), a *mad1Δ GAL-PDS1Δdb mcd1-1* strain exhibited a ME delay of 30 minutes or less. This result is qualitatively consistent with my observations in Figure 3.5A-B. Variable delays in ME could be due to different experimental systems or limited resolution.

Thus, I conclude that Esp1 is not required for ME in multiple experimental conditions, provided the requirement for cohesin cleavage is bypassed, although absence of Esp1 may cause a <30 min ME delay due to failure of FEAR network

activation. I propose that provided sufficient Clb-Cdk inactivation, the timing of ME is largely regulated by the spindle-positioning-checkpoint regulating MEN activation, as proposed by Bardin et al. (2000). Cohesin cleavage may be a requirement for efficient activation of the MEN by this mechanism, since anaphase spindle elongation requires cohesin cleavage, and anaphase efficiently drives one SPB into the bud.

Consistent with the hypothesis that allowing cohesin cleavage bypasses the Pds1-mdb block by allowing spindle elongation and consequent MEN activation, the *GAL1-PDS1-mdb* block to cytokinesis can be effectively bypassed by ectopic activation of the MEN by deletion of the MEN inhibitor *BUB2*; in the absence of chromosome separation (Queralt *et al.*, 2006); I have confirmed this result using HU block-release instead of *cdc20* block-release (Figure 3.6). I explore the connection between cohesin cleavage, spindle elongation and MEN activation further in the following sections.

Figure 3.6

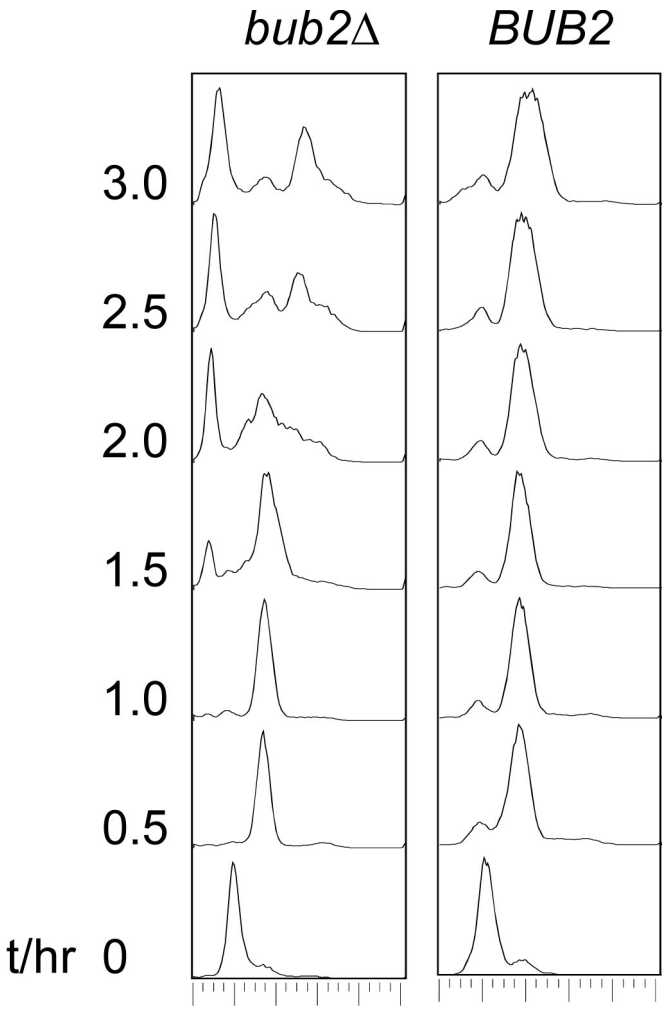

Figure 3.6. *GAL-PDS1-mdb bub2*Δ (YL0452) or *BUB2* (OCF1517.2) strains were arrested in raffinose medium containing hydroxyurea as described in Materials and Methods, and released into galactose media lacking hydroxyurea at 30º. DNA flow cytometry profiles are shown.

5. Direct block of Scc1 cleavage delays ME in cells with active Esp1.

The results above indicate that Esp1 contributes little to ME kinetics beyond its role in cohesin cleavage, leading to the conclusion that Esp1 is not necessary for quite efficient ME. A converse question, so far not addressed in my experiments, concerns the ability of Esp1 to drive ME in cells in which cohesin cleavage and sister chromatid separation fails – is Esp1 sufficient to drive ME without cohesin cleavage? This question has been examined previously with the use of the non-cleavable version of Scc1 expressed from the *GAL1* promoter (*GAL1-SCC1-RRDD*) (Uhlmann *et al.*, 1999). In these experiments, blocking sister chromatid separation does not block Esp1 activation, since endogenous Scc1 is cleaved on schedule even in the presence of ectopic Scc1-RRDD (Uhlmann *et al.*, 1999). Blocking sister separation with Scc1-RRDD in the presence of active Esp1 causes a delay in ME estimated between 20 to 60 minutes, depending on the assays for ME and/or on the exact experimental conditions (Stegmeier et al., 2002; Uhlmann et al., 2000). I examined this question using a different assay, by time-lapse microscopy of *GAL1-SCC1-RRDD* cells pregrown in raffinose (uninduced) and plated on galactose medium to induce *GAL1-SCC1-RRDD* expression. I observed a variable delay averaging ~1 hr between the first bud emergence (unaffected by *SCC1-RRDD* expression) and the second bud emergence, which requires prior ME, due to *SCC1-RRDD* expression (Table 3.1). I included a Myo1-GFP marker (Bi et al., 1998) to allow measurement of the time between budding and cytokinesis (determined by Myo1 ring

disappearance), and observed a delay of ~0.5 hr due to *SCC1-RRDD* expression. The difference in delay times between these two assays is interesting and suggests that even in cells that complete cytokinesis, defects due to failure of cohesin cleavage cause an additional ~0.5 hr delay in rebudding. Thus my results generally confirm the previous findings of a significant delay in ME solely due to failure of cohesin cleavage. An advantage of my assay is that it requires no previous synchronization of the cells, which avoids potential artifacts, and in addition allows determination of the variability among individual cells, which can give misleading results in population studies. Further, the method allows me to observe events preceding ME. Using cells labeled with GFP-tubulin and blocked in metaphase by Scc1-RRDD, I observed rapid spindle oscillations, which pushed one SPB back and forth between daughter and mother cells (Palmer *et al.*, 1989). This oscillatory movement could potentially activate the MEN by allowing one SPB to contact Lte1 near the bud cortex (Bardin *et al.*, 2000). This makes a complete assessment of Esp1's contribution to ME in this experimental context difficult, since the spindle oscillations might activate the MEN without any Esp1 activity. This difficulty was circumvented in the next section by using nocodazole to depolymerize the spindle.

Table 3.1. **Mitotic exit delay caused by noncleavable cohesin.** Strain *GAL-SCC1-RRDD TUB1-GFP MYO1-GFP* (YL066) was pre-grown in Raffinose medium, plated on galactose medium, and subjected to time-lapse analysis at 30°C or 37°C as described in materials and methods. Cells that were unbudded at the time of plating were timed for both the interval from first budding to first cytokinesis (Myo1-GFP ring contraction and disappearance), and from first budding to the second budding. For comparison to other published data, we also carried this experiment out at 37°C; at this temperature, high fluorescent background prevented reliable assignment of time of cytokinesis, so only bud-to-bud times were assayed for initially unbudded cells. Cells were classified according to whether the short spindle ended in the mother (Mo.) or the daughter cell (Da.). (At 30°C, almost 100% initially unbudded cells showed defective division, in which the spindle did not elongate but ended up intact in mother or daughter, in the first cell cycle. At 37°C, 35% initially unbudded cells elongated the spindle in spite of galactose addition, suggesting inefficient expression of *GAL1-SCC1-RRDD* at 37°C. Because we are tracking individual cells through time, we can exclude such cells from the analysis.) A *MYO1-GFP TUB1-GFP* strain lacking *GAL1-SCC1-RRDD* (BD78-2C) was treated in parallel as a control, pooling bud-to-bud data for mothers and daughters. All numbers are in min +/- standard deviation. The average differences (Δ) from wild-type are shown, and the P-value for these differences (by t-test). The numbers of cells (n) examined in each condition are shown in the last column.

Table 3.1

30°C		Myo1-GFP appearance to disappearance (min)	P-Value rel. to WT	Bud to rebud (min)	P-Value rel. to WT	n
WT		75±14		110±29		18
SCC1-RRDD	Mo.	102±20 (Δ 27 min)	$5x10^{-3}$	169±60 (Δ 59 min)	$1x10^{-2}$	11
	Da.	112±21 (Δ 37 min)	$1x10^{-4}$	228±59 (Δ 118 min)	$1x10^{-5}$	19
37°C						
WT		ND		102±8		12
SCC1-RRDD	Mo.	ND		153±28 (Δ 51 min)	$1x10^{-4}$	9
	Da.	ND		189±99 (Δ 87 min)	$1x10^{-2}$	12

In any case, based on my and others' results with *GAL1-SCC1-RRDD*, it is clear that blocking cohesin cleavage while allowing Esp1 activity causes a substantial delay in ME. In turn, this suggests that the kinetics of ME in the wild-type cell cycle are driven by cohesin cleavage, since the time from cohesin cleavage to ME in wild-type cells is only ~15-20 minutes (Stegmeier *et al.*, 2002), shorter than my estimate of the time required for ME in the presence of active Esp1, but without cohesin cleavage.

6. Mitotic exit promoted by Esp1 over-expression depends on spindle elongation and MEN activation

Esp1 over-expression, but not TEV-induced spindle elongation, was shown to drive ME in *cdc20*-depleted cells, without a requirement for Esp1 proteolytic activity (Queralt et al., 2006; Sullivan and Uhlmann, 2003). I have confirmed the finding that Esp1 overexpression drives ME in *cdc20*-depleted cells, even using the attenuated *GALS* promoter driving *ESP1* instead of 6 copies of *GAL1-ESP1* (Queralt et al., 2006; Sullivan and Uhlmann, 2003). Expression of *GALS-ESP1* still constitutes an approximately 30-fold overexpression based on comparison of accumulation of Myc-tagged Esp1 from the *GALS* vs. the endogenous promoter (data not shown). It is also an effective overexpressor based on rescue of *PDS1-mdb* lethality; see above. For most purposes I prefer the *GALS-ESP1* construct because it allows viability, unlike 6x*GAL1-ESP1*. I found efficient induction of ME by *GALS-ESP1*, with all markers of ME (cytokinesis, rebudding, Clb2 degradation and DNA replication in the next cell cycle) occurring promptly upon *GALS-ESP1* induction (Figure 3.7A). This Esp1-induced ME was much more efficient than that described previously (Sullivan and Uhlmann, 2003). This is likely a consequence of performing the experiment a. 30° rather than at 23°. *6X GAL1-ESP1* also drove much more efficient ME at 30° than at 23° (Figure 3.8D).

Thus, I confirm the previous finding (Sullivan and Uhlmann, 2003) that

overexpressed Esp1 drives ME in *cdc20*-blocked cells. To further analyze this response, I tested if overexpressed Esp1 could drive ME in the presence of nocodazole to depolymerize the spindle. Inclusion of nocodazole blocked ME in all aspects I have tested for at least 3 hours (Figure 3.7A). Thus, overexpressed Esp1 may not be intrinsically sufficient to drive ME in *cdc20*-depleted cells. This ability of Esp1 may rely on spindle elongation consequent to cohesin cleavage by the proteolytic function of Esp1. In these experiments I primarily used strains containing a *CDC14* allele endogenously tagged with YFP, in order to follow Cdc14 trafficking in later analysis (see below). This *CDC14-YFP* was previously shown to fully complement, and to be competent for FEAR- and MEN-induced nucleolar exit (Pereira et al., 2002). I also have confirmed key results in isogenic strains with untagged *CDC14* (Figure 3.8A). The involvement of the spindle integrity checkpoint surveillance system in this result seemed unlikely since the experiment was performed in a *cdc20*-depleted background, removing the target of the checkpoint (Hwang et al., 1998; Kim et al., 1998). In addition, I have performed the same experiment in the absence of the essential spindle checkpoint component Mad2, with identical results (Figure 3.8B).

Spindle elongation could promote ME by driving the daughter spindle pole into contact with the bud cortex, activating the MEN (Bardin et al., 2000; Stegmeier and Amon, 2004; Yeh et al., 1995). To test this, I inhibited MEN activation with a temperature-sensitive *cdc15-2* mutation (Cdc15 is an essential MEN component).

cdc15-2 completely inhibits *GALS-ESP1*-induced ME at 35.5°C (Figure 3.7B).

Thus, promotion of ME by Esp1 overexpression in *cdc20*-blocked cells requires both an intact and a functional MEN, even if Clb-Cdk inhibition is provided ectopically. I hypothesize that the requirement for spindle integrity for Esp1 promotion of ME arises because Esp1-mediated cohesin cleavage allows spindle elongation, promoting effective contact between the daughter SPB and the bud cortex and thereby promoting MEN activation (Bardin et al., 2000; Yeh et al., 1995).

Figure 3.7. **Mitotic exit promoted by Esp1 overexpression depends on an intact spindle and MEN activation.** **A**. A *MET3-CDC20 GALS-ESP1* strain (YL1361) was arrested by Cdc20 depletion, as in Fig. 3.1. Esp1 was expressed from the *GALS* promoter at time zero by adding galactose (G) in the absence or presence of nocodazole + benomyl (NOC) (methionine was kept in the medium throughout to maintain Cdc20 depletion). DNA flow cytometry and protein samples were taken. Microscopic examination allowed quantification of the following phenotypes: Black: large budded mononucleate cell. Red: large budded binucleate cell. Green: rebudded cell without cytokinesis. Blue: unbudded or small budded cell. (lower right). Squares: without nocodazole; circles: with nocodazole. Western blotting was used to assess the level of Clb2 (amido-black staining of the gels showed equal loading of all lanes [data not shown]). **B**. *MET3-CDC20 GALS-ESP1* strains, either *CDC15* (YL1361) or *cdc15-2* (YL1362) were treated and analyzed as in (A), except that the cultures were maintained at 35.5°C to inactivate *cdc15-2*. Squares: *CDC15-wt*; circles: *cdc15-2*. Nonspecific band "*" was used as a loading control.

Figure 3.7

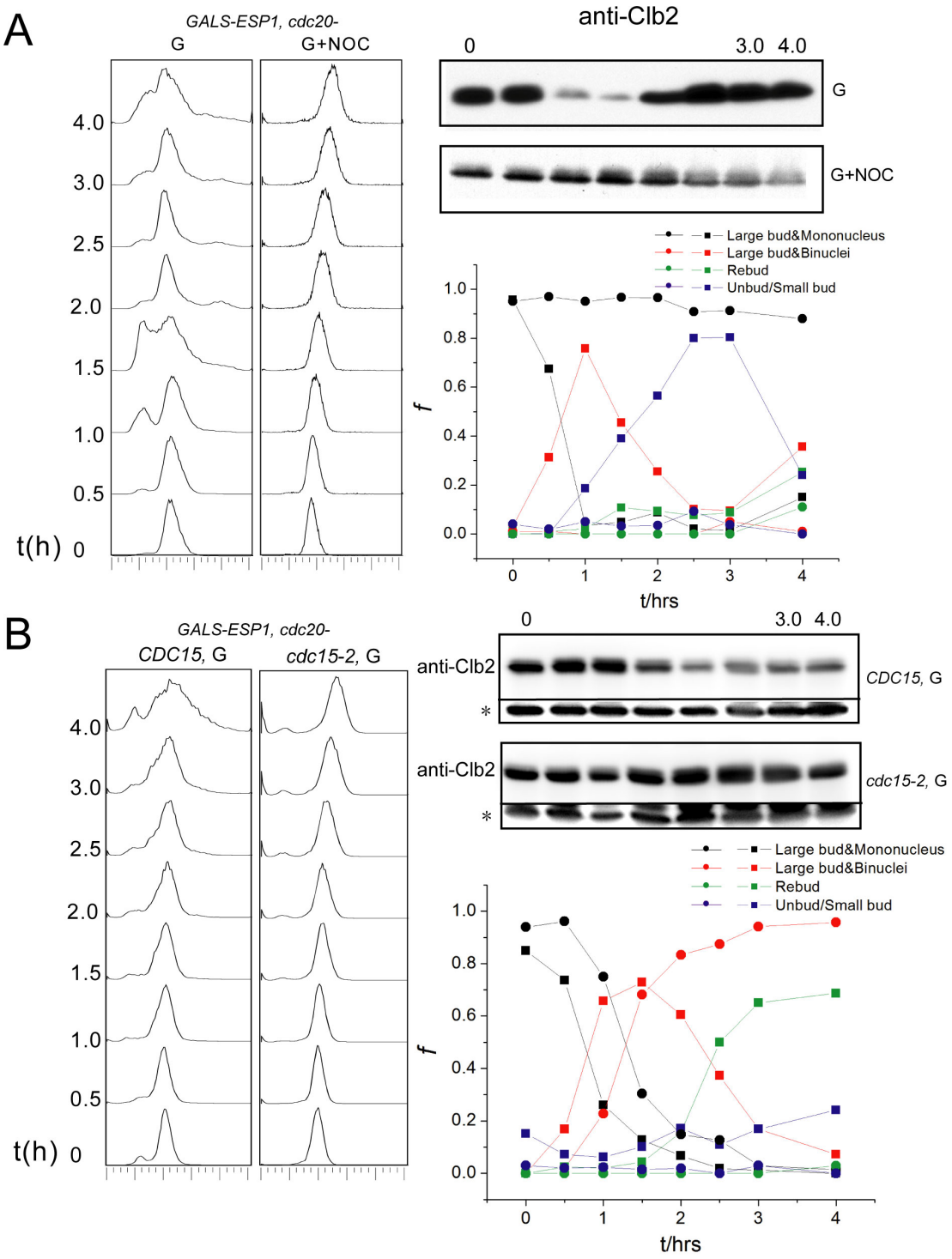
A
GALS-ESP1, cdc20-
G
G+NOC
4.0
3.0
2.5
2.0
1.5
1.0
0.5
t(h) 0
anti-Clb2
0
3.0 4.0
G
G+NOC
Large bud&Mononucleus
Large bud&Binuclei
Rebud
Unbud/Small bud
f
t/hrs
B
GALS-ESP1, cdc20-
CDC15, G
cdc15-2, G
anti-Clb2
CDC15, G
cdc15-2, G
*

Deletion of *CLB5* may lower the threshold of Cdc14 activity required for triggering ME, since it rescues viability of *cdc20 pds1* cells (Shirayama et al., 1999; Sullivan and Uhlmann, 2003). Thus, *CLB5* deletion might sensitize detection of an ability of Esp1 to drive ME, even without an intact spindle. However, the result in Figure 3.7A is robust to deletion of *CLB5*, implying that spindle function is strongly required for *GALS-ESP1*-induced ME (Figure 3.8C).

As shown in Figure 3.1, partial ME is obtainable with complete Clb-Cdk inhibition driven by *GAL1-SIC1-4A*, and ME becomes more efficient with concurrent expression of *GAL1-TEV* to provide cohesin cleavage. I examined the ability of *GALS-ESP1* to substitute for *GAL1-TEV* in this protocol, by a factorial experiment combining the presence or absence of *GALS-ESP1* and of nocodazole, all in the presence of *GAL-SIC1-4A*. *GALS-ESP1* promoted strong ME only in the absence of nocodazole. In the presence of nocodazole, I observed the partial ME attributable to *GAL1-SIC1-4A* (Figure 3.1B), independent of the presence or absence of *GALS-ESP1* (Figure 3.9). Thus, even with complete Clb-Cdk inhibition, I detect no ME-promoting activity of Esp1 in the presence of nocodazole.

Figure 3.8. **A**. *MET-CDC20 GALS-ESP1* (YL121) strain was arrested in Raffinose plus methionine, then experiments were performed as described in Fig. 3.7A. Results of DNA flow cytometry analysis and Clb2 western blot are shown. Even loading of samples were shown by amido-black staining (data not shown). **B**. A *MET-CDC20 mad2*Δ *GALS-ESP1* (YL169) strain was arrested by incubation in raffinose+methionine medium to deplete Cdc20. Galactose or Galactose+nocodazole+benomyl was added at time zero, keeping methionine present to maintain the cdc20 block. DNA flow cytometry and Clb2 western blot were performed as described in Materials and Methods. Pgk1 was employed as a loading control. **C**. Nocodazole inhibited ME caused by Esp1 overexpression in the absence of Clb5. *MET-CDC20 clb5*Δ *GALS-ESP1* (YL134) was arrested by incubation in raffinose+methionine medium to deplete Cdc20. Galactose or Galactose + nocodazole + benomyl was added at time zero, keeping methionine present to maintain the cdc20-block. DNA flow cytometry and Western blot analysis were done as described in Materials and Methods. Samples were evenly loaded as shown by Amido-Black staining of the membrane after protein transfer (data not shown). The lower right panel shows the fraction of large budded cells. **D**. Esp1 overexpression induced more efficient ME at 30˚. *MET-CDC20 6xGAL-ESP1* (strain 393, from F. Uhlmann) was arrested by incubation in raffinose+methionine medium to deplete Cdc20. Galactose was added at time zero, keeping methionine present to maintain the cdc20- block, at either 23˚ or 30˚. Results of DNA flow cytometry analysis are shown.

Figure 3.8

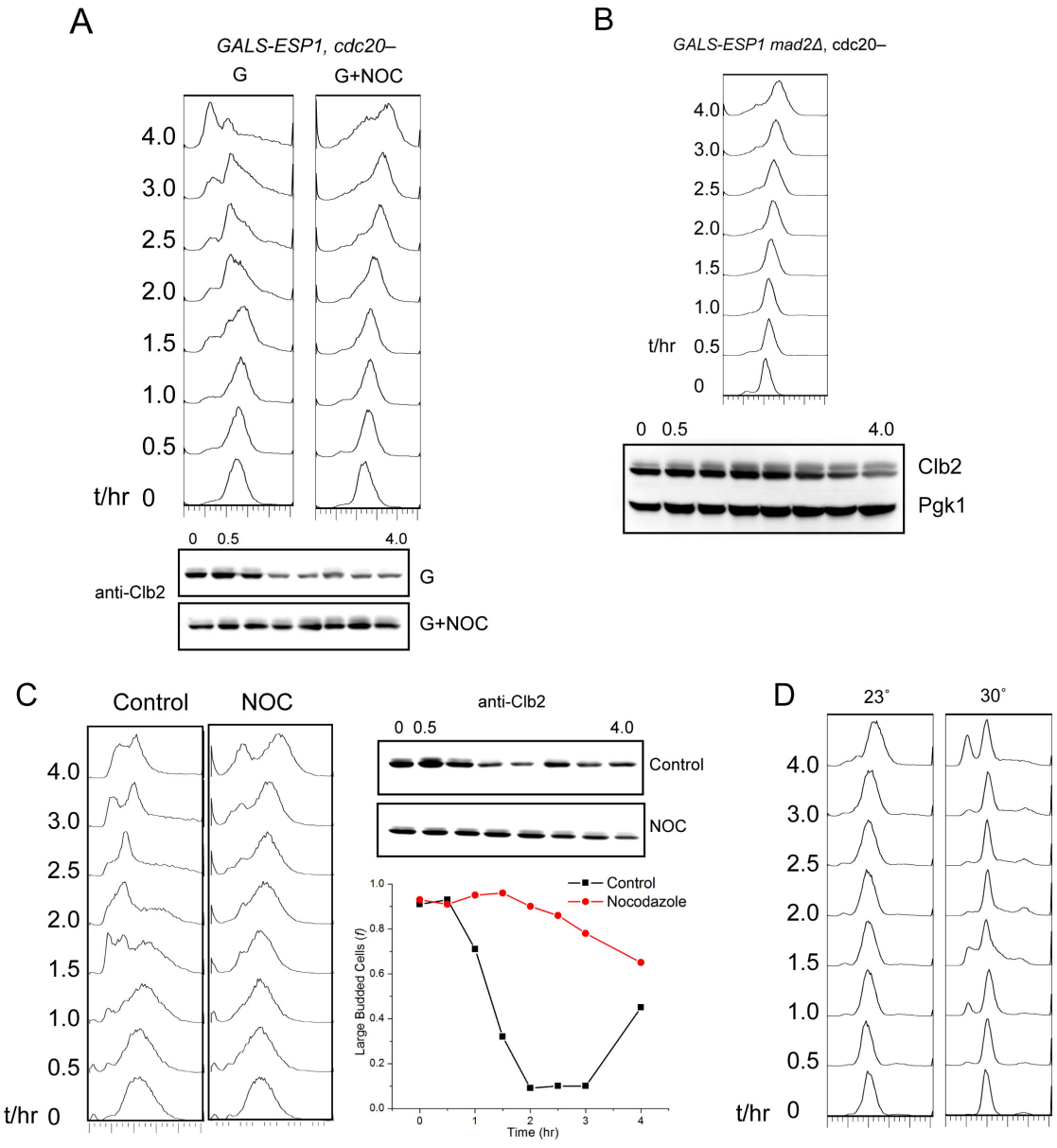
A
GALS-ESP1, cdc20–
G
G+NOC
4.0
3.0
2.5
2.0
1.5
1.0
0.5
t/hr 0
0 0.5 4.0
anti-Clb2
G
G+NOC
B
GALS-ESP1 mad2Δ, cdc20–
4.0
3.0
2.5
2.0
1.5
1.0
t/hr 0.5
0
0 0.5 4.0
Clb2
Pgk1
C
Control
NOC
4.0
3.0
2.5
2.0
1.5
1.0
0.5
t/hr 0
anti-Clb2
0 0.5 4.0
Control
NOC
Control
Nocodazole
Large Budded Cells (f)
Time (hr)
D
23˚
30˚
4.0
3.0
2.5
2.0
1.5
1.0
0.5
t/hr 0

Figure 3.9

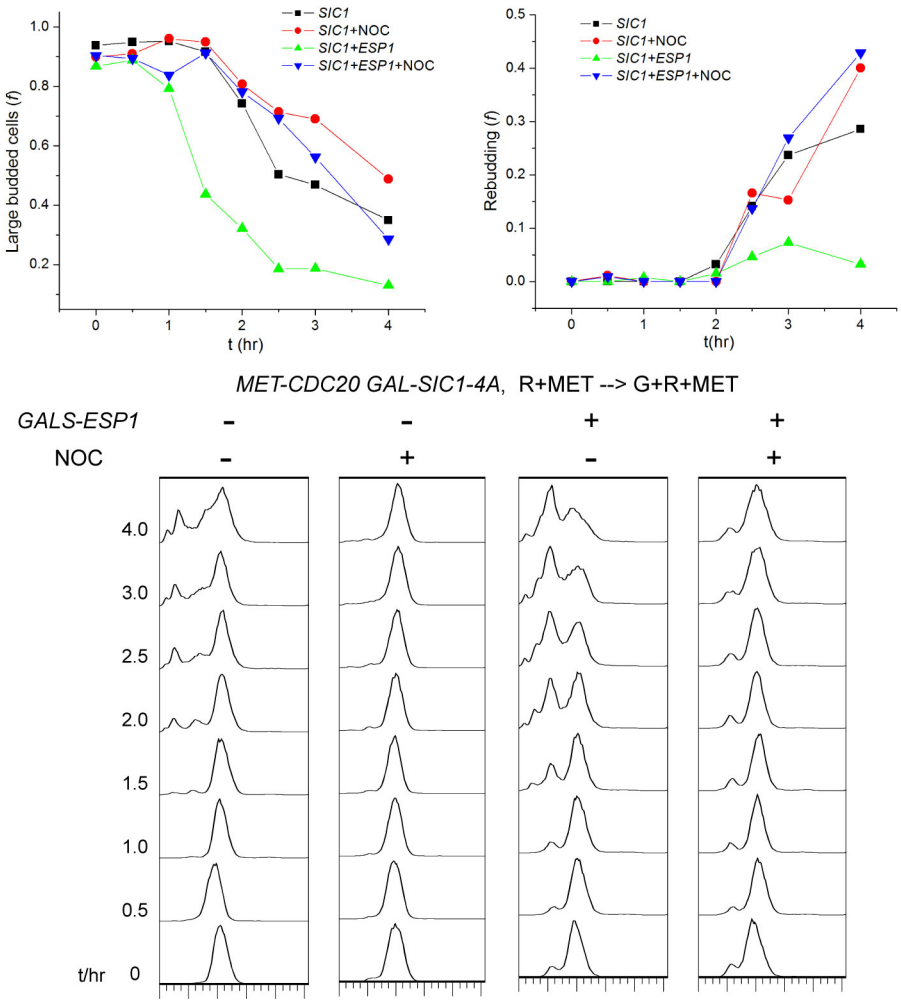

Figure 3.9. *MET-CDC20 GAL-SIC1-4A* strains, with (YL1721) or without (YL1722) *GALS-ESP1* were arrested by incubation in raffinose+methionine medium to deplete Cdc20. Galactose or Galactose+nocodazole+benomyl was added at time zero, keeping methionine present to maintain the cdc20 block. This experiment was carried out at 23º. Upper panels show the fraction of large budded cells (without rebudding) (left) and the fraction of rebudded cells, i.e. large-budded cells with extra small buds attached (right). Note that these graphs exclude cells produced by normal mitotic exit, which are not large-budded and are either unbudded, or contain a small bud. Lower panels show the results of DNA flow cytometry analysis.

7. Quantitative measurement of Esp1-induced Cdc14 release and activity

The ability of overexpressed Esp1 to promote ME was attributed to its ability to promote MEN-independent Cdc14 release from the nucleolus (Sullivan and Uhlmann, 2003). It is well established that the activity of Cdc14 is regulated by its localization in the nucleolus, where it is stably bound to its inhibitor Net1 and also sequestered from many potential dephosphorylation targets. The MEN is known to drive efficient release of Cdc14 from the nucleolus. (Shou et al., 1999; Visintin et al., 1999). It is important to note that the release status of Cdc14 is not all-or-none. The terms "partial release" and "full release" have been introduced to qualitatively describe Cdc14 localization (Stegmeier et al., 2002). Here, I use 2-color imaging with Cdc14-YFP and Net1-CFP (Pereira et al., 2002) and define a parameter "r" for any individual cell based on quantitative fluorescence microscopy.

$$r = \frac{\text{the mean intensity of 5\% brightest YFP pixels - the mean intensity of 5\% dimmest YFP pixels}}{\text{the mean intensity of 5\% brightest CFP pixels - the mean intensity of 5\% dimmest CFP pixels}}$$

This value will be high when Cdc14-YFP and Net1-CFP are colocalized, and low when Cdc14-YFP is significantly more dispersed than Net1-CFP (which is thought to remain nucleolar throughout the cell cycle). Thus, a lower r value should indicate higher Cdc14 release from Net1, and consequently increased Cdc14 activity. To establish the validity of this approach, I measured r throughout a *cdc20* block-release

experiment. At 30 minutes post release, cells with low r values appear exclusively in the anaphase subpopulation. 10 minutes later, Cdc14-YFP is resequestered into the nucleolus as the low-r fraction diminishes (Figure 3.10A). Thus, the r statistic clearly reflects the known dynamic localization behavior of Cdc14. (It is notable in these images that I essentially never observe complete absence of Cdc14 from the nucleolus; corresponding to this, the r value is never below ~0.3 in this experiment, where a value of 0 would correspond to uniform spreading of Cdc14 through the cell.)

Figure 3.10. **Quantitative measurement of Cdc14 release**. **A**. A *MET3-CDC20 CDC14-YFP NET1-CFP* strain (YL1452) was arrested in metaphase by incubation in +Met medium, and released at time zero by removal of Met. The "r" value (characterizing the degree of cellular dispersion of Cdc14 relative to Net1) for cells at various time-points was determined as described in Materials and Methods. Yellow curve: r value distribution in anaphase subpopulation. Green curve: r value distribution in unbudded/small-budded/rebudded cells. Red curve: r distribution in metaphase subpopulation. X axis is the r value; Y axis is frequency. The red, green and yellow distributions sum to the total histogram of r values (bars). Arrowhead on the picture highlights the bud-neck localization of Cdc14-YFP at ME. White numbers indicate r values for specific representative cells. Scale bar: 10 microns. In this and all the following experiments involving r value measurement, at least 50 cells were used to generate the distribution for each category at each time point. **B**. A *MET3-CDC20 6xGAL1-ESP1* strain (YL1451) was arrested in metaphase by incubation in +Met medium. Galactose (G) or Raffinose (R) were added at time zero in the presence (+NOC) or absence (-NOC) of nocodazole + benomyl (methionine was kept in the medium throughout to maintain Cdc20 depletion). At the indicated times, r values were determined as in A.

Figure 3.10

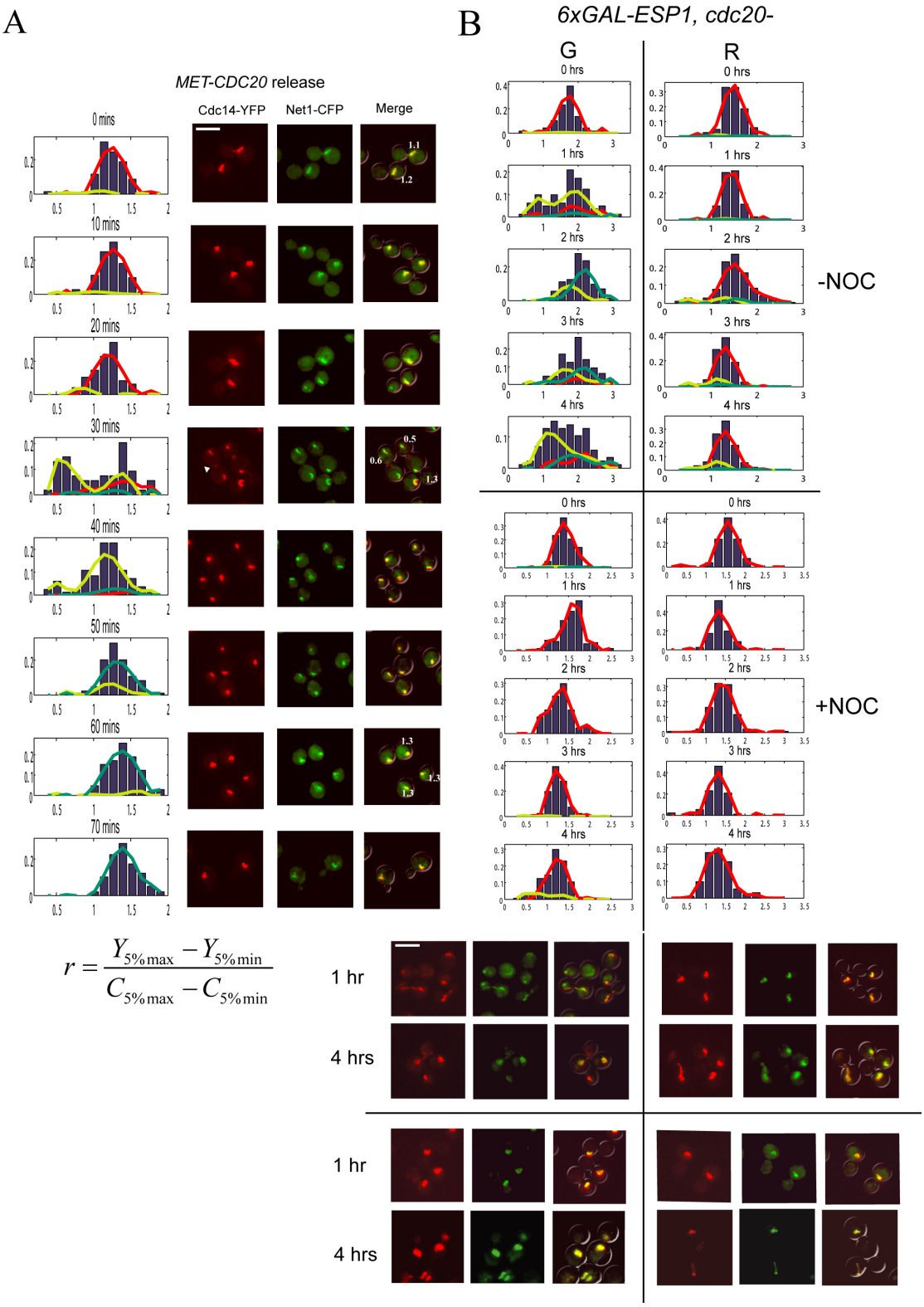

$$r = \frac{Y_{5\%\max} - Y_{5\%\min}}{C_{5\%\max} - C_{5\%\min}}$$

I then examined the ability of overexpressed Esp1 to drive Cdc14 release from the nucleolus in *cdc20*-blocked cells, with or without spindle depolymerization induced by nocodazole. In these experiments, I used *6xGAL1-ESP1* (Sullivan and Uhlmann, 2003) instead of *GALS-ESP1* because the higher overexpression produced a stronger and more synchronous phenotype. (Qualitatively similar results were also obtained with *GALS-ESP1*). I observe Cdc14 release (low r value cells) in Esp1-overexpressing cells undergoing spindle elongation and anaphase; strikingly, addition of nocodazole blocked Cdc14 release measured by this assay (Figure 3.10B)

I have quantified Cdc14 release in *CDC15* or *cdc15-2* cells, both *MET3-CDC20*, released from a *cdc20* block at 37° to inactivate *cdc15-2*. Upon release, r shifted strongly and transiently to a low value 20 minutes after release in the *CDC15* control. In contrast, I observed only a slight decrease in r in the *cdc15-2* cells; this decrease was maximal at 20 minutes after release. Some Cdc14-YFP speckles outside the nucleolus are observed in *cdc15-2* cells, but are largely absent in the CDC15-wt control (Figure 3.11); I do not know what these signify. Any MEN-independent Cdc14 release is apparently described by the small but reproducible decrease in r at 20 minutes after release, and the occurrence of the Cdc14-YFP speckles. Thus, Cdc14 release driven by the MEN is qualitatively and quantitatively stronger in my experiments than MEN-independent release.

Figure 3.11. (Left). *MET-CDC20 CDC14-YFP NET1-CFP* strains, either *CDC15* (YL1361) or *cdc15-2* (YL1362) were arrested in metaphase by incubation in methionine-containing medium to deplete Cdc20, then released into methionine-free media at 37° to inactivate cdc15-2. Samples were taken every 10 minutes, the cells were briefly fixed and quantitative fluorescence microscopy (see Materials and Methods) was used to calculate the r value for individual cells. The colored lines represent histograms of cells at each r value, with the morphology indicated in the cartoons below, based on Net1-CFP staining. The bars represent the complete histogram of r values (sum of the colored lines). Right: Sample pictures at indicated time points. Scale bar:10 μm. Images are linearly contrast-enhanced for better visualization.

Figure 3.11

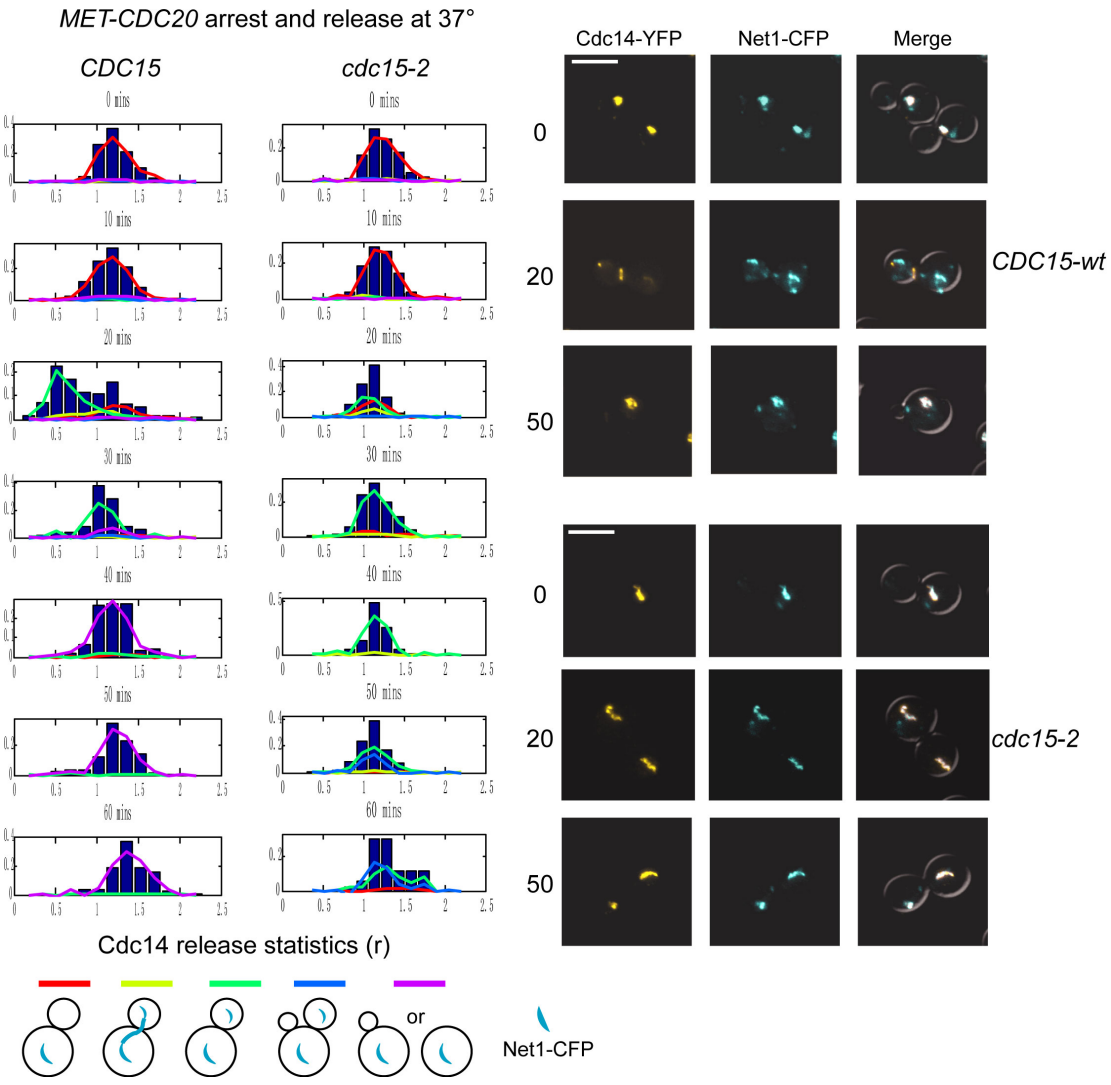
MET-CDC20 arrest and release at 37°
CDC15
cdc15-2
0 mins
10 mins
20 mins
30 mins
40 mins
50 mins
60 mins
Cdc14-YFP
Net1-CFP
Merge
0
20
50
CDC15-wt
cdc15-2
Cdc14 release statistics (r)
or
Net1-CFP

I conclude that separase Esp1 promotes ME in *cdc20*-blocked cells primarily via cohesin cleavage and consequent spindle elongation, rather than by a cohesin-cleavage-independent function of Esp1. The experiments described above implicate MEN activation as the proximal target of spindle elongation, resulting in effective Cdc14 release to drive ME.

A high level of CDK activity was shown to induce Cdc15 phosphorylation and lower Dbf2 kinase activity, and these reactions could have the potential to impair Cdc14 release (Jaspersen and Morgan, 2000; Menssen et al., 2001; Stegmeier et al., 2002). I were concerned, therefore, that my experimental manipulation of blocking Cdk inactivation was not truly independent of promotion or prevention of Cdc14 release. To investigate this, I quantified the release kinetics of Cdc14 in the presence of undegradable Clb2 (Clb2-kd, lacking the KEN boxes and destruction box. *CLB2-kd* at its endogenous locus is lethal, but can be rescued by Sic1 overexpression from the *GAL1* promoter (Wasch and Cross, 2002); *GAL1-SIC1* turnoff in this strain results in a block to ME (Wasch and Cross, 2002)). I synchronized a *GAL1-SIC1 CLB2-kd CDC14-YFP NET1-CFP MYO1-mCherry* strain in G1 with alpha factor, and released into glucose to shut off Sic1 expression, or into galactose as a control. Cell-cycle progression was monitored by budding, Myo1-mCherry to mark the bud neck and cytokinesis (Bi et al., 1998) and the separation of the Net1-CFP signal across the bud neck was monitored to assay anaphase. Clb2kd cells arrest in telophase as described (Wasch and Cross, 2002), but Cdc14 release was very efficient,

essentially coincident with anaphase and then persisting for about 30 minutes (Figure 3.12A). This result essentially confirms a previous finding of Cdc14 release in the presence of undegradable Clb2 (Stegmeier et al., 2002), obtained using *CLB2-db* overexpression from the *GAL1* promoter.

Figure 3.12

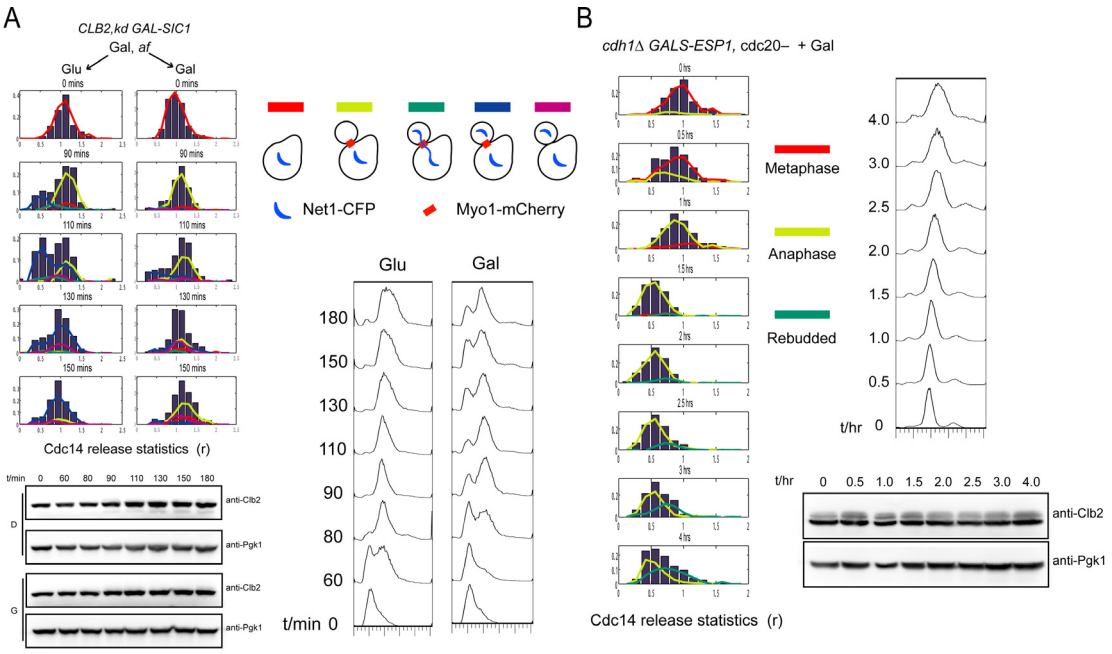

Figure 3.12. **Cdc14 release occurs despite persistent endogenous Clb-Cdk activity.** **A**: Strain *CLB2,kd GAL1-SIC1 CDC14-YFP NET1-CFP MYO1-mCherry* (ALG611) was arrested in alpha factor in galactose media, then released into either glucose to turn off *GAL1-SIC1* (Glu) or galactose media (Gal) to keep *GAL1-SIC1* on. Cdc14 localization was quantified as in Fig. 3.10. DNA flow cytometry, Clb2 western blot and r value test were performed as described in Materials and Methods. The inset cartoon shows the cell morphology of each category. **B**. *MET3-CDC20 cdh1Δ GALS-ESP1* (YL165) cells were first arrested in metaphase by incubation in raffinose plus methionine medium, then galactose plus methionine was added to induce Esp1 overexpression at time zero. DNA flow cytometry, Clb2 western blot and r value test were performed as described in Materials and Methods.

In a different experimental approach to the same question, I assayed *GALS-ESP1* induction of ME in *cdc20*-blocked cells (as in Figure 3.7A), in the absence of *CDH1*. These cells lack any factor to activate the APC for Clb degradation, since at least one of either Cdc20 or Cdh1 is required for Clb degradation (Wasch and Cross, 2002). Unlike *CDH1* controls (Figure 3.7A), the *cdh1* cells maintained a stable telophase block without any evidence of ME in this protocol, for up to four hours (when some degree of rebudding occurs). Despite this stable block, very efficient Cdc14 release was observed throughout this period (Figure 3.12B).

These results show that stabilized Clb cyclins cannot block Cdc14 release when expressed at endogenous levels. Therefore spindle elongation is likely to be the primary mechanism driving full Cdc14 release, rather than a separase-dependent but cohesin cleavage-independent mechanism, such as a Cdc14-Cdc15 positive feedback triggered by Esp1 (Queralt et al., 2006).

The experiments in Figures 3.7 and 3.12 allow me to propose a model for induction of ME by *ESP1* overexpression in *cdc20*-blocked cells: the overexpressed Esp1 cleaves cohesin and allows spindle elongation, prompting MEN activation when the daughter spindle pole reaches the bud cortex (Bardin et al., 2000; Yeh et al., 1995). MEN activation promotes Cdc14 release, which can activate Cdh1 by dephosphorylation (Zachariae et al., 1998), leading to Clb degradation. My results with nocodazole, *cdc15-2*, and *cdh1* suggest that all of these steps are required for

overexpressed Esp1 to induce effective ME.

8. Mitotic exit network controls Cdc14 nuclear export

Net1 sequestration in the nucleolus is the only characterized mechanism for regulation of Cdc14 activity; hence *net1* deletion would be expected to completely relieve any MEN-dependent regulation of Cdc14. However, I were surprised to find that in *net1Δ* cells, Cdc14-YFP localization is still cell-cycle regulated, being concentrated in the nucleus for most of the cell cycle, but spread throughout the cell transiently at ME (Figure 3.13B).

Figure 3.13. **Mitotic Exit Network controls Cdc14 nuclear export.** **A**. WT and *net1Δ* cells containing *CDC14-YFP* (YL1701) were briefly fixed and stained with DAPI to label DNA (top); *net1 CDC14-YFP* strains containing *NOP1-dsRed* (YL1702) or *dsRed-NLS* (YL174) were examined separately. **B**. Selected frames of a time-lapse movie (Bean *et al.*, 2006) with indicated strain genotypes. In *net1Δ CDC14-YFP* (YL1701) cells, Cdc14-YFP was transiently excluded from the nucleus approximately at the time of ME. This transient nuclear exclusion was not observed in *net1Δ CDC14-YFP cdc15-2* (YL161) cells at 37°C. **C**. The percentage of cell cycles, tracked using fluorescent time-lapse microscopy, in the course of which Cdc14-YFP release from nucleus was observed. 50 cell cycles were examined in each condition. **D**. Quantification of Cdc14 release from nucleus in a *net1Δ* background. The coefficient of variation (CV) of Cdc14-YFP signal inside a single cell, computed from fluorescent time-lapse microscopy data, is the standard deviation of YFP pixel intensity across the cell, divided by the mean intensity; this number will be high in cells with Cdc14-YFP concentrated in specific regions, and low when Cdc14-YFP is dispersed through the cell. Four examples of *CDC15-wt* (blue) and *cdc15-2* (red) cells, both at 37°, are shown. Curves are aligned by nuclear division as judged by initial stretching of the Cdc14-YFP signal across the bud neck, at t=0. Color bars indicate rebudding in the next G1.

Figure 3.13

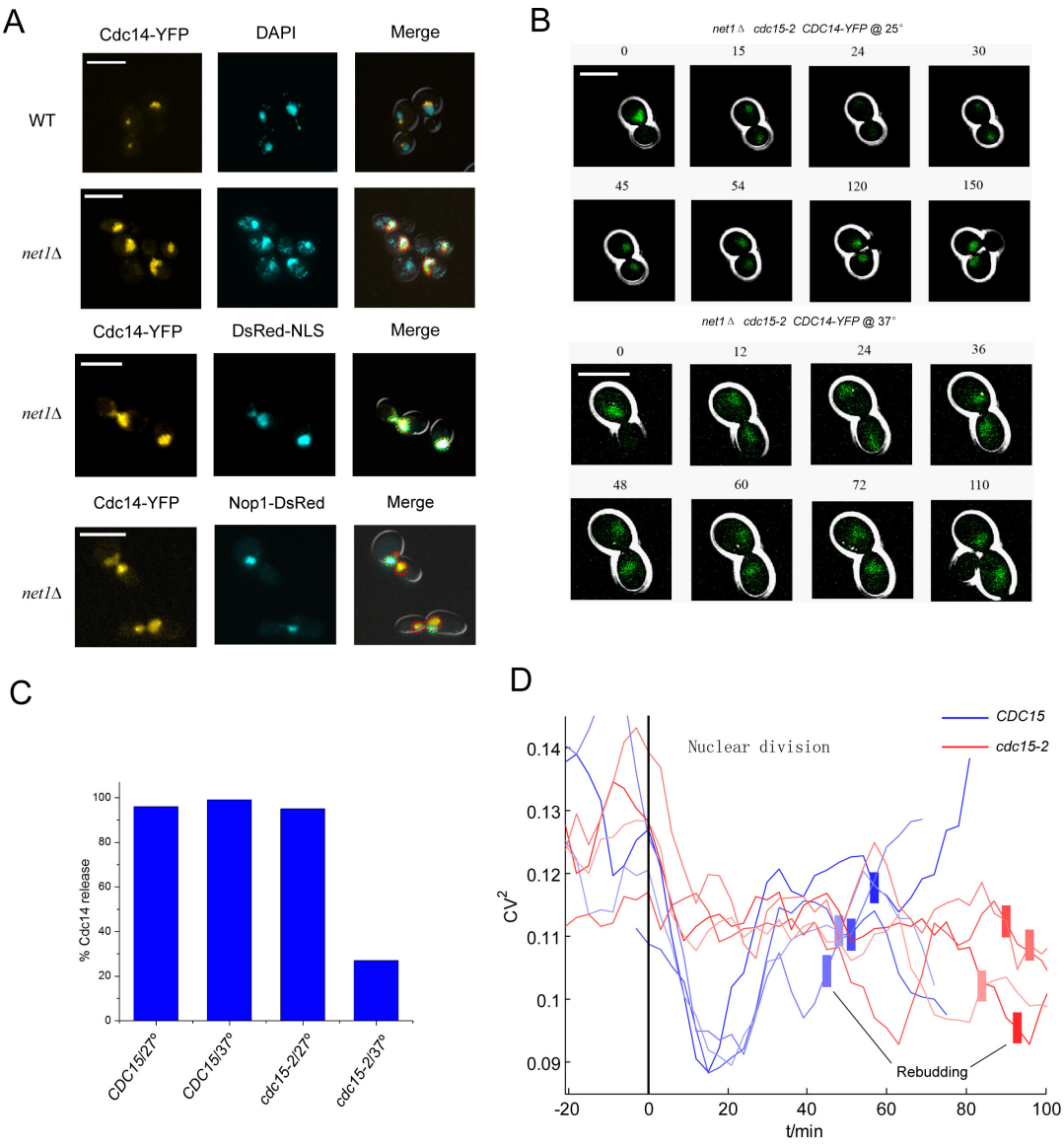
A
Cdc14-YFP
DAPI
Merge
WT
net1Δ
Cdc14-YFP
DsRed-NLS
Merge
net1Δ
Cdc14-YFP
Nop1-DsRed
Merge
net1Δ
B
net1Δ cdc15-2 CDC14-YFP @ 25°
0
15
24
30
45
54
120
150
net1Δ cdc15-2 CDC14-YFP @ 37°
0
12
24
36
48
60
72
110
C
% Cdc14 release
100
80
60
40
20
0
CDC15/27°
CDC15/37°
cdc15-2/27°
cdc15-2/37°
D
CDC15
cdc15-2
Nuclear division
Rebudding
CV2
0.14
0.13
0.12
0.11
0.1
0.09
-20
0
20
40
60
80
100
t/min

To examine the possibility that this result is due to residual binding of Cdc14 to other nucleolar components, I examined colocalization of Cdc14-YFP with DNA, with the nucleolar marker Nop1-dsRed (Gadal et al., 2001), and with a general marker of nuclear volume, dsRed-NLS (Rodrigues et al., 2001). In *NET1* cells, Cdc14 is in a typical crescent-shaped nucleolar distribution flanking the bulk of nuclear DNA, while in *net1* cells, Cdc14-YFP staining is enlarged to contain the DNA signal. In *net1* cells, Cdc14-YFP is localized much more broadly than the Nop1-DsRed nucleolar marker, but is coincident with the dsRed-NLS marker for the nuclear interior. Thus, in *net1* cells, Cdc14 is not retained in the nucleolus but is nevertheless restricted to the nucleus (Figure 3.13A), through most of the cell cycle.

I used time-lapse fluorescence microscopy to study whether the MEN is responsible for Cdc14 nuclear export in the absence of Net1. When the MEN is inactivated at restrictive temperature in a *cdc15-2 net1Δ* strain, Cdc14-YFP remains concentrated in the nucleus throughout the cell cycle, in contrast to *CDC15 net1Δ* cells with an intact MEN (Figure 3.13B,C). (Note that the *net1* deletion bypasses the *cdc15* block to telophase exit, as expected (Shou et al., 1999)). The Cdc14 nuclear export phenotype can be quantified using time-lapse microscopy to calculate the dispersion of Cdc14-YFP signal inside individual cells. A decrease of CV (Coefficient of Variation) corresponds to Cdc14 nuclear export (because Cdc14 is no longer concentrated, therefore the signal across the cell is less variable). A drop in the CV for Cdc14-YFP is clearly detected in *CDC15* cells at low and high temperatures,

but absent in *cdc15-2* cells specifically at 37° (Figure 3.13D). CDK activity by itself is unlikely to control Cdc14 export, since the timing of Clb2 degradation in *cdc15-2 net1Δ* is almost identical to *CDC15 net1Δ* (Figure 3.14) as expected (Shou et al., 1999). Cdc14 nuclear export is probably not directly driven by Esp1 activity, because the timing of this Cdc14 nuclear export correlates with ME rather than anaphase (which is directly promoted by Esp1 activity), and because Cdc14 nuclear export is impaired in *net1Δ cdc15-2* cells where Esp1 activity is presumably normal. Consistent with my observation, a nuclear export sequence in yeast Cdc14 has been reported. Mutations of that sequence cause Cdc14 to fail to localize to the bud neck during mitotic exit (Bembenek et al., 2005). Functions of the Cdc14 nuclear export signal may be tied to MEN activation.

These observations implicate the MEN in a previously unsuspected aspect of Cdc14 activation: its release from the nucleus and dispersal throughout the cell. This activity may contribute to the ability of the MEN, but not FEAR- or Esp1-induced Cdc14 release, to promote complete mitotic exit. A recent publication showing that the MEN component Dbf2 is involved in Cdc14 nuclear export, independent of its role in promoting Cdc14 nucleolar release, confirmed my observation (Mohl et al., 2009).

Figure 3.14

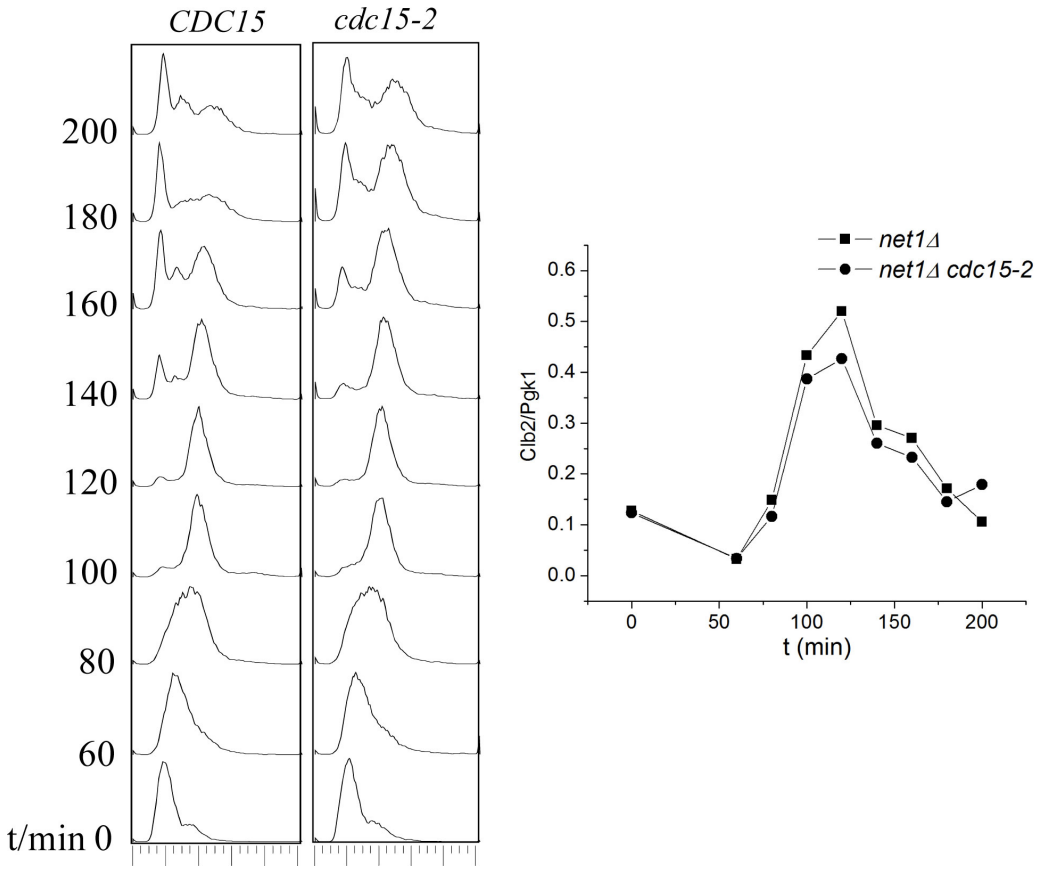

Figure 3.14. ***net1*Δ bypasses the MEN requirement for Clb2 degradation but not for cytokinesis.** *net1*Δ *cdc15-2* (YL1541) or *net1*Δ *CDC15* (YL1542) strains were arrested in alpha factor at 27˚. At time zero, the cultures were released by removal of alpha factor. Release was at 37˚ to inactivate cdc15-2. Alpha factor was added back at 100 minutes to prevent cells from entering the next cell cycle. Cytokinesis was assessed by the occurrence of a 1C DNA peak in DNA flow cytometry profile. Clb2 degradation was assessed by Western blot and quantified relative to a control Western blot of Pgk1.

9. Clb-Cdk activity may cooperate with Cdh1 to prevent Cdc14 from returning into the nucleolus

I demonstrated that Esp1 overexpression induced long-term release (~3 hours) of Cdc14-YFP in *cdc20- cdh1-* cells (Figure 3.12B). Since Cdc14 release normally only lasts for 15~20 minutes, it is interesting to know which factor prevents Cdc14 from returning into nucleolus in this condition.

In *cdc20- CDH1+* cells, Esp1 overexpression induces Cdc14 release of normal duration (~20 minutes), which leads to mitotic cyclin-Cdk inactivation and ME events (Figure 3.10B). Addition of NOC to the medium prevents induction of Cdc14 release and cyclin-Cdk degradation by Esp1 overexpression (Figure 3.7A, 3.10B). Therefore, the spindle could serve as a signaling center to sustain Cdc14 release status until its disassembly at ME. Alternatively, Cdc14 release could also be sustained by Clb-Cdk activity. To test those hypothesis, *MET-CDC20 cdh1* cells were blocked by depleting Cdc20, and Esp1 was overexpressed from *GALS* promoter at t=0. After 90 minutes when >95% cells had went through anaphase and released Cdc14, the culture was split into two. NOC was added into one culture to disassemble spindle, and Cdc20 was re-induced in the other culture to degrade mitotic cyclins. ME events and Cdc14 release were monitored during the time-course. In *cdc20- cdh1-* cells, NOC did not cause also any appreciable changes to either Cdc14 release or rebudding kinetics compared with NOC-free culture (Figure 3.15A, Figure 3.12B). In the

culture where Cdc20 was re-induced at 90 minutes, I initially observed a further release of Cdc14-YFP at 115 minutes reflected as a lower-shift of the r-value distribution. Then, Cdc14 rapidly returned into nucleolus (Figure 3.15A). Since Cdc20 re-induction causes mitotic cyclin inactivation, mitotic cyclin-Cdk activity may prevent Cdc14 from returning into nucleolus in *cdc20- cdh1-* cells. In this experiment, I observed that Cdc14 release by Esp1 overexpression in *cdc20- cdh1-* cells was quantitatively incomplete. I compared the pictures from maximum Cdc14-release time point in *CDH1+* and *cdh1-* cells, induced by Esp1 overexpression. Cdc14-YFP localization appeared to be more nuclear concentrated in *cdh1-* cells (Figure 3.15B). (Note: even in control experiments, I never observe complete Cdc14 release from the nucleolus; there is usually a weak Cdc14-YFP signal in the nucleolus even if Cdc14 release already reached its maximum by quantification.) *cdc20- pds1Δ* cells can achieve a similar telophase arrest with high mitotic cyclins and released Cdc14 (Shirayama et al., 1999) without Esp1 overexpression. In those cells, Cdc14-YFP localization also appeared to be nuclear concentrated (Figure 3.15B). Therefore, mitotic cyclin-Cdk activity could retain Cdc14 in the nucleus and prevent Cdc14 from returning into nucleolus, which potentially explains why the FEAR network-induced Cdc14 tends to regulate events in the nucleus (such rDNA segregation, spindle elongation), but does not induce cytokinesis. The relationship between this nuclear concentration of Cdc14, induced by mitotic cyclin-Cdk, and the MEN-induced nuclear exit of Cdc14 (even after nucleolar exit) documented in the preceding section, remains to be clarified.

Figure 3.15. **A**. Strain *MET-CDC20 cdh1*Δ *GALS-ESP1* was grown in raffinose medium and blocked with cdc20- by adding methionine to the culture. 90 minutes after *GALS-ESP1* induction at t=0, the culture was split into two. NOC was added to one culture (left), and Cdc20 was reinduced in the other culture by washing away methionine (right). Samples were taken at indicated time points, and Cdc14 localization was analyzed as described in Materials and Methods. Bar plot: r value distribution for the entire population. Red/green/blue/purple curve: r value distribution for metaphase/anaphase/rebudded/small-budded subpopulations. **B**. *MET-CDC20*, *MET-CDC20 cdh1*Δ *GALS-ESP1*, and *cdc20::GALL-CDC20 pds1*Δ strains, containing *CDC14-YFP NET1-CFP* were blocked with cdc20-. *MET-CDC20* cells were released into cell cycle progression by washing away methionine, and the picture showing Cdc14 release was taken at 30 minutes after release. Galactose was adding to *MET-CDC20 cdh1*Δ *GALS-ESP1* cell culture to overexpress Esp1, and the picture was taken 2 hours later. The *cdc20::GALL-CDC20 pds1*Δ picture was taken 4 hours after adding glucose in the culture to turn off the expression of Cdc20.

Figure 3.15

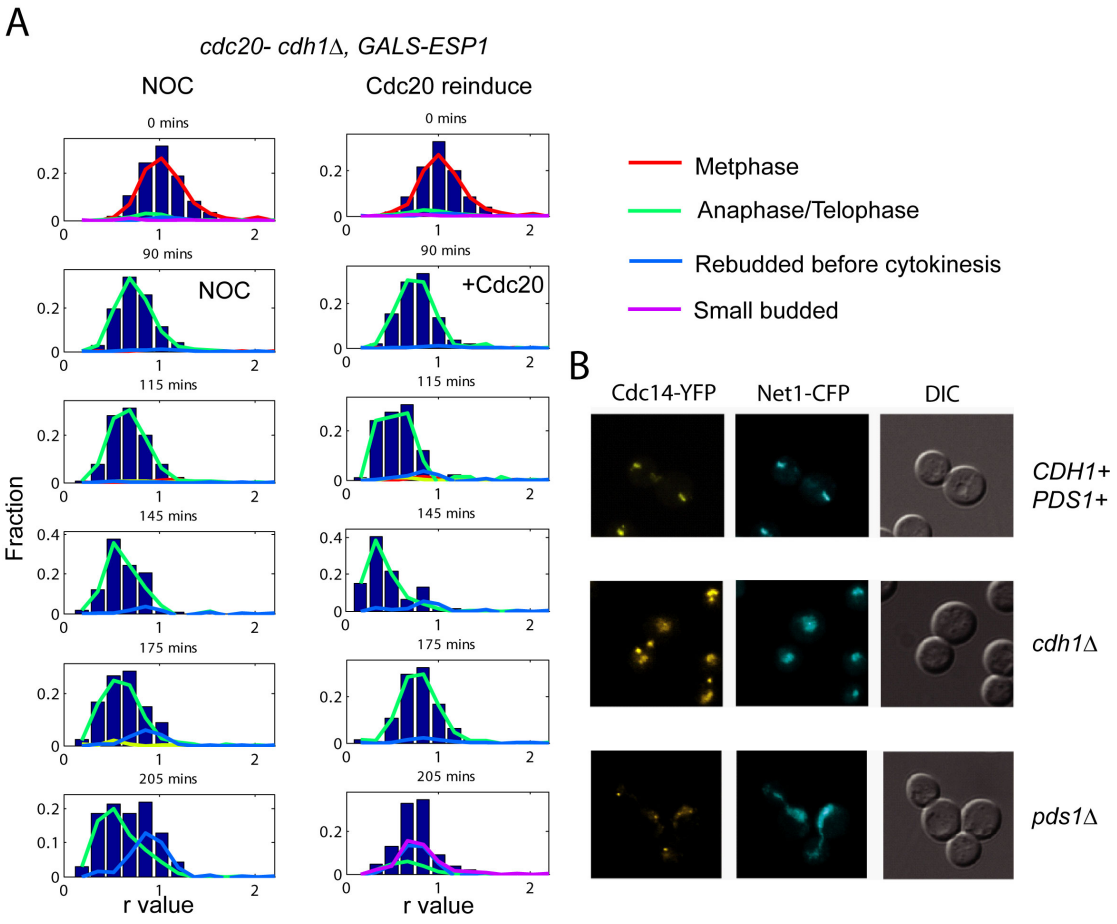
A
cdc20- cdh1Δ, GALS-ESP1
NOC
Cdc20 reinduce
0 mins
90 mins
NOC
+Cdc20
115 mins
145 mins
175 mins
205 mins
Fraction
r value
Metphase
Anaphase/Telophase
Rebudded before cytokinesis
Small budded
B
Cdc14-YFP
Net1-CFP
DIC
CDH1+
PDS1+
cdh1Δ
pds1Δ

10. Spindle checkpoint inactivation by FEAR-induced Cdc14 release

I showed in Figure 3.7A that Esp1 ovexpression did not induce ME or Clb2 degradation in *cdc20-* cells with NOC added. However, it is known that Esp1 overexpression induces efficient Clb2 and Pds1 degradation in NOC arrested cells (with Cdc20p present, but presumably inhibited by the spindle checkpoint)(Tinker-Kulberg and Morgan, 1999), suggesting that Esp1 overexpression can inactivate spindle checkpoint in NOC, likely through releasing Cdc14.

If FEAR-released Cdc14 can activate Cdc20 to degrade Pds1 and release inhibition of Esp1, Esp1 will cause more Cdc14 release by activating FEAR network, potentially forming a positive feedback loop to accelerate cell cycle recovery from spindle checkpoint arrest. I tested this idea by comparing Pds1p degradation kinetics in *slk19, cdc14-1, esp1-1,* and *esp1-1 ESP1C1531A* cells following release from NOC arrest. Consistently, I found that Pds1p degradation was delayed in both *slk19Δ* and *cdc14-1* cells by 10~15 minutes, compared with WT cells (Figure 3.16). But interestingly, Pds1 degradation was not affect by the non-proteolytic function of Esp1. In a recent publication, Cdc14 is shown involved in a positive feedback loop with Cdc20 to achieve a coherent metaphase-anaphase transition(Holt et al., 2008); the

involvement of Esp1 (with or without its proteolytic activity) was not addressed in this publication, but the work is still consistent with the idea proposed above that Cdc14 accelerates escape from checkpoint arrest.

Figure 3.16

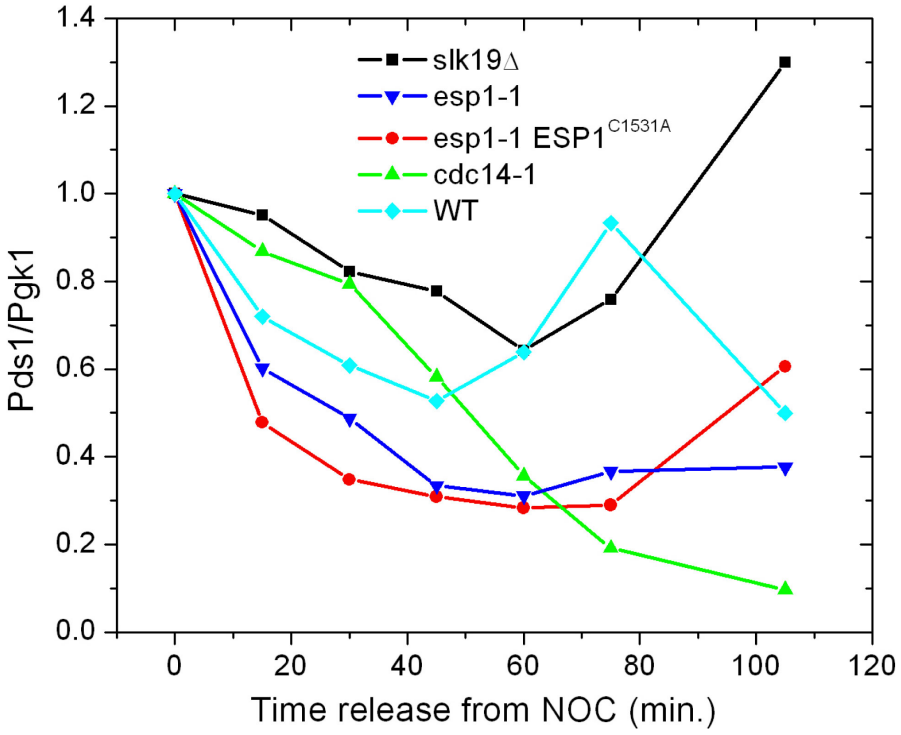

Figure 3.16. *slk19Δ, esp1-1, esp1-1 ESP1C1531A, cdc14-1* and wild-type cultures were arrested in glucose medium + NOC +BEN at 25℃ as described in Materials and Methods. Then, temperature was shifted to 37℃ to inhibit temperature-sensitive alleles, and the cultures were released into cell cycle by washing away NOC+BEN, still at 37℃. Protein samples were taken at indicated time points to analyze Pds1-18Myc levels using western blot with anti-Myc antibody. Pgk1 was the loading control.

11.Discussion

In budding yeast, Cdc14 is absolutely required for ME, and much evidence indicates that Cdc14 can not promote ME until it is released from its nucleolar anchor Net1. My results in this chapter show that efficient ME requires CDK inactivation and spindle elongation driving MEN activation, but Esp1 is not required beyond the need for cohesin cleavage. Furthermore, I devised a quantitative method to measure Cdc14 activity, which revealed that Cdc14 release driven by Esp1 overexpression depends on spindle elongation and MEN activation. My conclusion is consistent with previous findings that the FEAR network is dispensable for the cell cycle, while MEN activation is essential for effective release of Cdc14 from Net1 (Hofken and Schiebel, 2002; Shou et al., 1999; Stegmeier et al., 2002; Visintin et al., 1999). Interestingly, separase is also not required for ME in mammalian cells or fission yeast (Hirano et al., 1986; Wirth et al., 2006)

An absolute requirement for Esp1 in ME was supported by the finding that Esp1 overexpression, rather than TEV-protease induced spindle elongation, triggered ME (Sullivan and Uhlmann, 2003). These results, which I have confirmed (data not shown), were obtained in a *cdc20*-deficient background, and I interpret the apparent Esp1 requirement to be due to high Clb-Cdk activity levels because of Cdc20

depletion. In my experiments where anaphase is promoted by TEV protease or by mutational inactivation of cohesin, ME can occur in the absence of Esp1 activity if Cdc20p is kept active (allowing mitotic cyclin degradation), or if Clb-Cdk activity is inhibited by *GAL1-SIC1-4A*. In the presence of high Clb-Cdk levels, TEV protease may promote transient spindle elongation which only partially activates MEN, causing failure to exit from mitosis in *cdc20* arrest (Higuchi and Uhlmann, 2005).

The requirement for inactivation of Clb-Cdk1 activity before ME places APC-Cdc20 in a uniquely important position in the ME control system. Mitotic cyclin degradation in budding yeast is biphasic (Yeong et al., 2000). APC-Cdc20 degrades Clb5,6 and partially degrades Clb1,2 at the metaphase to anaphase transition, which may lower the overall Cdk activity level sufficiently to allow ME, once the MEN is triggered by spindle elongation. Consistently, deleting *CLB5* to lower Clb-Cdk activity can restore viability to *cdc20Δ pds1Δ* strains (Shirayama et al., 1999). Thus, the stable arrest observed in *cdc20* cells cannot be overcome simply by allowing Esp1 to escape from Pds1 inhibition (either by *pds1* deletion or by *ESP1* overexpression); Cdk inactivation is independently required, and is provided in the first phase of Clb degradation in the wild-type system by Cdc20. Cdc20 is even required to recover from *cdc15-2* arrest (Yeong et al., 2000). A likely explanation is that depletion of Cdc20 during a *cdc15-2* arrest increases the Clb cyclin level, making the cell unable to recover from telophase arrest after being shifted to permissive temperature. The mechanism by which Clb-Cdk inhibits ME is unknown. High

Clb-Cdk may block cytokinesis and rebudding directly (Eluere et al., 2007; Padmashree and Surana, 2001). These results thus suggest that Esp1 is not sufficient to drive ME, even when overexpressed.

The *esp1-2td* allele is thought to completely remove separase activity (Queralt et al., 2006). In my hands this allele only causes a 2 hour delay in ME (data not shown), confirming recent results (Visintin et al., 2008). These results support my conclusions derived using Pds1 as an Esp1 inhibitor (see above) in suggesting that Esp1 is not necessary for ME. Its absence does clearly delay ME very significantly, but I suggest that most or all of this delay is due to failure of cohesin cleavage, which prevents spindle elongation, greatly delaying MEN activation and Cdc14 release. It is clear from much work that Cdc14 release is essential for ME.

Cdc14 release is thought to be biphasic: Esp1 induces the FEAR network, promoting the first wave of Cdc14 release in early anaphase. ME is delayed until the second wave of Cdc14 release, promoted by the MEN; the reason for this delay is unknown. My quantification of Cdc14 release suggest that Esp1 and the FEAR pathway, in the absence of spindle elongation or MEN activity, do not promote a quantitatively or qualitatively sufficient degree of Cdc14 release to trigger ME. Esp1-induced Cdc14 release has been reported to fulfill ME-independent functions, such as stabilizing the anaphase spindle (Jensen et al., 2001). The functional diversification of Cdc14 at early and late anaphase might in part be due to the ability

of MEN to control Cdc14 nuclear export, independent of its restriction to the nucleolus; nuclear export could allow access of Cdc14 phosphatase to additional substrates. Consistently, in *net1Δ* cells, the bud-neck localization of Cdc14-YFP only appears at ME when the MEN is activated and Cdc14 release from the nucleus is promoted. I do not observe bud-neck localization of Cdc14 upon *ESP1* over-expression, if spindle elongation is inhibited by nocodazole (Figure 3.10B). Intact microtubules are not likely to be intrinsically required for ME or Cdc14 release, since in a *mad2 bub2* double mutant, lacking all known spindle surveillance pathways, microtubule depolymerization with nocodazole has no effect on the kinetics of Clb2 degradation, rebudding and DNA replication in the subsequent cell cycle (Alexandru et al., 1999), strongly suggesting that Cdc14 phosphatase was properly released and activated at ME in this context. I cannot completely exclude the possibility that the FEAR network could require an intact spindle to function for reasons unrelated to ultimate spindle elongation. However, my conclusions are consistent with the finding that both Cdc14 release and ME (assessed by spindle disassembly) in the *dyn1Δ* mutant coincide with SPB moving into the bud, rather than spindle elongation *per se* (i.e. separase activation) which frequently happens within the mother cell body in this mutant (Bardin et al., 2000). In these cells, the spindle is intact, but Esp1 still appears unable to promote ME on its own.

Esp1-induced Cdc14 release was previously reported to occur in nocodazole (Visintin et al., 2003). I observe a spreading of the Cdc14-YFP signal in

cdc20-depleted cells after long-term induction of *ESP1*–overexpressing cells in nocodazole, but an essentially identical spreading of Net1-CFP was also observed, which colocalized with Cdc14-YFP, accounting for the maintenance of a high r value (Figure 3.10B). I do not know whether this spreading is due to the release of Net1 as well as Cdc14 from the nucleolus, or to a general disruption of nucleolar structure. The tight colocalization suggests that Net1 has the potential to bind and inactivate Cdc14 in this condition, which could explain the lack of mitotic exit in this context. Deletion of *CDC55* has been reported to hyper-activate the FEAR network and cause constitutive Cdc14 release in *cdc20*-blocked cells (Queralt et al., 2006). I observed essentially the same scenario of co-spreading of both Cdc14-YFP and Net1-CFP in *cdc20*- blocked *cdc55Δ* cells (data not shown).

ME is a complex system, governed by an interdigitated control network. Here, I have attempted to elucidate the system with all major control parameters taken into consideration in a balanced way, in order to gain an understanding of the relative importance of various pathways in controlling ME. My results lead to the conclusion that Cdk inactivation is absolutely required for ME. In my analysis, Esp1 does not make a quantitatively major contribution to kinetics of ME beyond that due to its ability to cleave cohesin. Cohesin cleavage and consequent spindle elongation strongly increases the speed and reliability of ME, most likely by allowing MEN activation.

12. Remaining issues from my experiments:

1. How is the MEN activated? The prevailing model is that spindle elongation pushes one SPB close to the bud cortex where Lte1 localizes. Lte1 can activate GTPase Tem1 probably as its guanine exchange factor to induce the Tem1-Cdc15-Dbf1 signaling cascade. However, Let1 is not essential for cell viability. There should be parallel mechanisms activating MEN by sensing anaphase. It is also unclear whether SPB has to directly contact the bud cortex to activate MEN, or just needs to get close to it. It has been reported that some proteins (like Kar9 and Bim1) can travel along cytoplasmic microtubules. It is imaginable that cell polarization proteins (like Cdc42, Lte1, Ste20 et al.) might reach the SPB by traveling along microtubules to activate Tem1 at the SPB.

2. Does Cdc14 localize differently in early and late mitosis in normal cell cycles? My data and previous publications suggested that Cdc14 might localize in nucleus/spindle in early mitosis, and switch to cytoplasm and bud-neck in later mitosis. However, most experiments were performed with the cell cycle blocked by various means. It is important to know whether Cdc14 localization really follows this rule in normal cell cycles.

3. What causes Cdc14 to return into nucleolus? Although Cdc5 degradation by Cdh1 has been reported to promote Cdc14 re-sequestration, in cycling *cdh1Δ* cells,

Cdc14 resequestration was delayed by at most 3 minutes (i.e., any difference is at frame resolution) in my single cell time-lapse analysis. So there must be parallel mechanisms promoting Cdc14 resequestration. Since both polo kinase and the MEN are essential for Cdc14 release, inactivation of MEN may lead to Cdc14 re-sequestration. My data showed that in the absence of Cdh1, mitotic cyclin-Cdk activity can maintain Cdc14 in released state for 3 hours, indicating Clb-Cdk may prevent MEN inactivation. It is unclear how the MEN is inactivated at the end of mitosis. Cdc14 has been shown to dephosphorylate Bub2 to inactive the MEN. The MEN could also be inactivated directly due to budding which translocates MEN activators into the incipient bud. Cdc14 can promote Lte1 delocalization from bud cortex into cytoplasm at least under overexpression, pointing to another possible way for MEN inactivation by Cdc14, though the causal relationship has yet to be demonstrated.

One problem that makes it difficult to reason effectively on these issues is that it remains unclear how the MEN and the FEAR network release Cdc14 from nucleolus. One model suggests that Dbf2, Cdc5 and Cdk can phosphorylate Net1 and Cdc14 to promote their disassociation, but solid evidence is still missing. Effective Cdc14 release could be coupled directly to nucleolar division, providing a direct cell biological coupling between anaphase and ME. This model could explain the requirement I observed for intact microtubules for promotion of Cdc14 release by Esp1.

4. Cdc14 released by FEAR network has been shown to promote rDNA segregation. In my experiments, Clb2kd expression can delay rDNA segregation, but not bulk DNA segregation, in single cell analysis. Therefore, phosphorylation/dephosphorylation may be a way to coordinate rDNA segregation with anaphase, but the potential Cdk/Cdc14 targets are unknown.

Chapter 4: Cell Cycle Control by Phase-Locking: Study of the Cdc14 Release Endocycle

1. Background information

The eukaryotic cell cycle is driven by oscillations in levels and activity of cyclin-dependent kinase (Cdk) (Morgan, 2007). These oscillations are accompanied by ordered progression of cell cycle events. There are at least two mechanisms to ensure correct ordering of these events. Checkpoint surveillance mechanisms delay subsequent events until previous ones are finished (Elledge, 1996; Weinert et al., 1994). However, checkpoints are dispensable for correct ordering of cell cycle events, at least in budding yeast.

Order can be established independent of checkpoints by a 'ratchet'-like mechanism under direct control of cyclin-Cdk oscillations: initiation of an event is triggered by high cyclin-Cdk, but completion of the event is inhibited by high cyclin-Cdk (Nasmyth, 1996; Stern and Nurse, 1996). The consequence of this regulation is that cell cycle events occur exactly once per cyclin-Cdk cycle in a regular sequence. There is abundant evidence for this mechanism in control of DNA replication (Kearsey and Cotterill, 2003). Division of regulatory function among multiple cyclins complicates this simple picture; nevertheless, a generally similar

ratchet-like mechanism may apply to many cell cycle processes, such as spindle and bud morphogenesis (Bloom and Cross, 2007).

Ratchet control can be attained by many molecular mechanisms. For the proposed ratchet control of DNA replication, many different redundant mechanisms coexist in any given species, and very different mechanisms can operate in different species (Kearsey and Cotterill, 2003). Nevertheless, *all* ratchet mechanisms, controlling *any* cell cycle process, have one unavoidable prediction: blocking the cyclin-Cdk cycle by locking Cdk activity at any constant level should arrest a ratchet-controlled process at a single defined step in its trajectory. The dose-response of where the process arrests in response to cyclin-Cdk level is then informative as to mechanism and the overall structure of the control system.

Some cell cycle events may occur cyclically and repetitively in the likely absence of oscillation of mitotic cyclin-Cdk activity. Examples include the SPB/centrosome duplication cycles in budding yeast and various animal embryos, and the periodic budding and cell-cycle-regulated transcription in budding yeast. These 'endocyclical' events are not likely driven by oscillations of other cyclins (Gard et al., 1990; Haase and Reed, 1999; Haase et al., 2001; McCleland and O'Farrell, 2008; Sluder et al., 1990). DNA endoreduplication could also be considered under this category since it occurs in the absence of mitotic B-cyclin activity. However, in this case, a ratchet-like mechanism driven by other cyclins such as cyclin E has been

proposed (Inze and De Veylder, 2006; Weiss et al., 1998).

On their face, these endocycles pose a significant challenge to the concept of cyclin-Cdk-based ratchet control. However, the relevance of these endocycles to the mitotic cell cycle, and what mechanism, if any, entrains them to mitotic cyclin-Cdk cycles, remains unclear (Murray and Kirschner, 1989).

Recently, we carried out an analysis of dose-response of mitotic exit to locked cyclin-Cdk activity levels, using titrated pulses of undegradable mitotic cyclin Clb2 and correlating steps of mitotic exit to Clb2 levels in individual cells (Drapkin et al., in press). High Clb2 levels have long been known to block mitotic exit (Surana et al., 1993); however, we found that the peak level of Clb2-Cdk activity attained in a normal cell cycle was inefficient at restraining multiple aspects of mitotic exit. These results strongly suggested that the simple cyclin-based ratchet model accounted poorly for control of mitotic exit, and a better fit was obtained by incorporating the activity of Cdc14 phosphatase as a general cyclin-Cdk antagonist, capable of dephosphorylating multiple cyclin-Cdk phosphorylation targets. (This specificity is consistent with structure and in vitro activity of Cdc14 (Gray et al., 2003)).

Effective regulation of Cdc14 localization and activity is probably essential for normal cell cycle progression. Cdc14 is restrained and inhibited in the nucleolus by the constitutively nucleolar Net1 protein, except in mitosis (Shou et al., 1999; Visintin

et al., 1999). The spindle orientation checkpoint (SPOC, regulating the mitotic exit network MEN) is an important regulator of Cdc14 release (Bardin et al., 2000; Pereira et al., 2000; Stegmeier and Amon, 2004). Anaphase sends the daughter-oriented spindle pole body (SPB) into the bud, activating the Tem1-Cdc15-Dbf2 MEN cascade which promotes Cdc14 release and activation (Bardin et al., 2000). However, removing the key SPOC inhibitor Bub2 has almost no effect on Cdc14 release in an unperturbed cell cycle (data not shown), despite strong deregulation of SPOC function, indicating the need for additional mechanisms to account for regulation of Cdc14 release, which is likely associated with cyclin-Cdk oscillations. Although connections between Cdc14 release and Clb-Cdk activity have been described (Azzam et al., 2004; Jaspersen and Morgan, 2000; Queralt et al., 2006; Stegmeier et al., 2002), it is as yet unclear how Cdc14 localization responses to difference Clb levels and whether these controls constitute a ratchet mechanism sufficient to lock Cdc14 release to once per cell cycle.

In this work, I aim to understand how cyclin-Cdk activity controls Cdc14 localization and activity, and whether this control constitutes a 'ratchet' mechanism. In initial experiments, I treated the Cdc14 control system as a 'black box', and to study its input (cyclin-Cdk) – output (Cdc14 localization) relationship at various mitotic cyclin levels. Again, I used pulses of undegradable mitotic cyclin Clb2. As noted above, for a process under cyclin-Cdk ratchet control, this approach is predicted to result in arrest of the process at a specific step defined by the locked cyclin-Cdk

levels. In exact contrast to this prediction, though, I observed Cdc14 cycling in and out of the nucleolus multiple times at high but physiological fixed mitotic cyclin levels.

These observations, along with other cell cycle endocycles reported previously (see above), suggest that many cell cycle events have intrinsic 'clocks' controlling their occurrence. This concept stands in sharp contrast to the cyclin-Cdk-ratchet model, and pose the question of how these events occur only once per Clb-Cdk cycle and in a very specific sequence despite the ability to oscillate autonomously.

Based on my study of Cdc14 endocycles, I propose that the cyclin-Cdk oscillator entrains ('phase-locks') other cell cycle oscillators. Phase-locking is well-established for circadian systems (as well as many other biological and physical systems) (Glass, 2001). Extrinsically applied phase locking has been implemented experimentally to control the timing of the budding yeast cell cycle (Charvin et al., 2009).

My experiments and analysis suggest that Cdc14 localization, likely other cell cycles events, is controlled by an intrinsically oscillatory module(s). In wild-type cell cycles, cyclin-Cdk oscillations phase-lock those oscillators to once-per-cell-cycle, and the Cdk-response properties of those oscillators determine the timing and order of downstream cell cycle events. The phase-locking model reconciles previous

observation of autonomous oscillators with once-per-cell-cycle control of multiple cell cycle events, and is compatible with experimental results from my study.

2. Blocking mitotic exit with undegradable Clb2kd reveals Cdc14 release endocycles

Cdc14-release status is not “all or none” but contains intermediate states (Stegmeier et al., 2002). I designed a quantitative, single cell measurement for Cdc14 localization based on variation of cellular Cdc14-YFP pixel intensities, standardized to variation of nucleolar Net1-mCherry, which is an improved version of my previous assay (Lu and Cross, 2009) (this Cdc14 release measure is mathematically predicted to vary linearly with the fraction of Cdc14 released into cytoplasm, Materials and Methods). Fig. 4.1A illustrates the measure applied to a *CDC14-YFP NET1-mCherry* cell undergoing a normal Cdc14 release following anaphase. I used Myo1-GFP as a budding and cytokinesis marker (Bi et al., 1998). Since the bud-neck region was always manually excluded from quantification, the Myo1-GFP signal didn’t interfere with Cdc14 measurements.

Figure 4.1

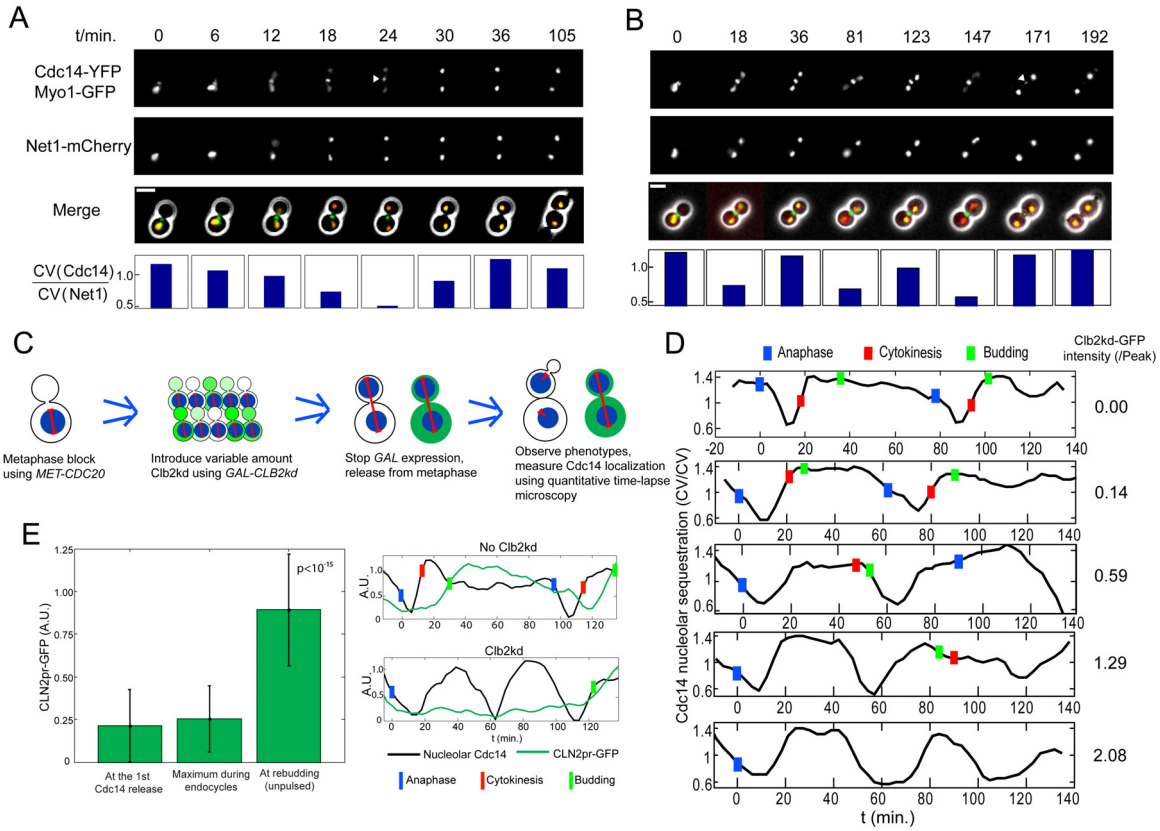

Figure 4.1. **Cyclical Cdc14 release uncoupled from cell cycle progression. A, B.** *MET3-CDC20 CDC14-YFP NET1-mCherry MYO1-GFP* cells were released from a *MET3-CDC20* block (t=0). Bottom: Cdc14 release was quantified at each time point. Triangle: Myo1 ring. Scale bar: 5 microns. **A:** control. **B.** Clb2kd was pulsed for 30 minutes before release. **C.** Schematic of procedure for loading cells with undegradable Clb2kd (green) before ME. Nucleolus is shown in red. **D.** Pulsed Clb2kd-GFP was quantified (right column) in units standardized to the peak level of Clb2 attained in a normal cell cycle, and Cdc14 release quantified. Blue bars: anaphase (nucleolar separation, marked by Net1-mCherry); Red bars: cytokinesis (Myo1 ring disappearance); green bars: bud emergence. **E**. *CLN2* promoter expression during Cdc14 endocycles. A *CLN2pr-GFP-PEST* strain was pulsed with Clb2kd as in (B) for 35 minutes. GFP intensities at the first Cdc14 release, maximum during endocycles (n=40), and at rebudding in unpulsed control cells ($P<10^{-15}$. Error bars: standard deviation).

I followed a procedure described in 'Materials and Methods' to load cells with physiological levels of stable Clb2 during a pre-anaphase block, and then release the block and examine events of mitotic exit in single cells as a function of Clb2 level. I blocked cells in metaphase by depleting the essential anaphase-promoting complex (APC) activator Cdc20, by shutoff of *MET3-CDC20* (Sullivan et al., 2001). Cdc20 promotes proteolysis of the separase inhibitor Pds1, driving anaphase, and promotes initial proteolysis of B-type cyclins (Shirayama et al., 1998; Wäsch and Cross, 2002; Yeong et al., 2000) ; later in mitosis and in G1, B-type cyclin proteolysis is maintained by the related Cdh1 activator (Schwab et al., 1997). I transiently pulsed these *cdc20*-blocked metaphase cells with Clb2kd; Clb2kd lacks the Clb2 destruction and KEN boxes recognized by Cdh1 and Cdc20, and is therefore almost completely stable (Wäsch and Cross, 2002)). Clb2kd was labeled with GFP to allow single-cell quantification of Clb2kd levels. This procedure yielded a population with variable levels of stable Clb2kd-GFP, averaging around the peak Clb2-GFP level in a wild-type cell cycle (I refer to this level as '1X peak' Clb2kd; accurate single-cell quantification of Clb2kd levels in these units has been documented elsewhere [Drapkin et al, in press]).

Re-inducing *MET3-CDC20* induced anaphase, which proceeded on schedule independent of stable Clb2kd-GFP (data not shown). Clb2kd-GFP was stable after expression, only being slowly diluted with cell growth (Fig. 4.2). Clb2kd-associated kinase activity was essentially constant through this protocol (Drapkin et al, in press).

I assayed post-anaphase ME events as a function of single-cell Clb2kd-GFP levels (Fig. 4.1C), using quantitative time-lapse microscopy.

~1X peak Clb2kd-GFP and above induced dose-dependent delays in cytokinesis and bud emergence (Drapkin et al., in press; Fig. 4.3). In contrast, Cdc14-YFP was released from the nucleolus and subsequently resequestered, with essentially normal kinetics up to at least 3X peak Clb2kd-GFP concentrations (Fig. 4.1D and Fig. 4.4; Drapkin et al., in press). Strong overexpression of stable Clb2 was shown previously to cause extended Cdc14 release. I confirmed this observation by constitutively overexpressing *GAL1-CLB2kd* in galactose medium, which results in at least 10-fold peak Clb2kd levels (Fig. 4.5). I assume that results at approximately physiological Clb2kd levels are more biologically relevant, and I have not pursued the basis for the effect of extreme Clb2kd overexpression on Cdc14 release.

Remarkably, cells with moderately more than 1X peak Clb2kd-GFP frequently exhibited multiple cycles of Cdc14-YFP release and resequestration, before finally undergoing cytokinesis and rebudding (Fig. 4.1B,D). I call these 'Cdc14 endocycles'.

Figure 4.2

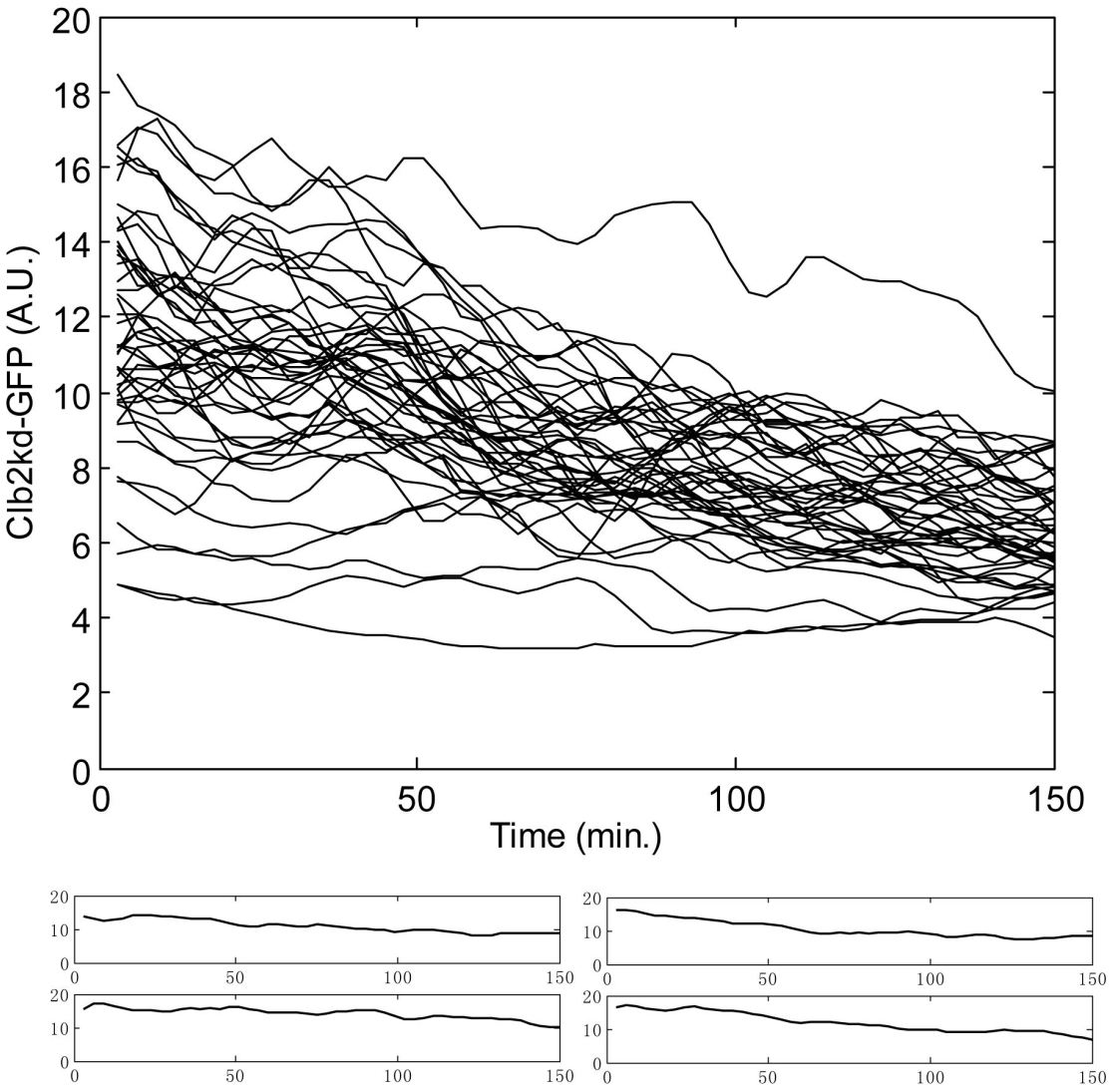

Figure 4.2. **Clb2kd-GFP is stable in vivo.** GAL1-CLB2kd-GFP was pulsed for 30 minutes as described in Materials and Methods. The average GFP intensity inside a cell was measured, and ploted in the upper panel. 4 traces were picked up to plot in the lower panels. Fitting the GFP curve with an exponential decay function, we obtain the median decay constant of 112 minutes.

Cells exhibiting Cdc14 endocycles did not show overt cell cycle progression as determined by budding, cytokinesis, or nuclear or nucleolar division. The G1 cyclin *CLN2* is expressed at cell cycle Start, as part of a large regulon (Wittenberg et al., 1990). To examine whether some aspects of cell cycle progression were proceeding despite the absence of morphological events, I examined *CLN2* promoter activity using a *CLN2pr-GFP-PEST* construct (Bean et al., 2006; Mateus and Avery, 2000) as a molecular marker for cell-cycle progression in Clb2kd-blocked cells. I observed no significant *CLN2pr* expression while cells were undergoing Cdc14 endocycles, while a burst of *CLN2pr* expression occurred when these cells finally budded (Fig. 4.1E). This result also implies that the Cdc14 endocycle is not driven by oscillations in G1 cyclin expression (also see below).

Figure 4.3

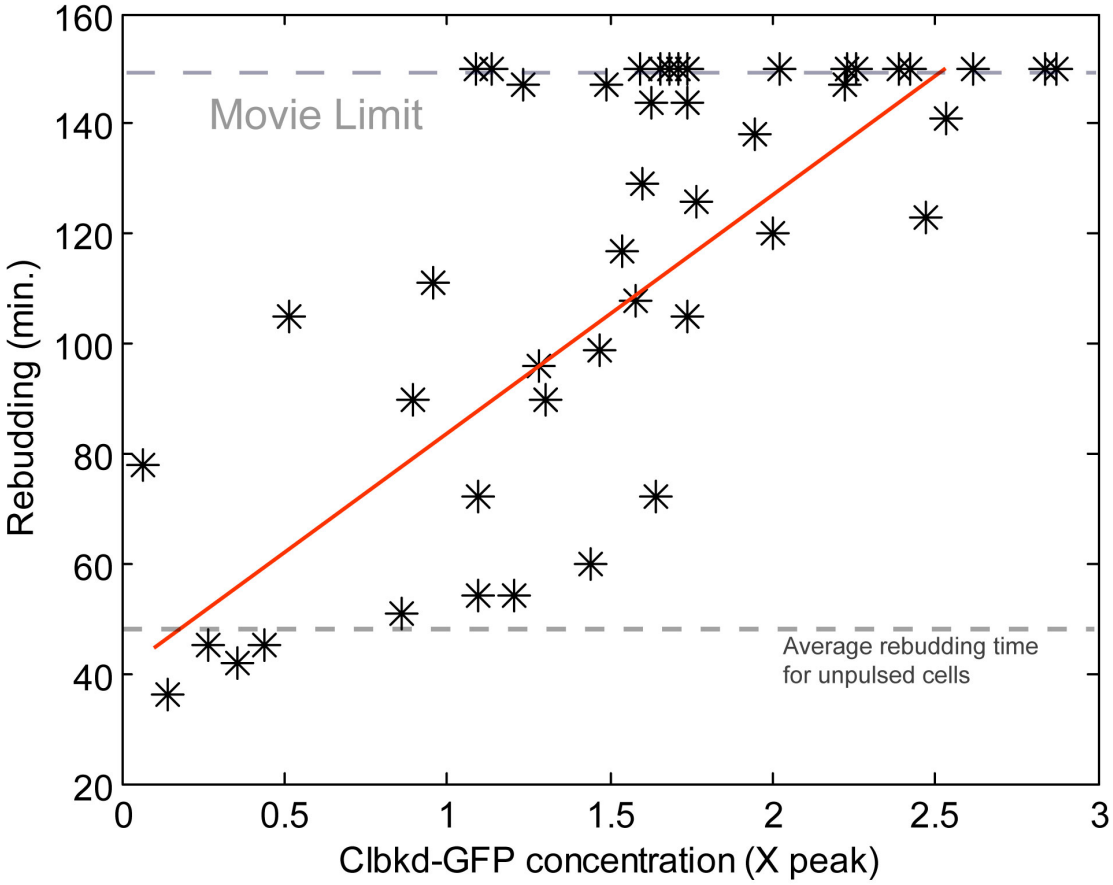

Figure 4.3. **Clb2kd-GFP activity leads to graded delay in rebudding.**

GAL1-CLB2kd-GFP strain was treated as in Fig. 4.1D. The rebudding time was plotted against Clb2kd-GFP concentration for each cell. Red line shows a fitting with a linear function ($r=0.8$, $p=8\times10^{-4}$). The average rebudding time for unpulsed cells was shown with a dashed grey line.

Figure 4.4

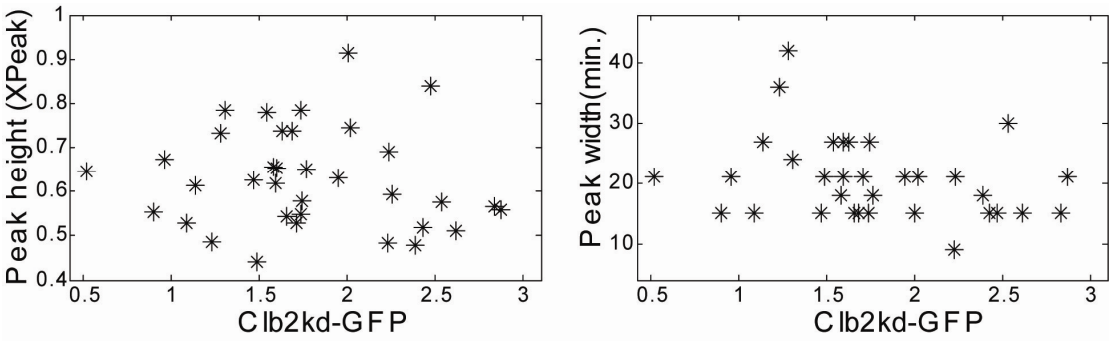

Figure 4.4. **Height and width of Cdc14 release peak are not affected by Clb2kd-GFP concentration up to 3-fold wild-type peak level**. Cells were treated as in Fig. 4.1D. In cases of Cdc14 endocycles, the height and width of the release peak is plotted against Clb2kd-GFP concentration. Cdc14 release in wildtype cells lasts for about 20 minutes.

Figure 4.5

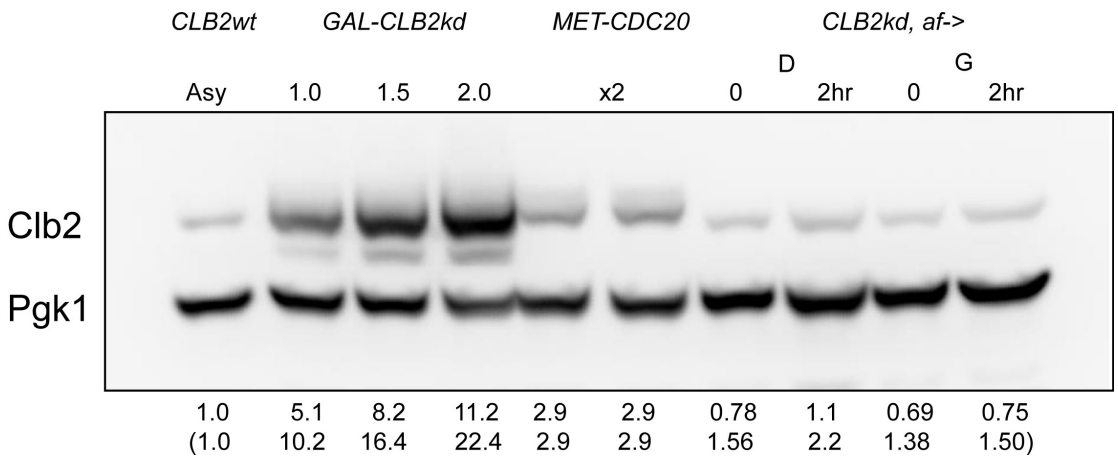

Figure 4.5. **Comparison of Clb2(kd) levels under various conditions.** Asy: asynchronous culture; *GAL-CLB2kd*: asynchronous culture of *GAL-CLB2kd* strain growing in raffinose. Galactose is added at time zero. *MET-CDC20: MET-CDC20* strain in R+MET; *CLB2kd:CLB2kd* strain is first synchronized with alpha factor in galactose medium, and is released into either glucose or galactose (t=0). Numbers under lanes: Clb2/Pgk1 value, normalized by the value for asynchronous culture. Numbers in bracket: Adjusted Clb2/Pgk1 value. Anti-Clb2 antibody recognizes Clb2 and Clb2kd with different affinity. We calibrate the Clb2 antibody using Clb2-YFP and Clb2kd-YFP, obtaining the correction factor ~2.0 (Clb2/Clb2kd).

In yeast, the MCM replicative helicase complex is excluded from the nucleus throughout the cell cycle except for late M and G1, and this regulation contributes to preventing pre-replicative complex formation except during these cell cycle stages (Kearsey and Cotterill, 2003). Mcm2-GFP nuclear relocalization occurs sharply at ME. ~1X peak Clb2kd-YFP was sufficient to completely block Mcm2-GFP nuclear accumulation before rebudding in the next G; lower levels of Clb2kd-YFP strongly but incompletely inhibited Mcm2 nuclear reentry (Fig. 4.6; Drapkin et al., in press). Consistent with this observation, I observed little or no DNA endoreduplication during Cdc14 endocycles by DNA flow cytometry (no accumulation of 4C peak, which would indicate an extra round of replication in undivided cells; Fig. 4.7). These observations confirm continuous high Clb2kd-associated kinase activity *in vivo*, and further confirm absence of molecular markers of cell cycle progression during Cdc14 endocycles.

Despite constancy of Clb2kd levels and activity through this protocol (see above, and Drapkin et al., in press), I needed to determine whether endogenous mitotic cyclins might be oscillating and potentially controlling Cdc14 localization in cells exhibiting Cdc14 endocycles. I tagged endogenous Clb2 with GFP in *GAL1pr-CLB2kd* cells, and found that Clb2-GFP was uniformly degraded after the initial Cdc14 release regardless of Clb2kd levels. Clb2-GFP signal remained at the basal level through the period of Cdc14 endocycles, only reaccumulating upon exit from the endocycling state and re-entry into the next cell cycle (Fig. 4.8). Thus, the

Cdc14 endocycle is most likely not driven by endogenous mitotic cyclin oscillations.

Cdc14 endocycles are not driven by oscillations of stoichiometric inhibitors of Cdk, such as Sic1 (Verma et al., 1997), because pulsed Clb2kd was associated with constant histone H1 kinase activity, and Sic1 levels stayed low, and insufficient for Clb2kd inhibition, during the protocol (Drapkin et al. in press). Consistently, Cdc14 endocycles were independent of Swi5, the major *SIC1* transcription factor (Toyn et al., 1997)(Fig. 4.9).

Overall, I conclude that Cdc14 release endocycles were not driven by oscillations of Clb2kd or Clb2-Cdk activity, and was likely independent of endogenous G1 or mitotic cyclins. Cdc14 endocycles were observed in cells that failed to undergo cell cycle progression, as indicated by failure of cytokinesis, rebudding, Mcm complex nuclear reaccumulation, DNA replication, G1 cyclin expression and endogenous Clb2 reaccumulation.

Figure 4.6

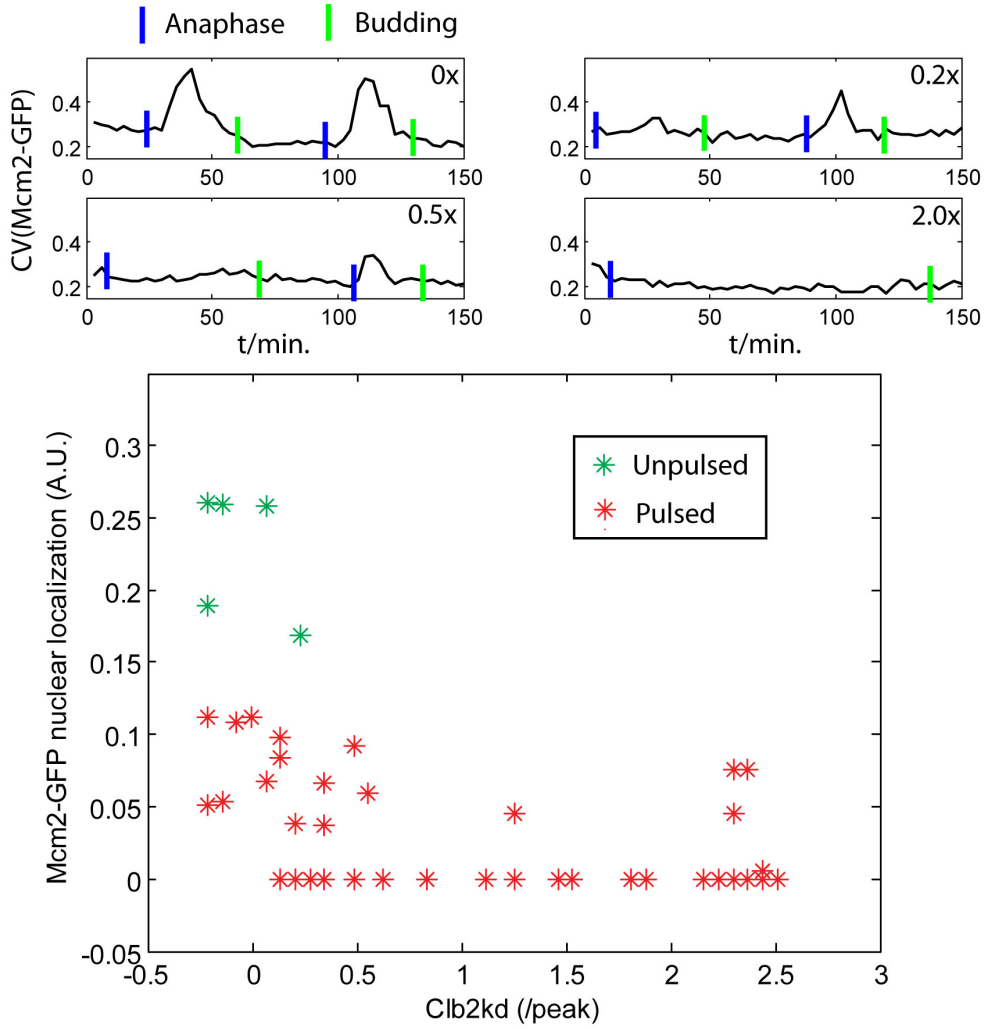

Figure 4.6. **The response of Mcm2 nuclear localization to Clb2kd.** *MCM2-GFP* cells was pulsed with *GAL1-CLB2kd-YFP* for 30 minutes as in Fig. 4.1D, and released into cell cycle progression. Coefficient of Variation(CV) of Mcm2-GFP in a single cell was used as a proxy for Mcm2 nuclear localization. An increase of CV indicates an increase of Mcm2-GFP nuclear concentration. Top four traces show CV(Mcm2-GFP) during the time course under various Clb2kd-YFP concentrations in the 'peak' unit (Materials and Methods). Bottom panel shows the height of CV(Mcm2-GFP) peak before budding vs. Clb2kd-YFP levels for both unpulsed control and pulsed cells. Note: due to cellular background fluctuations, the apparent 'Clb2kd-YFP' level for unpulsed controls is not strictly zero. Blue bars: anaphase; green bars: budding.

Figure 4.7

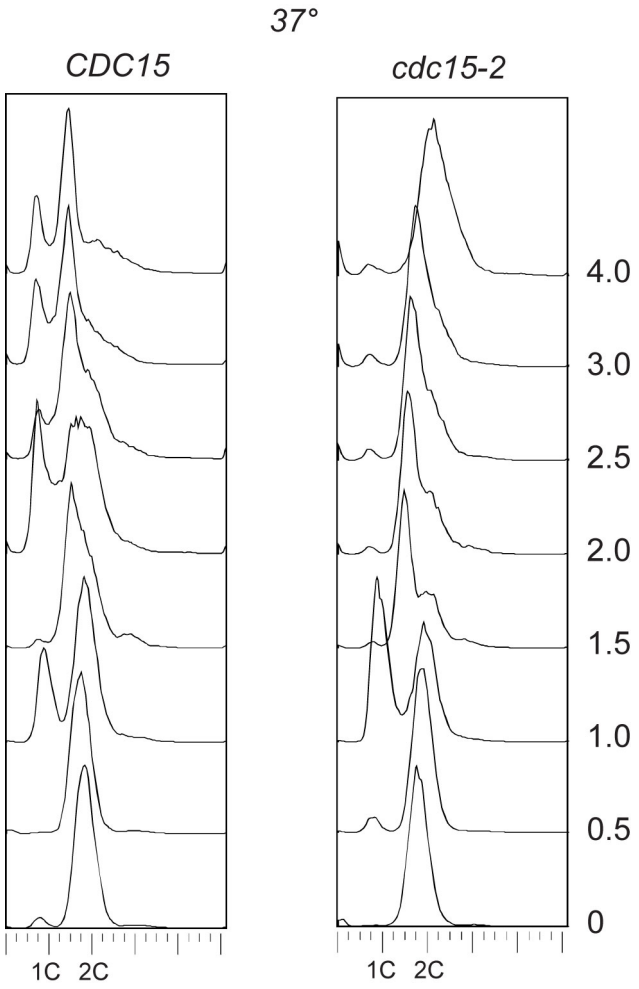

Figure 4.7. *MET-CDC20 CDC15/cdc15-2* cells were pulsed with GAL1-Clb2kd for 35 minutes at 28° permissive temperature before released from cdc20- block. After incubated at 28° for 40 minutes to allow anaphase and initial Cdc14 release, cultures were shifted to 37° restrictive temperature (t=0). FACS samples showing DNA content were taken at indicated time points.

Figure 4.8

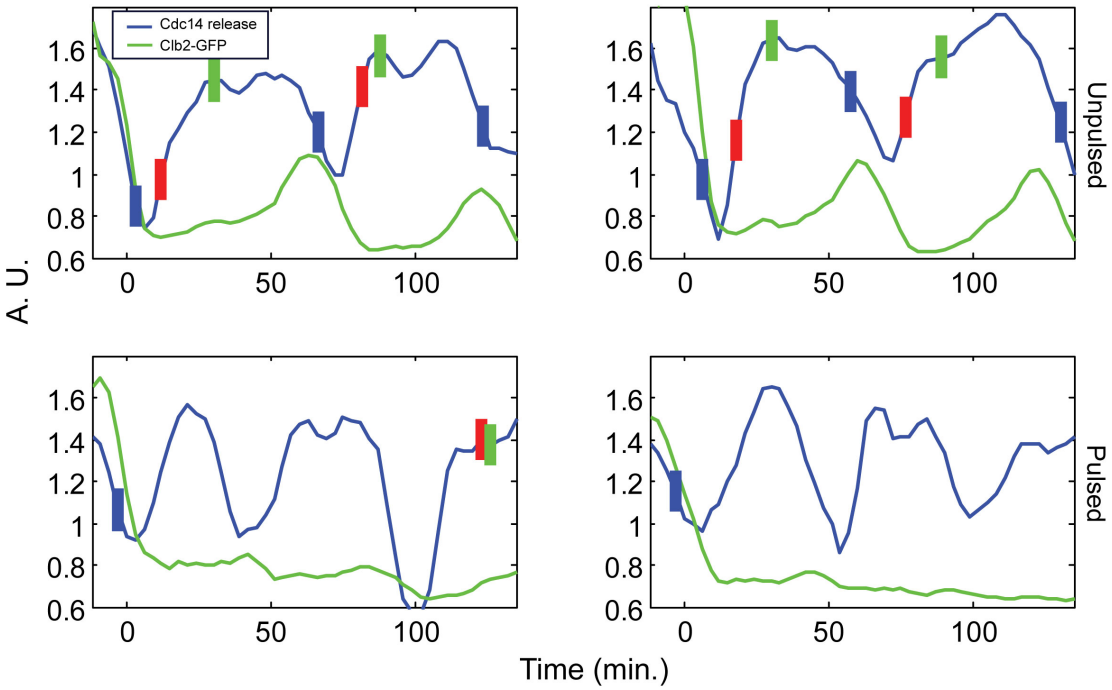

Figure 4.8. **Endogenous Clb2 was degraded regardless of Clb2kd, and did not accumulate during Cdc14-release endocycles.** *GAL1-CLB2kd* was pulsed for 35 minutes in cells whose endogenous Clb2 was tagged with GFP. Cdc14 release curve (blue) and GFP signal (green) were shown for 4 examples. In the case of Cdc14 release endocycles (lower two panels), Clb2-GFP signal remained low during the oscillation period (n=36). Vertical blue bar: nucleolar separation (anaphase); Vertical red bar: cytokinesis; Vertical green bar: bud emergence.

Figure 4.9

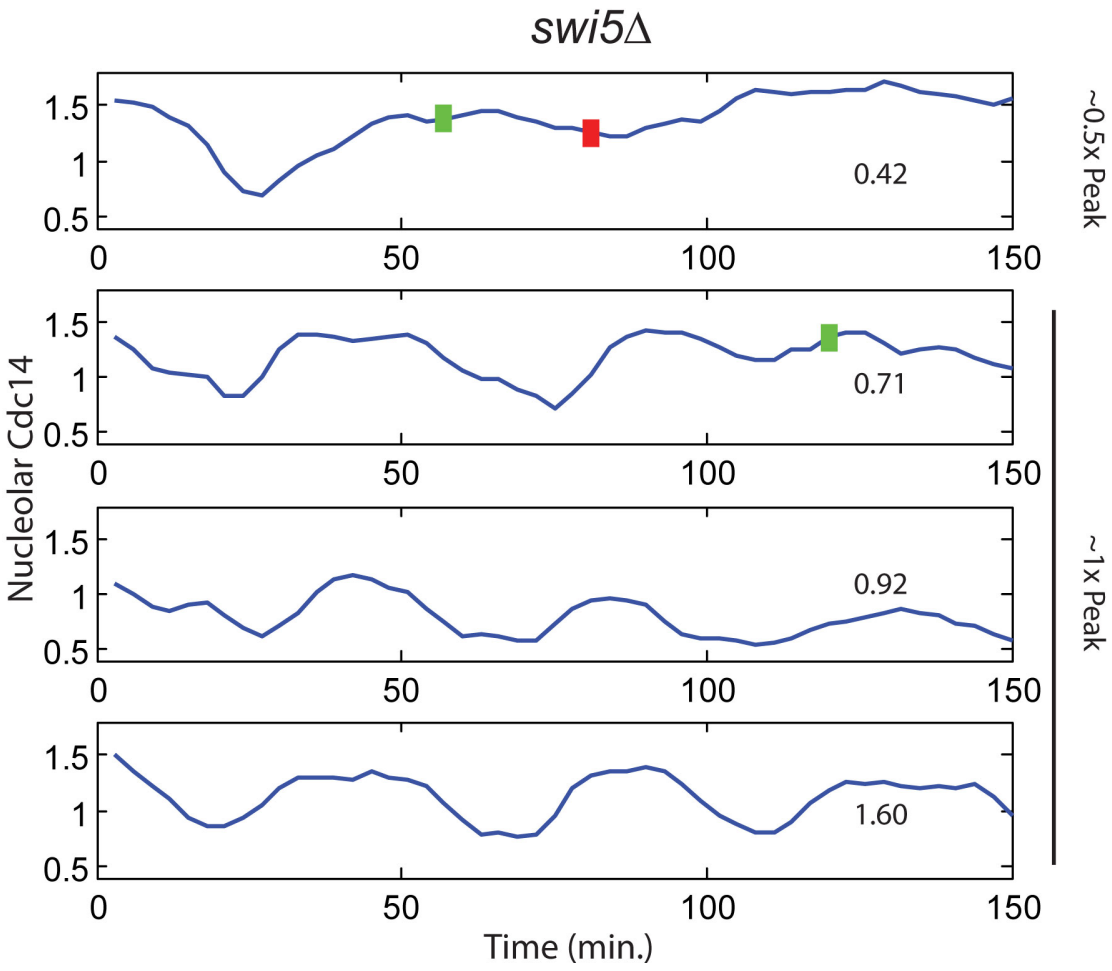

Figure 4.9. **Cdc14 endocycle is not disrupted by SWI5 deletion**.

GAL1-CLB2kd-GFP was pulsed for 30 minutes in *swi5*Δ cells before observation. representative samples show that Cdc14 endocycles persisted in *swi5*Δ cells(n=66). The number on each panel is Clb2kd-GFP concentration in the 'peak' unit (Materials and Methods). Blue bars: anaphase; Green bars: budding; Red bars: cytokinesis.

3. Clb2kd levels quantitatively control the frequency of the Cdc14 release endocycle

Cdc14 release cycles exhibited an interesting dose-response to Clb2kd. In cells with a relatively low level of Clb2kd-GFP (less than ~0.5X peak), cell-cycle progression was not greatly disturbed, and a single cycle of Cdc14 release and resequestration followed anaphase (marked by nucleolar Net1 separation), as in normal cell cycles (Fig. 4.10A, category 1). Cdc14 release in the next cell cycle of 'category 1' cells was frequently delayed, possibly due to 2^{nd}-cycle defects caused by low Clb2kd (Drapkin et al. in press). At intermediate levels of Clb2kd-GFP (around 0.75X peak), cytological ME was delayed but not blocked by Clb2kd, as reported (Drapkin et al., in press). In some of these cells, a 2^{nd} Cdc14-release event occurred rapidly after bud emergence, without an associated anaphase (Fig. 4.10A, category 2). At >=1X peak Clb2kd concentrations, the 2^{nd} (and frequently additional) Cdc14 release/resequestration cycles happened without cytokinesis, rebudding, *CLN2pr* expression or any other markers of cell cycle progression; these category 3 cells exhibits the endocycle phenotype characterized above (Fig. 4.10A, category 3).

Figure 4.10. **Clb2kd level controls the Cdc14 endocycle period.** **A.** Trajectories for Clb2kd-pulsed cells. Category 1: essentially normal cell-cycle progression (though with 2nd cycle Clb2kd-induced delays; Drapkin et al., submitted); Category 2: a second Cdc14 release occurred between rebudding and nucleolar separation in the next cell cycle; Category 3: Cdc14 endocycles without cytokinesis or rebudding. Below: category means and standard deviations of Clb2kd-GFP concentration (blue) and Cdc14 release intervals (red) . **B.** Cdc14 release frequencies plotted against Clb2kd-GFP level for cell categories: inverse of intervals between first and second Cdc14 release (categories 1 and 2), or average frequencies of one cell's Cdc14 endocycles (category 3). Shaded: range of cell cycle frequencies for cycling *MET3-CDC20* mother cells.

Figure 4.10

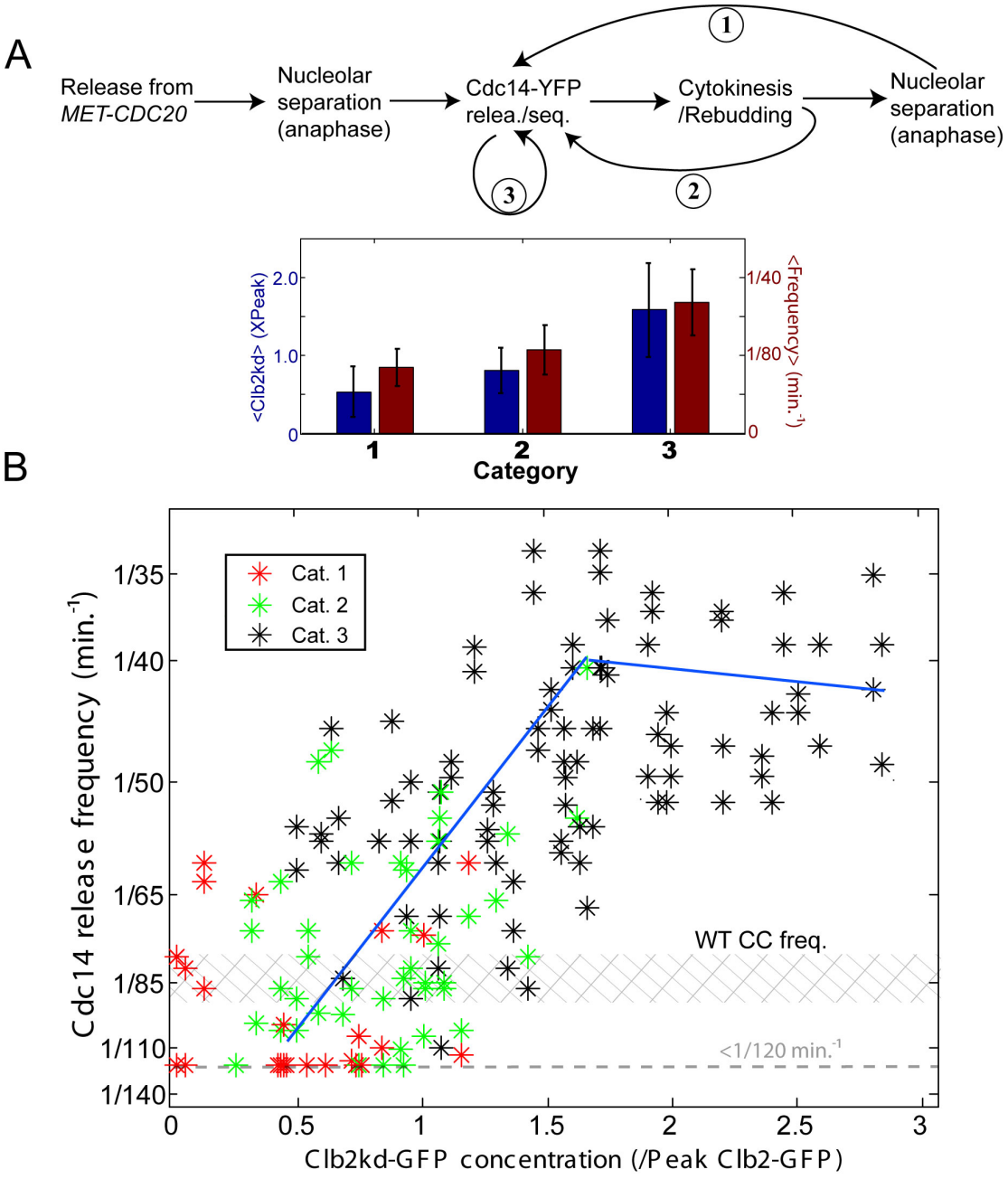
A
Release from
MET-CDC20
Nucleolar
separation
(anaphase)
Cdc14-YFP
relea./seq.
Cytokinesis
/Rebudding
Nucleolar
separation
(anaphase)
1
2
3
<Clb2kd> (XPeak)
<Frequency> (min.-1)
Category
B
Cat. 1
Cat. 2
Cat. 3
Cdc14 release frequency (min.-1)
Clb2kd-GFP concentration (/Peak Clb2-GFP)
WT CC freq.
<1/120 min.-1

It is interesting to note that category 2 cells represent an intermediate phenotype between normal tight linkage of Cdc14 release to cell cycle progression, and complete uncoupling as in category 3 endocycling cells. Therefore, there is likely a continuous transition from normal Cdc14 release cycles to endocycle phenotypes with increasing Clb2kd concentrations.

By plotting the frequencies of Cdc14-release oscillation versus the concentration of Clb2kd-GFP, I observed a positive correlation below ~1.7x peak Clb2kd concentration ($P<2*10^{-7}$, using only data from cells that undergo endocycles without apparent cell cycle progression; 'category 3' in Fig. 4.10. A quantitatively similar and highly significant positive correlation was observed using all three categories of cells). This continuous response across the different phenotypic categories suggests that frequency of Cdc14 release may be directly controlled by Clb2 levels, independent of occurrence of some events of cell cycle progression. At higher Clb2kd, the endocycle frequency saturated at about once every 45 minutes (Fig. 4.10B). For simplicity, I fitted this correlation with a linear step function. This correlation is highly significant, and the slope determined with rather narrow confidence intervals (Fig. 4.10B legend). There is obviously very considerable noise about this linear fit, which could be due to the intrinsic heterogeneity in the cell population. In what follows, I will make use solely of the average dose-response relationship.

Although the frequencies of Cdc14 release cycles were positively controlled by Clb2kd, the amplitude and duration of Cdc14 release (whenever it occurred) did not significantly correlate with Clb2kd-GFP concentration (Fig. 4.4).

These quantitative observations are important for my theoretical analysis below.

4. Requirement for Cdc14 release endocycle

A free-running oscillator may drive G1 events in the absence all B-type cyclins (Haase and Reed, 1999; Orlando et al., 2008). It was important to determine if this oscillator might also drive Cdc14 endocycles. To test this, I overexpressed a stable Clb-Cdk inhibitor Sic1-4A from a *GAL1* promoter to inhibit all B-type cyclin-Cdk activity (Verma et al., 1997). Multiple budding without cell division (manifesting the free-running G1 oscillator, as described (Haase and Reed, 1999)) was observed following Clb inhibition. However, I did not detect any Cdc14-release events in a 6 hour time-course in these cells (Fig. 4.11) (this result, when compared to the Clb2kd results, also has the interesting implication that Cdc14 release endocycles may have a minimum 'permissive' level of mitotic cyclin activity required for their occurrence). Conversely, to test if Cdc14 was an essential component for the G1 oscillator, I constructed a strain harboring a temperature-sensitive mutant of *cdc14-1* with all B-cyclin deleted. I counted the multiple-budding phenotype in a time-course experiment from small G1 cells by elutriation, and found that *cdc14-1* cells formed a second bud as efficiently as wild-type cells (Fig. 4.12). Therefore, I conclude that the Cdc14 release and G1 endocycles are driven by distinct and independent mechanisms.

The mitotic exit network (MEN) is a major regulator of Cdc14 release during late

anaphase (Stegmeier and Amon, 2004). Cdc14 endocycles required the MEN component Cdc15, even after allowing an initial round of Cdc14 release (showing that the MEN is required for maintenance as well as initiation of endocycling) (Fig. 4.13D). The FEAR network is involved in a transient wave of early anaphase Cdc14 release (Stegmeier et al., 2002); Cdc14 endocycles did not require the FEAR network component Spo12, or Net1 phosphorylation by Clb-Cdk, a key event in FEAR pathway activation (Azzam et al., 2004; Queralt et al., 2006) (Fig. 4.14). In *bub2Δ* cells, MEN activity is likely to be near-constitutive (Alexandru et al., 1999; Pereira et al., 2000; Xu et al., 2000). The Cdc14 release endocycles persisted in *bub2Δ* cells in the presence of Clb2kd (Fig. 4.14), suggesting that the Cdc14 endocycle may not be driven by oscillations of MEN activity.

Figure 4.11

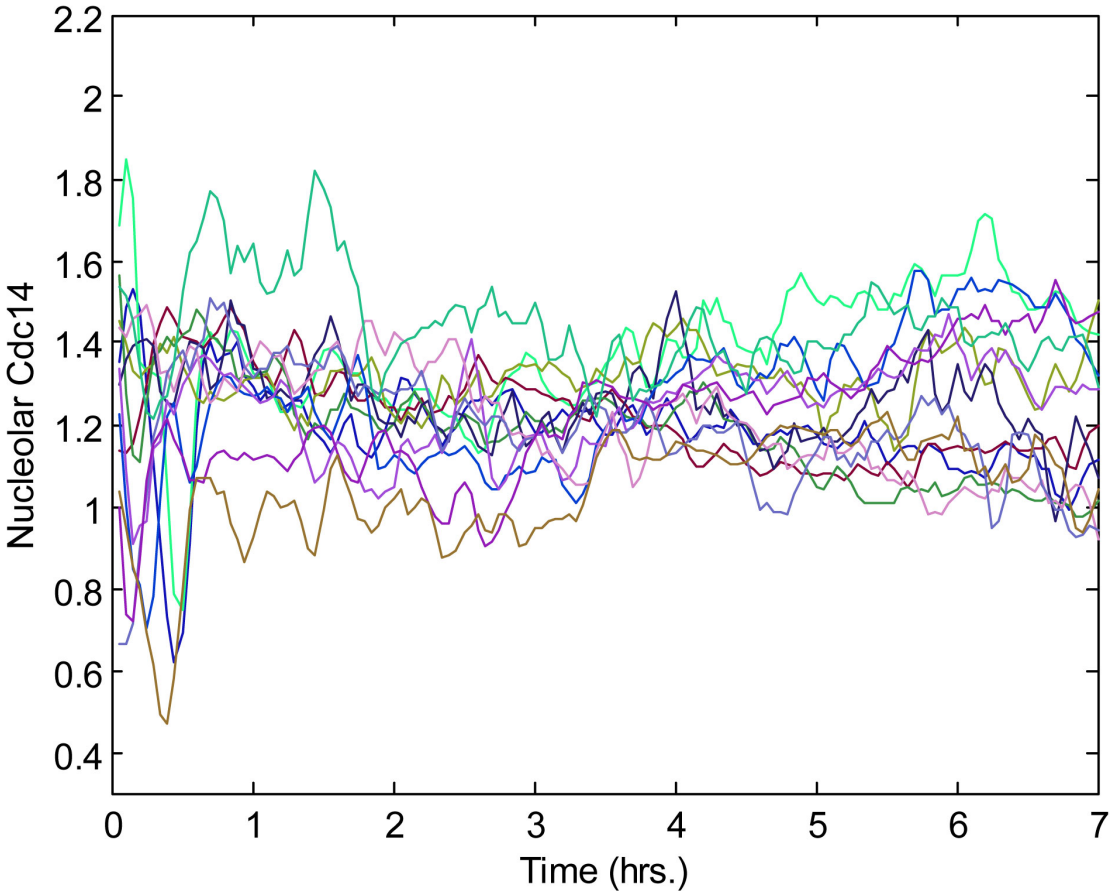

Figure 4.11. **Cdc14 release did not happen in Sic1-4A expressing cells.**

GAL1-SIC1-4A cells were grown in raffinose medium, then transfered to galactose medium to make time-lapse movies (t=0). No Cdc14 release was detected during the experiment except in the initial cell cycle. 14 independent cells are shown here (n=36).

Figure 4.12

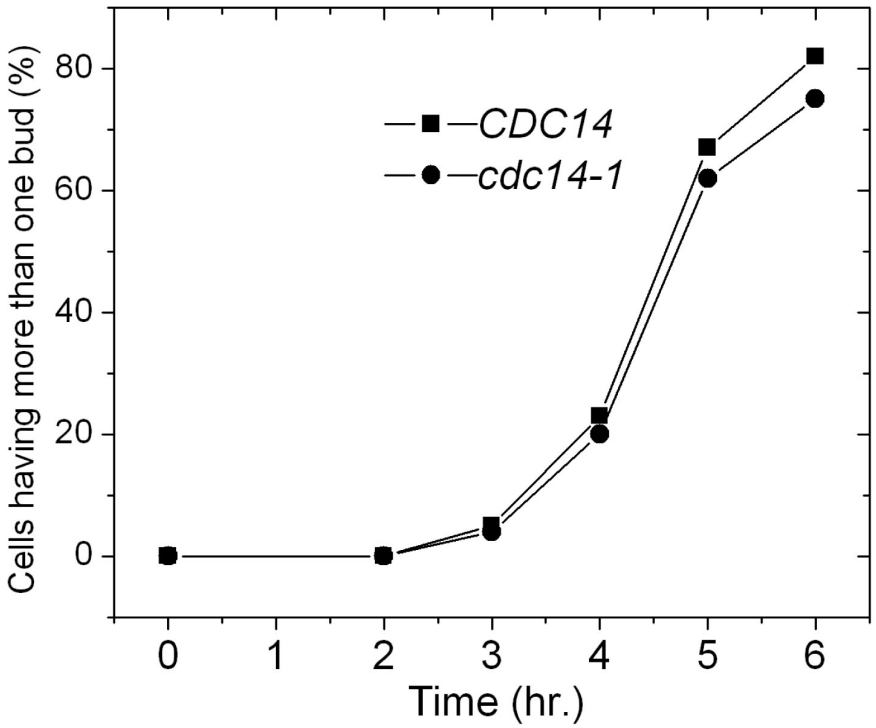

Figure 4.12. **The budding endocycle in *clb1~6*Δ cells was independent of Cdc14.** *clb1~6*Δ *GAL1-CLB2 swe1*Δ with *CDC14* or *cdc14-1* was grown in galactose medium at 23˚. Small G1 cells were collected through elutriation, and released into glucose medium at 37˚. Cells were harvested and counted for multi-budding phenotype at indicated time points.

Figure 4.13. **Requirements for Cdc14 endocycles.** **A.** As in Fig. 4.1B, but cells also *cdc5::3XCDC5ΔNT* . Among cells whose rebudding was delayed for at least 25 minutes (implying >1X peak Clb2kd, Fig. 4.3), 19/36 cells showed fast Cdc14 release and resequestration, followed by prolonged Cdc14 release. 8/36 showed only prolonged Cdc14 release. **B.** As in Fig. 4.1D, but also *cdh1Δ*; 30 min Clb2kd-GFP pulse; typical traces for the indicated Clb2kd-GFP ranges. Among cells with >1X peak Clb2kd-GFP (n=86), 41% showed a prolonged Cdc14 release period (middle two traces); 43% (cells with highest Clb2kd-GFP) showed release endocycles with a reduced amplitude (bottom trace); Blue bars: anaphase; Red bars: cytokinesis; green bars: bud emergence. **C.** *CDC5pr-GFP* cells, as in Fig. 4.1B. Trough GFP intensities before rebudding plotted against rebudding times; rebudding delay indicates Clb2kd levels; sample traces below. **D.** Cells as in Fig. 4.1D, but also *cdc15-2* or *cdc5-1*; after 35 min to allow initial Cdc14 release, cells were plated for time-lapse at 37^{o}C (restrictive temperature) (t=0). CHX: as above, except that time-lapse medium contained 0.2ng/µl cycloheximide (CHX). Among cells with >1X peak Clb2kd-GFP, 18/24 *CDC15 CDC5* cells, 0/22 *cdc15-2*, 0/30 *cdc5-1* and 3/64 cells in CHX exhibited Cdc14 release endocycles.. Blue bars: anaphase; green bars: bud emergence. **E**: As in Fig. 4.1B, but *CDC5-GFP* cells; 30 min Clb2kd pulsed; typical traces of Cdc14 release and Cdc5-GFP levels are shown. In 36/45 Cdc14-endocycling cells, Cdc5-GFP signal oscillated in-phase with Cdc14 release. **F.** ODE model simulating Cdc14-Cdh1-Cdc5 negative feedback (Materials and Methods).

Figure 4.13

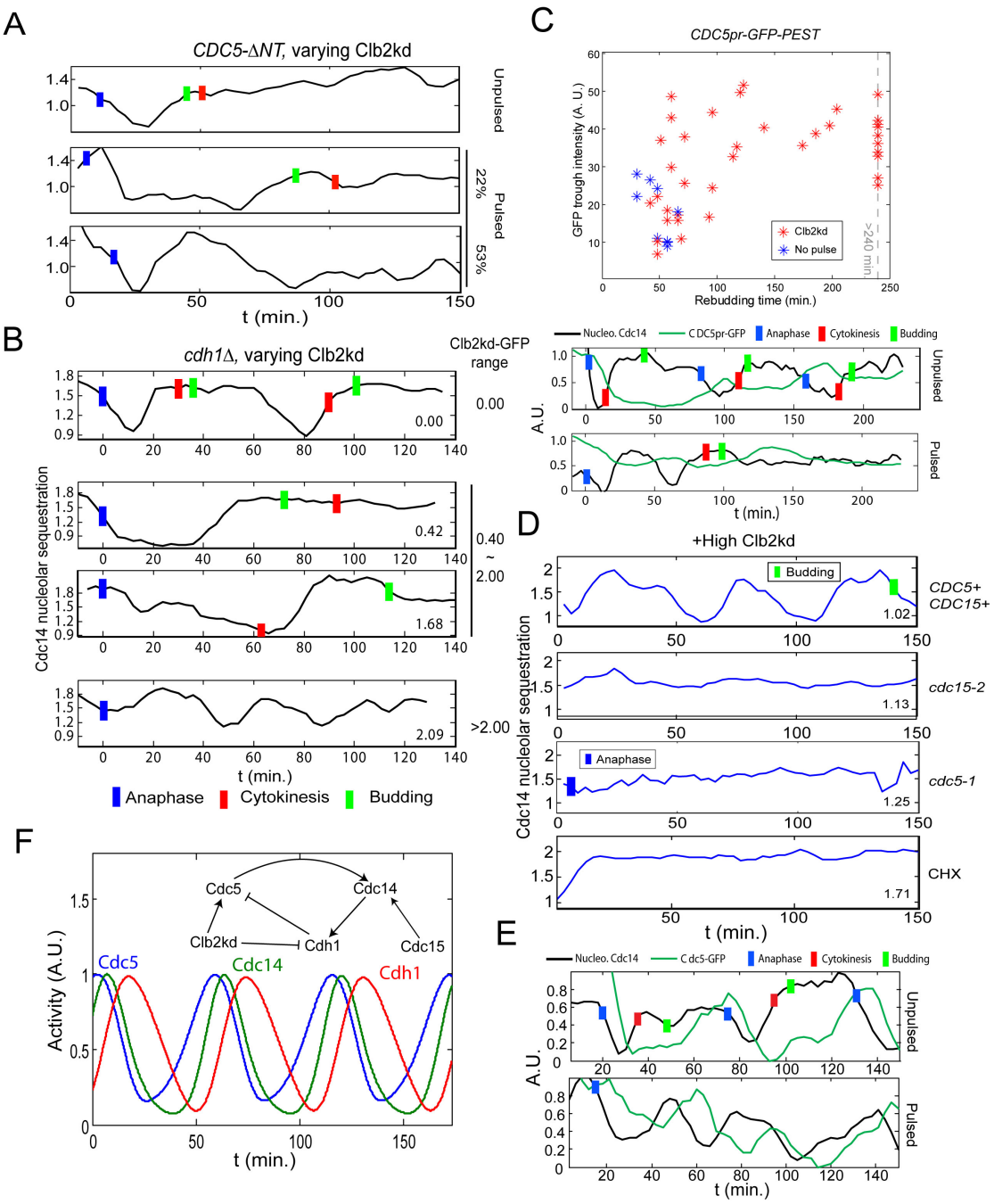
A
CDC5-ΔNT, varying Clb2kd
Unpulsed
Pulsed
22%
53%
t (min.)
B
cdh1Δ, varying Clb2kd
Clb2kd-GFP range
0.00
0.40 ~ 2.00
>2.00
Cdc14 nucleolar sequestration
t (min.)
Anaphase
Cytokinesis
Budding
C
CDC5pr-GFP-PEST
GFP trough intensity (A. U.)
Clb2kd
No pulse
>240 min.
Rebudding time (min.)
Nucleo. Cdc14
CDC5pr-GFP
Anaphase
Cytokinesis
Budding
A.U.
Unpulsed
Pulsed
t (min.)
D
+High Clb2kd
Budding
CDC5+ CDC15+
cdc15-2
Anaphase
cdc5-1
CHX
Cdc14 nucleolar sequestration
t (min.)
E
Nucleo. Cdc14
Cdc5-GFP
Anaphase
Cytokinesis
Budding
A.U.
Unpulsed
Pulsed
t (min.)
F
Cdc5
Cdc14
Clb2kd
Cdh1
Cdc15
Activity (A.U.)
t (min.)

Polo kinase Cdc5 is essential for Cdc14 release, in both the FEAR and MEN pathways, and Cdc5 overexpression can drive ectopic Cdc14 release in S-phase-blocked cells (Visintin et al., 2003). Using a *cdc5-1* temperature-sensitive mutation, I determined that Cdc5 activity was absolutely required for maintenance of Cdc14 endocycles (Fig. 4.13D).

Thus, Cdc14 endocycles in Clb2kd-blocked cells share requirements with normal late-anaphase Cdc14 release, supporting the idea that the endocycles may involve mechanisms controlling Cdc14 release in the free-running cell cycle.

Cdc14 endocycles in Clb2kd-blocked cells require resequestration into the nucleolus after each release. Cdc5 is essential for normal Cdc14 release, and Cdc5 is down-regulated at the end of mitosis by inactivation of its transcription and by Cdh1-APC-dependent proteolysis (Charles et al., 1998; Shirayama et al., 1998); Cdc5 proteolysis contributes to Cdc14 resequestration into the nucleolus (Visintin et al., 2008). Therefore, to ask if resequestration in endocycles shared requirements with resequestration in the free-running cycle, I tested Cdh1-resistant Cdc5-*ΔNT* (using *3X CDC5-ΔNT*, an allele that produces near-wild-type Cdc5 kinase levels, without proteolytic regulation of Cdc5 protein abundance (Visintin et al., 2008)). *3X CDC5-ΔNT* severely inhibited Cdc14 endocycles. In *3X CDC5-ΔNT* cells deduced to contain >1X peak Clb2kd, I did not detect multiple Cdc14 release endocycles. Instead, 22% of cells showed an extended Cdc14 release period, and 52% of cells had

a short Cdc14 release/re-sequestration cycle prior to a long release period (Fig. 4.13A). As noted above, the release period in Cdc14 endocycles in *CDC5+* cells are of normal duration and amplitude, unlike the very long release periods in *3X CDC5-ΔNT* cells.

CDH1 is required for cell-cycle-regulated Cdc5 degradation. Consistent with results with *CDC5-ΔNT*, *cdh1Δ* but not *CDH1* cells containing 0.5X to 2X peak Clb2kd released Cdc14 for up to 80 minutes, and did not exhibit Cdc14 endocycles (Fig. 4.13B). Surprisingly, however, I observed Cdc14 endocycles in *cdh1Δ* cells with > 2X peak Clb2kd, but release was incomplete (about half the normal amplitude) (Fig. 4.13B). This result indicates the existence of a parallel Cdh1-independent pathway allowing Cdc14 endocycles; but the primary mechanism likely requires Cdh1-dependent proteolysis of Cdc5, dependent on the Cdc5 N-terminal destruction box.

Figure 4.14

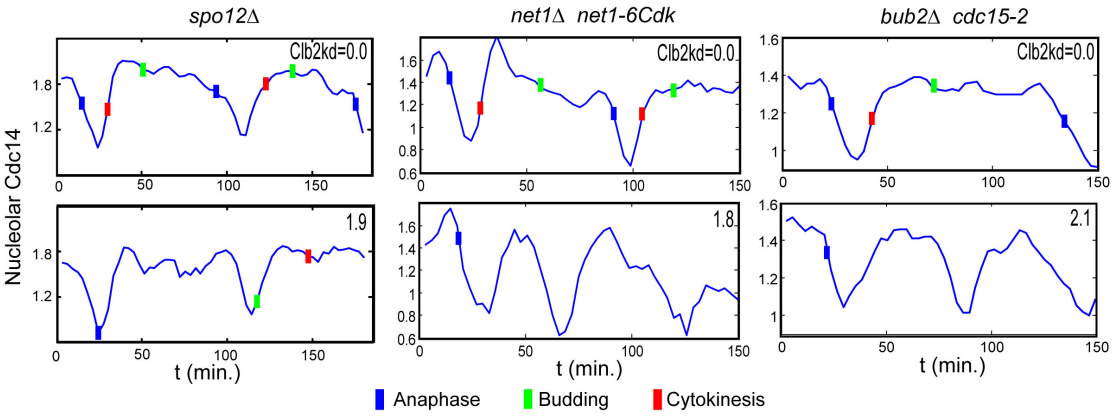

Figure 4.14. **Cdc14 endocycles occured in *spo12*Δ, *net1-6Cdk, bub2*Δ cells.** All three strains contain *MET-CDC20 CDC14-YFP NET1-mCherry MYO1-GFP GAL1-CLB2kd-GFP GAL4-rMR* with additional genotypes indicated above. Cultures were pulsed with Clb2kd-GFP for 30 minutes, and subjected to time-lapse microscopy analysis as in Fig. 4.1D. Unpulsed controls are shown in the top row. *bub2*Δ *cdc15-2* cells were arrested and pulsed at 34°, and released at 27° (Using cdc15-2 is to achieve a stable arrest at cdc20-). Among cells with >1X peak zation.pdf</url></*pdf-ur*ls></urls><la*nguage*>*eng*</language></*record*></Cite></EndNote>¶ (Visintin et aphenotypes.

5. A Cdc14-Cdh1-Cdc5 negative feedback mechanism contributes to Cdc14 endocycle

Cdc14 endocycles are abrogated either by loss of Cdc5 (in *cdc5-1* cells), or by blocking Cdc5 degradation, presumably increasing Cdc5 levels (in *CDC5-ΔNT* or *cdh1Δ* cells). This could reflect a requirement for *cyclical* Cdc5 activity for Cdc14 endocycles, since they are prevented by either constitutively high or constitutively low Cdc5.

I hypothesized that mitotically active Cdc5 would promote Cdc14 release, Cdc14 would activate Cdh1 leading to Cdc5 proteolysis, and Cdc14 would reaccumulate in the nucleolus. In the wild-type cell cycle, Cdc5 cannot reaccumulate until the next M-phase: *CDC5* is co-transcribed with *CLB2* under Clb2-dependent positive feedback control (Wittenberg and Reed, 2005), so Clb2 removal at anaphase blocks further *CDC5* transcription. In addition, absence of Cdk activity in G1 keeps Cdh1 active until later cyclin-Cdk reactivation. In Clb2kd-blocked cells, though, persistent Clb2kd could both maintain *CDC5* transcription, and inactivate Cdh1, in the absence of counterbalancing dephosphorylation by Cdc14, allowing rapid reaccumulation of Cdc5 and endocyclic Cdc14 release and resequestration. This negative feedback hypothesis would explain the absence of endocycles in *cdc5-1*, *CDC5-ΔNT* and *cdh1Δ* cells.

Consistent with this hypothesis, I observed higher trough levels and rapid rebound of *CDC5* transcription in Clb2kd-pulsed cells compared to unpulsed controls (Fig. 4.13C), using a cell-cycle-regulated *CDC5pr-GFP* reporter (J. Skotheim, pers. comm.).

Also consistent with the hypothesis, Cdc14 endocycles required new protein synthesis, since endocycles were blocked by addition of cycloheximide after an initial Cdc14 release (Fig. 4.13D). Finally, in cells undergoing Cdc14 endocycles, I observed cyclical accumulation and degradation of Cdc5-GFP fusion protein expressed from the endogenous promoter, in approximately the expected phase relative to Cdc14 release (Fig. 4.13F).

A qualitative ODE model (Fig. 4.13E) of a Cdc5-Cdc14-Cdh1 negative feedback loop reproduced my major qualitative results, including dependence of Cdc14 endocycle frequency on Clb2kd concentrations (Fig. 4.10B; Fig. 4.15).

Figure 4.15

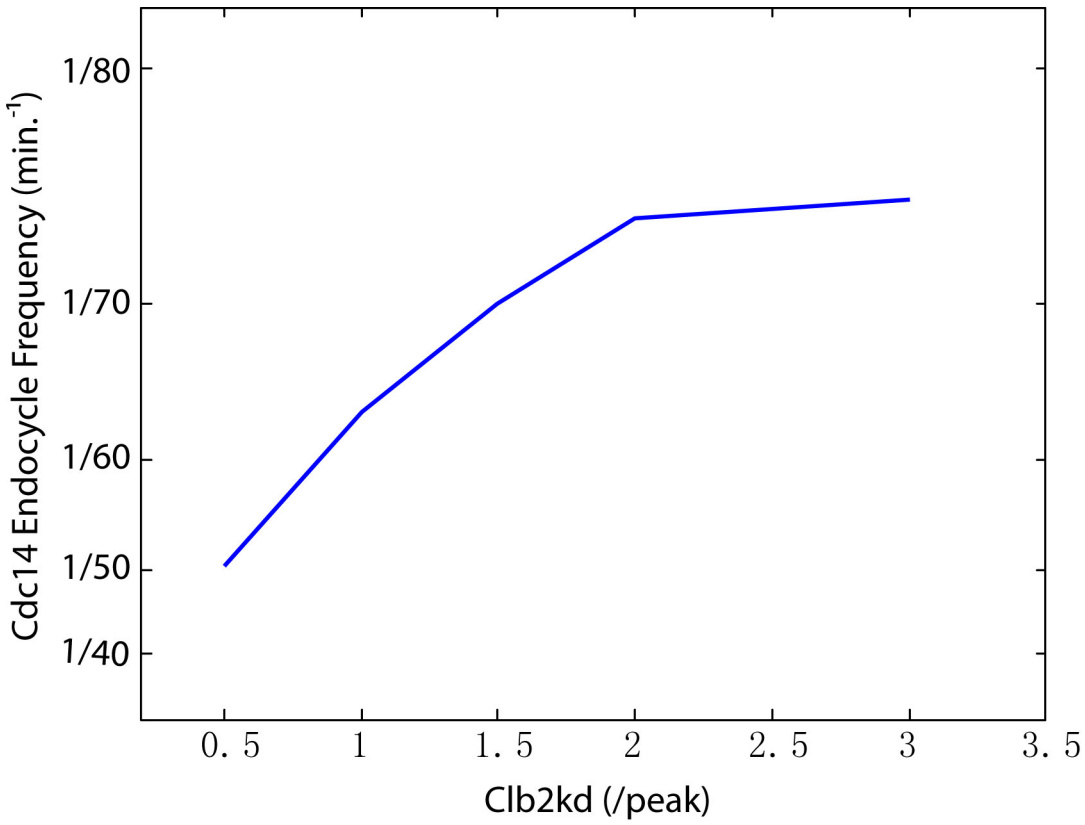

Figure 4.15. **Cdc14 endocycle frequency vs. Clb2kd level by ODE simulation.** Clb2kd concentration was changed continuously as a parameter in the ODE model simulating Cdc5-Cdc14-Cdh1 negative feedback (Materials and Methods). Cdc14 release frequency was calculated from the simulation.

This negative feedback mechanism is probably the main but not the only source of Cdc14 endocycles. Cdh1-dependent Cdc5 degradation cannot be strictly essential for resequestration, since resequestration was delayed but not blocked in *CDC5-ΔNT* and *cdh1Δ* cells, and I observed low-amplitude endocycles in *cdh1Δ* cells at very high (>2X peak) Clb2kd levels.

6. An intrinsic oscillatory module may control normal Cdc14 release in unperturbed cell cycles

I used cell cycle block with undegradable Clb2 to demonstrate an oscillatory module controlling Cdc14 localization in the absence of cyclin-Cdk oscillations.

The emergence of Cdc14 release endocycles at high (but physiological) Clb2kd levels could come about because Clb2kd accelerates the Cdc14-release-control module (Fig. 4.10B) and greatly delays Clb-Cdk oscillation, temporally separating these oscillators. Mechanistically, acceleration of the Cdc14 module could derive from rapid rebound of the Cdc5-Cdc14-Cdh1 negative feedback oscillator with high locked Clb2 levels (see above); the stalling of the Clb-Cdk oscillation is a direct consequence of blocking Clb2 degradation.

Cdc14 endocycle phenotypes are only of clear physiological importance only if this module and its self-oscillatory behavior are coupled to normal Cdc14 release in unperturbed cell cycles. However, any experiments trying to reveal the module's intrinsic behavior will inevitably perturb normal cell cycle progression. Therefore, I try to answer this question in two steps: 1. whether the Cdc14-release module can oscillate autonomously in free-running cell cycles; 2. whether normal Cdc14 release cycles are also promoted by self-oscillatory behavior of this module. To study the

first question, I looked for ways to uncouple the hypothetical Cdc14 oscillatory module from the Clb-Cdk oscillator, without blocking the cell cycle. Genetic manipulations providing sufficient uncoupling could allow detection of Cdc14 release endocycles in a free-running cell cycle. Plausible coupling components include: 1. *CDC5* transcription, activated by Clb-Cdk; 2. Cdh1, activated by Cdc14 and degrading Clbs and Cdc5; 3. the MEN, indirectly activated by mitotic cyclin-Cdk, since anaphase (promoted by cyclin-Cdk (Fitch et al., 1992)) in turn activates the MEN (Fig. 4.16).

Figure 4.16. **Cdc14 release endocycles in free-running cell cycles or with low Clb2kd.** **A.** Cdc14 release and Clb-Cdk control mechanisms. Left: potential autonomous Cdc14 release oscillator; right: Clb-Cdk negative-feedback oscillator. SPOC: spindle orientation checkpoint. **B.** Cdc14 release analyzed as in Fig. 4.1D, in *bub2Δ cdh1Δ* and *GAL1-URL-CDC5* cells (cycling cells, without *cdc20* block-release or Clb2kd pulse). A representative lineage (M0: mother, D1, D2...sequential daughters) exhibiting ectopic Cdc14 release (red) before bud emergence. Cdc14 release curves shifted for visualization. Below: frequencies of G1 Cdc14 endocycles. **C.** 67μM Latrunculin-B (LAT-B) was added to the medium (t=0) to inhibit budding of a cycling *bub2Δ cdh1Δ* strain. 32/44 cells demonstrated G1 Cdc14 endocycles. 14/19 daughter cells and 13/19 mother cells exhibited endocycles (maximum 4 endocycles; average=2.8). **D**. *MET-CDC20 bub2Δ cdc15-2* cells were arrested in metaphase at 34℃ and pulsed with Clb2kd-GFP for 20 minutes (using *cdc15-2* is to achieve a stable cdc20- block), then released into cell cycle at 27℃ with 67μM LAT-B to observe. The first anaphase (nucleolar separation) happened with normal kinetics. LAT-B effectively blocked budding, cytokinesis, and all subsequent anaphase in ~90% cells. 39/46 cells containing 0.2~1.0x peak Clb2kd-GFP demonstrated Cdc14 endocycles. Four traces are shown. The 'Cdc14 endocycle frequency vs. Clb2kd-GFP levels' information is plotted together with the data in Fig. 4.10B. Blue bars: anaphase; green bars: budding.

Figure 4.16

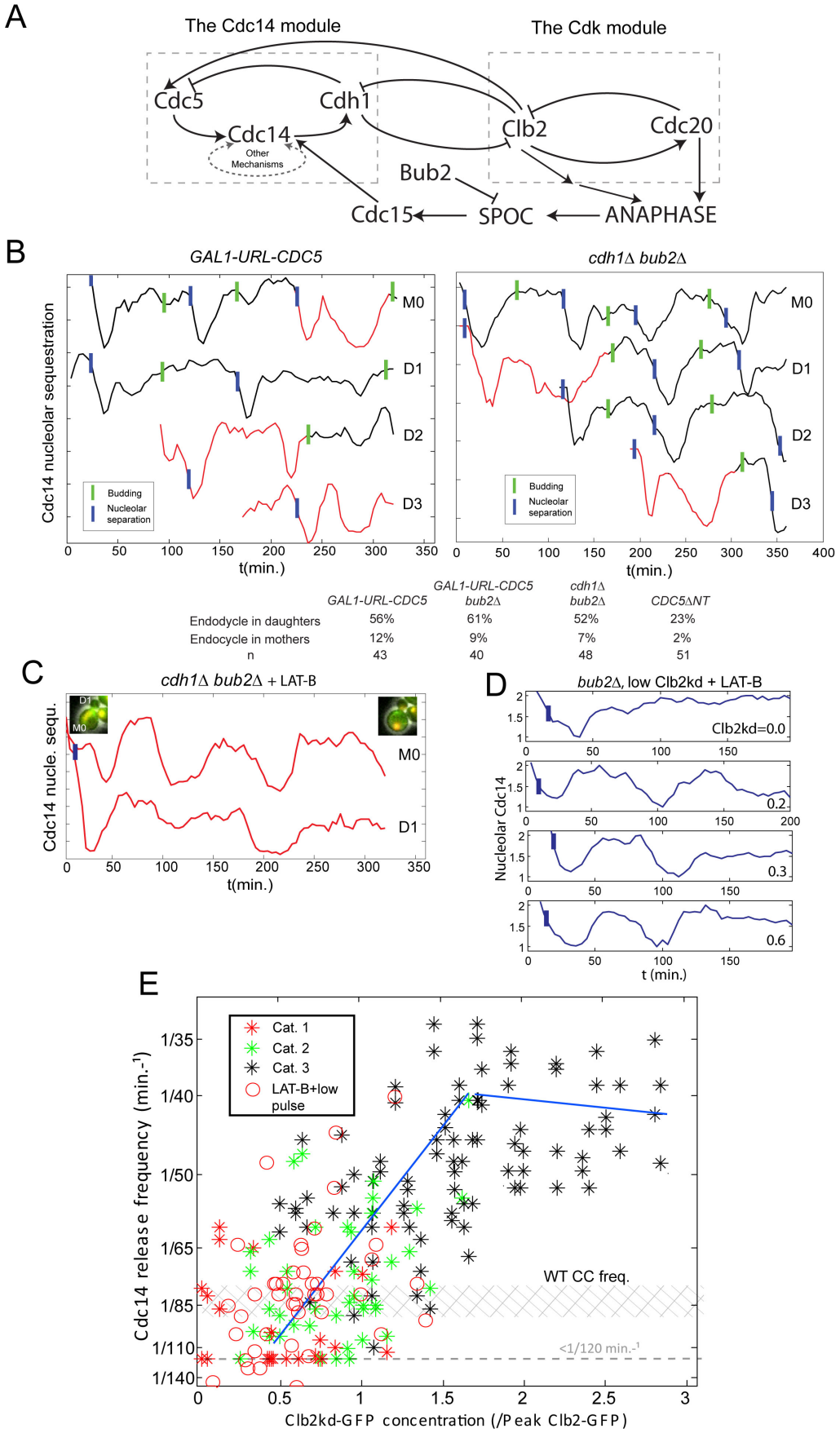
A
The Cdc14 module
The Cdk module
Cdc5
Cdh1
Cdc14
Other Mechanisms
Clb2
Cdc20
Bub2
Cdc15
SPOC
ANAPHASE
B
GAL1-URL-CDC5
cdh1Δ bub2Δ
Cdc14 nucleolar sequestration
M0
D1
D2
D3
Budding
Nucleolar separation
t(min.)
GAL1-URL-CDC5
GAL1-URL-CDC5 bub2Δ
cdh1Δ bub2Δ
CDC5ΔNT
Endocycle in daughters 56% 61% 52% 23%
Endocycle in mothers 12% 9% 7% 2%
n 43 40 48 51
C
cdh1Δ bub2Δ + LAT-B
Cdc14 nucle. sequ.
D1
M0
t(min.)
D
bub2Δ, low Clb2kd + LAT-B
Clb2kd=0.0
0.2
0.3
0.6
Nucleolar Cdc14
t (min.)
E
Cat. 1
Cat. 2
Cat. 3
LAT-B+low pulse
Cdc14 release frequency (min.-1)
1/35
1/40
1/50
1/65
1/85
1/110
1/140
WT CC freq.
<1/120 min.-1
Clb2kd-GFP concentration (/Peak Clb2-GFP)

Following this reasoning, I tested the effects of making *CDC5* transcription independent of Clb-Cdk, using a *GAL1-URL-CDC5* construct (Visintin et al., 2008); the destabilizing *URL* tag was required to keep Cdc5 at a non-lethal level). *GAL1-URL-CDC5* cells are fully viable in galactose medium. Consistent with the oscillatory module hypothesis, I observed a G1-specific Cdc14 release endocycle in ~70% of daughter cells (Fig. 4.16B). The observation of Cdc14 endocycles in G1 is completely unexpected on the basis of any model involving ratchet-type control by cyclin-Cdk. (G1 cells stably contain almost no cyclin-Cdk activity (Mendenhall and Hodge, 1998), so any event controlled by a cyclin-Cdk ratchet event has no basis for repeated activity in G1 cells).

Deletion of *CDH1* could also be predicted to weaken the coupling. However, I did not observe Cdc14 endocycles or Cdc14 release anomalies in cycling *cdh1Δ* cells. One explanation for this could be that Cdh1 plays an important role not only in coupling, but in the Cdc14 intrinsic oscillatory mechanism itself (see above; Fig. 4.13B). My data suggest, though, that Cdh1 is not absolutely essential for Cdc14 cycles, since Cdc14 resequestration is eventually observed in Clb2kd-pulsed *cdh1Δ* cells, and at high Clb2kd levels, low amplitude Cdc14 endocycles re-emerge. If this idea is correct, more complete decoupling could reveal Cdc14 release endocycles in the absence of Cdh1, if they can be driven by parallel coupled pathway(s). I further reduced the coupling by deleting *BUB2*, removing an MEN inhibitor that keeps MEN activation dependent on anaphase (Fesquet et al., 1999; Pereira et al., 2000), and thus,

indirectly, dependence on mitotic cyclins that are required for anaphase (Fitch et al., 1992). Similar to *GAL1-URL-CDC5* cells, I observed G1-specific Cdc14 release endocycles in cycling *cdh1Δ bub2Δ* cells (again only in daughter cells and with incomplete penetrance) (Fig. 4.16B). *BUB2* deletion slightly increased the penetrance of Cdc14 endocycle phenotypes in *GAL1-URL-CDC5* cells (Fig. 4.16B; 4.17), but did not alone induce endocycles (data not shown). *CDC5-ΔNT* in a *CDH1 BUB2* background also induced G1 Cdc14 endocycles (Fig. 4.18).

Figure 4.17

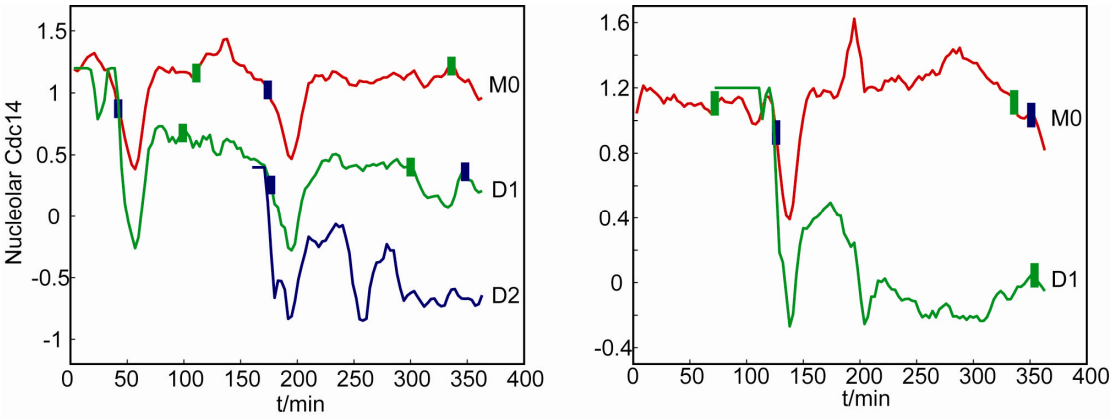

Figure 4.17. **Cdc14 endocycles in G1 *bub2*Δ *cdc5::GAL1-URL-CDC5* cells.**

Asynchronous *bub2*Δ *cdc5::GAL1-URL-CDC5* cells were grown in galactose medium and subjected to time-lapse microscopy analysis. Two examples here show Cdc14 release endocycles in G1 daughter cells. Traces are shifted along Y-axis for presentation. In the whole population, 61% daughter cells show the endocycle phenotype(n=18). Only 9% mother cells show this phenotype(n=22). The mother cell M0 gave rise to the first daughter cell D1, and the second daughter cell D2. Blue bar: anaphase; green bar: budding.

Figure 4.18

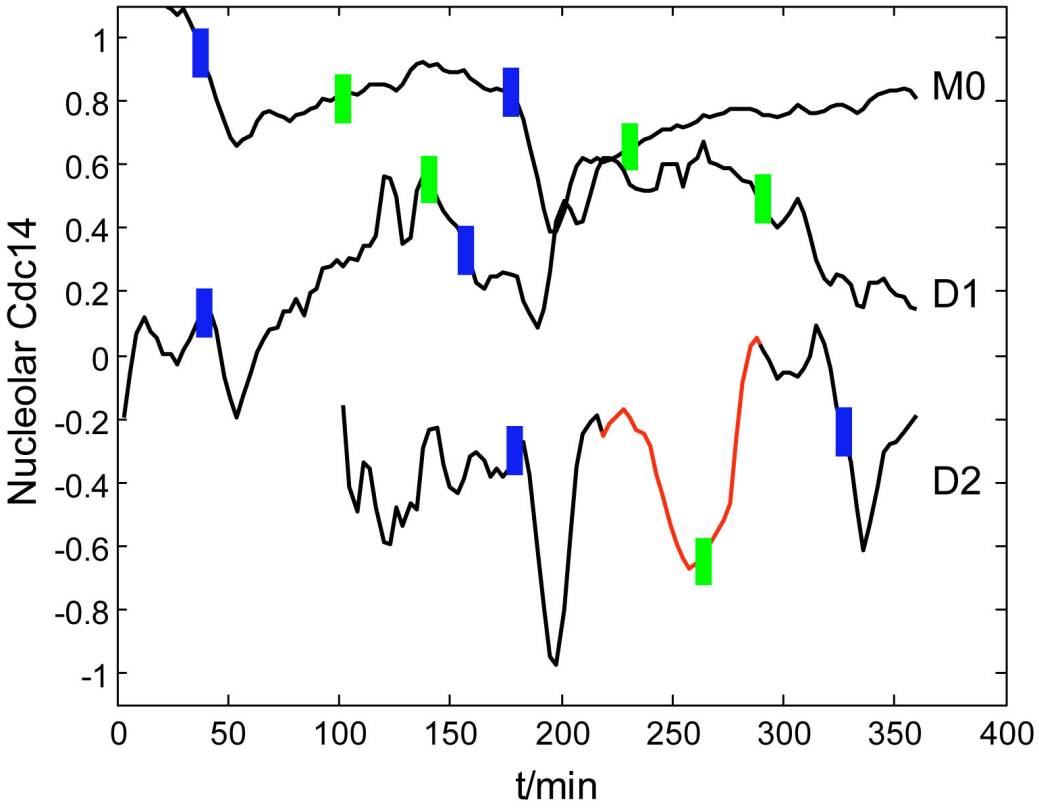

Figure 4.18. **Cdc14 endocycles in G1 *cdc5::3xCDC5*Δ*NT* cells.** Log phase *cdc5::3xCDC5*Δ*NT* culture was subjected to time-lapse microscopy analysis. An example shows Cdc14 release endocycles in a G1 daughter cell (D2). The mother cell M0 gave rise to the first daughter cell D1, then the second daughter cell D2. In the whole population, 23% daughter cells showed the endocycle phenotype in G1 (red; n=21); Only 3% mother cells showed this phenotype (n=30). Traces were shifted along Y-axis for presentation. Blue bars: anaphase; green bars: budding.

The daughter-preference of the endocycle phenotype could be due to G1-cyclin-dependent relocalization of MEN activators such as Lte1 to the incipient bud (Jensen et al., 2002), thus sequestering these activators until spindle pole entry into the bud in the next cell cycle. Mothers bud and express G1 cyclins much earlier than daughters (Di Talia et al., 2007), which could forestall any G1 Cdc14 endocycles, explaining the observed daughter preference of endocycles. Actin depolymerization with latrunculin B prevents budding; G1-cyclin-dependent Lte1 relocalization to the cortex still occurs but cortex-bound Lte1 cannot be sequestered in a bud (Jensen et al., 2002). Addition of latrunculin B to *cdh1Δ bub2Δ* cells allowed Cdc14 endocycles in G1 mothers as well as G1 daughters with equal probability (Fig. 4.16C). I observed up to four cycles of Cdc14 release and resequestration in these cells, in most cases without associated anaphase.

These results establish that the genetic network controlling Cdc14 localization has the intrinsic ability to oscillate even in free-running cell cycles. This demonstration required some alteration of normal control circuits, leaving the question open as to whether the Cdc14-release control module still exhibits self-oscillatory behavior when promoting normal Cdc14 release cycles in wild-type cells. There are some suggestions in the data so far presented that this could be the case. First, 'category 2' cells described above form an intermediate phenotype in a continuous transition from normal Cdc14 release cycles to the endocycle phenotype (Fig. 4.10A and text). The simplest explanation is that normal Cdc14 cycles and endocycles are driven by the

same network whose kinetic parameters are tuned by mitotic cyclin activity. Second, my estimate of the frequency of Cdc14 release oscillation at approximately mid-cell cycle Clb2 levels, by extrapolation, is ~95 minutes, i.e., close to the normal cell cycle frequency (Fig. 4.10B). Third, genetic requirements for Cdc14 endocycles and for normal Cdc14 release are similar. Both required Cdc5 and Cdc15, and shared a requirement for Cdh1-dependent degradation of Cdc5 for efficient Cdc14 resequestration. Fourth, the complete absence of Cdc14 endocycles at zero Clb-Cdk activity and the appearance of endocycles at ~1X peak Clb2kd (Fig. 4.11; 4.1), suggests that the Cdc14-release-control module undergoes a 'Hopf' bifurcation to give rise to limit cycle behaviors at a specific Clb2-Cdk level less than the peak. Direct measurement of the critical Clb2-Cdk level is difficult currently since Cdc14 release oscillation is coupled with cell cycle progression and endogenous Clb2 expression at sub-peak Clb2kd levels. However, 'Hopf' bifurcation is known to have a generic (independent of functional forms or parameters) property that the oscillation amplitude scales as $\sim\sqrt{(\boldsymbol{Clb2kd} - \boldsymbol{Clb2kd}^{Critical})}$ around the bifurcation point. In my experiments, Cdc14 endocycle always oscillates with full amplitude around 1X peak Clb2kd (Fig. 4.1; 4.4), suggesting that the critical Clb2kd level at bifurcation point should be significantly lower that 1x peak, which supports the idea that the Cdc14 control system also operates at an oscillatory zone in wild type cells.

To explore this question further, I study if the intact Cdc14-release module can still generate Cdc14 release cycles of a cell-cycle period under low Clb2 conditions

(comparable to average Clb2 in a cell cycle). With <1X peak Clb2kd, I used LAT-B to inhibit cytokinesis, budding and anaphase to study the autonomous behavior of this module. I also deleted *BUB2* to avoid the interference of SPOC. In the absence of cell cycle progression by LAT-B, Cdc14 release cycles of a 90-minute period emerged at 0.2X peak Clb2kd-GFP (Fig. 4.16D). With <1X peak Clb2kd, 39/46 cells exhibited Cdc14 endocycles, and the frequency-Clb2kd relationship followed a similar rule as in Fig. 4.10B (Fig. 4.16E). This result suggests that when promoting normal Cdc14 release, this module still exhibits self-oscillatory behavior, though entrained to cell cycle progression. Overall, those experiments suggest that this module and its oscillatory behavior may control normal Cdc14 release in unperturbed cell cycles, and the coupling of this module with cyclin-Cdk oscillator is required for maintaining once-per-cell-cycle Cdc14 release in mitosis.

Control of Cdc14 release by an autonomous oscillator must be compatible with the well-established restriction of Cdc14 release to late mitosis, at the end of the cyclin-Cdk cycle. In the following sections, I propose that the Cdc14 oscillator is entrained by the cyclin-Cdk oscillator, and extend this concept to other likely oscillatory modules controlling different cell cycle events.

7. Cyclin-Cdk oscillations could order cell cycle events through phase-locking

Besides the Cdc14 endocycle, other key cell cycle events can occur 'endocyclically' in the absence of mitotic cyclin-Cdk oscillation or overall cell cycle progression (see Introduction), and thus have the capacity to be driven by intrinsic oscillating modules. These observations are difficult to fit into the Cdk-ratchet model, since two essential components of the ratchet model, Cdk activity oscillation as the sole driver for cell cycle periodicity, and specific distinct Cdk thresholds for multiple steps in each process, are irrelevant in such situations. Therefore, I considered other ways that cyclin-Cdk oscillations could still order cell cycle events, independent of ratchet-like mechanisms.

My observation that the frequency of Cdc14 release endocycle was controlled by Clb2kd concentration (Fig. 4.10B) within a physiological range suggests that cyclin-Cdk oscillations could entrain other autonomous oscillatory modules to form an orderly and coherent cell cycle progression (Fig. 4.19A). Such entrainment, or 'phase-locking', is a known phenomenon in which oscillators with difference intrinsic frequencies can synchronize, if the frequency of one is controlled by the activity of the other (Glass, 2001; Winfree, 1967). When phase-locked, their stable phase offset is determined by their intrinsic frequency difference and simple properties of their

interactions (Winfree, 1967).

Figure 4.19

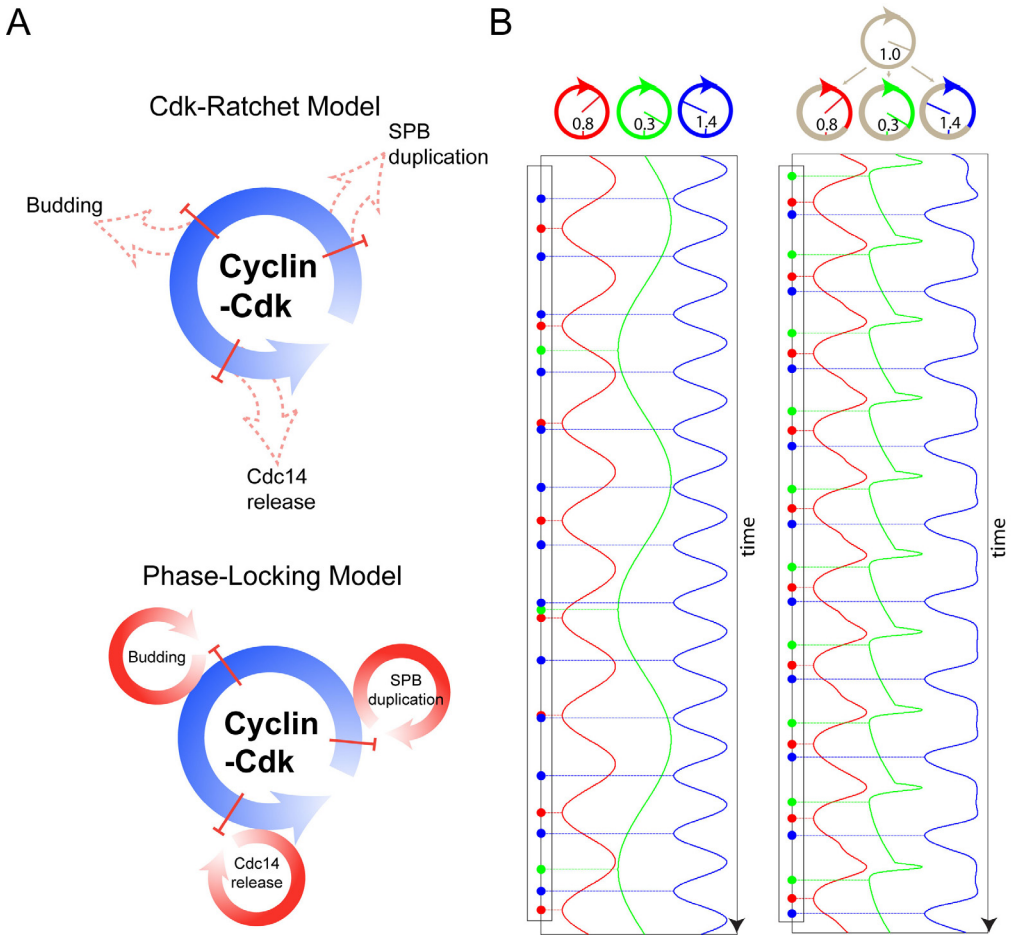

Figure 4.19. **Cell cycle control through phase-locking.** **A.** Schematic of ratchet (above) and phase-locking (below). **B.** Conceptual model: three Kuramoto oscillators ((Kuramoto, 1975), Materials and Methods) with different frequencies (indicated) control different cell cycle events. Without entrainment there is no fixed order (left) among events they generate. Allowing a cyclin-Cdk oscillator to advance or delay part of the peripheral oscillators' cycles leads to phase-locking and a stable order of events (Right).

To demonstrate how phase-locking could order cell cycle events controlled by independent modular oscillators, I built a conceptual model containing four oscillating modules. One is the cyclin-Cdk oscillator, and the other three are autonomous 'peripheral' oscillators controlling specific cell cycle events (in this example, loosely modeled after budding, SPB duplication, [see Introduction] and Cdc14 release). Without any coupling, the different intrinsic frequencies of the peripheral oscillators results in a disordered and irregular relative sequence of cell cycle events (Fig. 4.19B, left). Computer simulations showed that allowing the cyclin-Cdk master oscillator to affect the frequencies of the peripheral oscillators resulted in the three peripheral modules oscillating at a common frequency, producing events occurring once per cyclin-Cdk cycle in a fixed order (Fig. 4.19B, right).

The model in Fig. 4.19B is only a cartoon representation of a possible cell cycle control mechanism. However, the qualitative result of a distinct, dynamically *stable* phase-locking solution for each oscillating module, given sufficient interactions with the Cdk oscillator, may be robust to true biological complexity, since the stability of the phase-locking solution is only determined by the local dynamical structure near the fixed point (Winfree, 1967), meaning that phase-locking can occur largely independent of detailed mechanism. The only requirements are sufficiently strong linkage, combined with reasonably close intrinsic frequencies; both of these features are likely highly evolvable given initially independent oscillators (see Discussion).

8. Reducing amplitude of the cyclin-Cdk oscillator results in disordered cell cycle events

Phase-locking models of the general sort shown in Fig. 4.19B lead to a key prediction: lowering the amplitude of Clb-Cdk oscillation should simultaneously weaken entrainment between the Clb cycle and other Clb-controlled events, potentially perturbing the *order* of cell-cycle events (Fig. 4.20A). Thus, if other cell cycle events are under control of other independent oscillators, then reducing the amplitude of Clb-Cdk oscillations could result in scrambling of the order of these events.

Importantly, this prediction is largely independent of the detailed structure or parameters of the phase-locking model. An entirely different prediction is made based on ratchet-type control (again, largely independent of detailed mechanism): lowering amplitude should either block events or delay some steps, but not put events out of order.

Figure 4.20. **Experimental test of phase-locking predictions.** A. Model as in Fig. 4.19B, but the amplitude of cyclin-Cdk oscillation is reduced by 15%, resulting in event disorder (compare Fig. 4.19B, right). **B.** *2XGAL1-SIC1 bub2Δ* or *cdh1Δ sic1Δ bub2Δ* strains may reduce the amplitude of cyclin-Cdk oscillation by lowering the peak Cdk activity or raising the trough (cartoon below). *2XGAL1-SIC1* cells (n=37) were grown in raffinose medium prior to time-lapse analysis on galactose medium to induce Sic1 (t=0). *cdh1Δ sic1Δ GALL-CDC20* cells (n=35) were imaged on glucose to turn off *GALL-CDC20*. Quantification of the phenotype of the first cell cycle (right) and representative traces. Blue bars: nucleolar separation; Green bars: budding; red bars: cytokinesis. **C.** Cdc14 release and SPB duplication timing in free-running cell cycles predicted by a quantitative phase-locking model. Red: best estimation of parameters; blue: sine wave simulation of Clb-Cdk cycle. Light-red: solutions with parameters altered +/- one standard deviation for one or both of the two parameters (for two combinations no solution could be obtained due to mathematical restrictions of the model; Materials and Methods). Right panel: phase-locking could entrain SPB duplication oscillator (red) to the correct position early in the Clb-Cdk cycle (blue) (Materials and Methods).

Figure 4.20

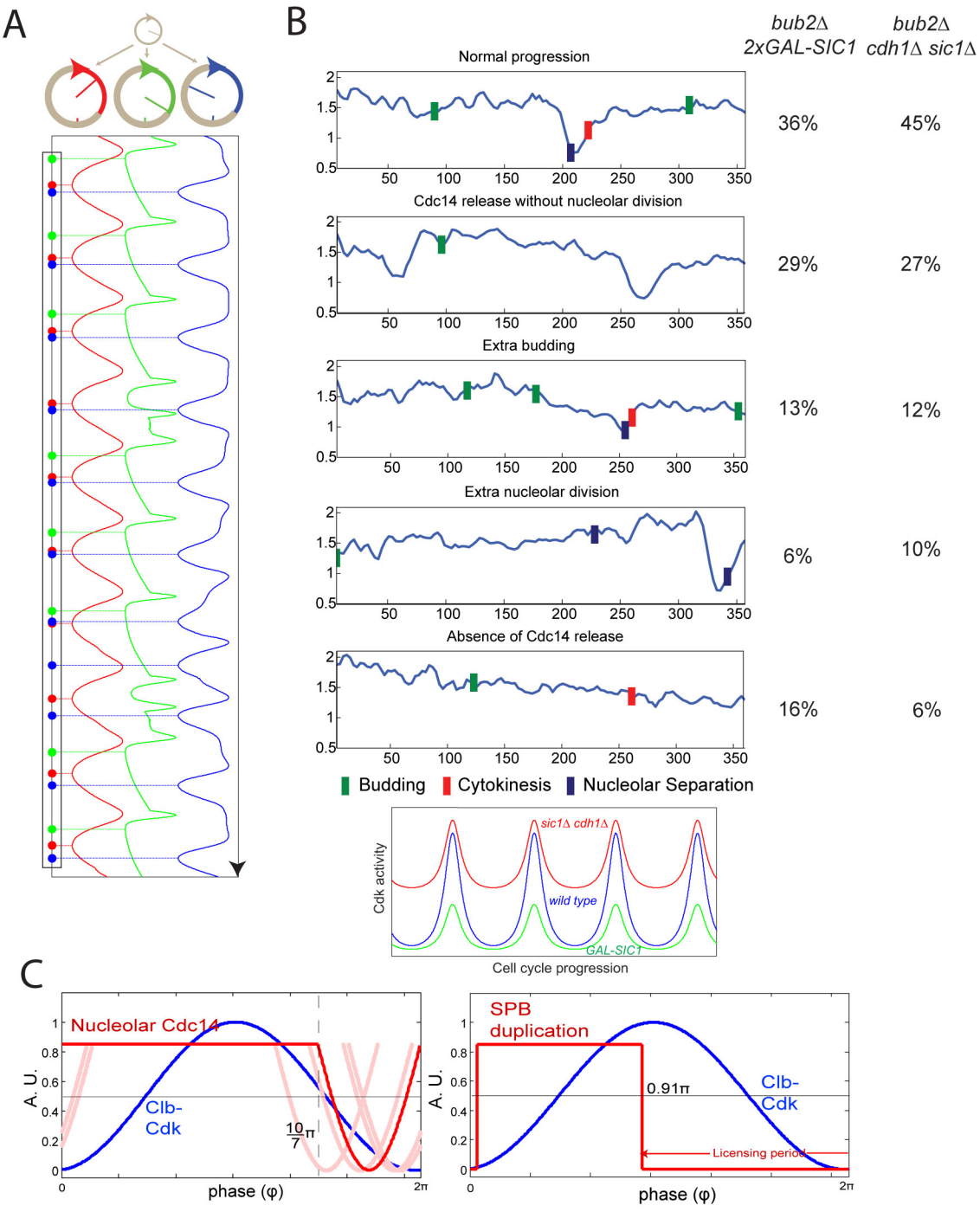
A
B
bub2Δ 2xGAL-SIC1
bub2Δ cdh1Δ sic1Δ
Normal progression
36%
45%
Cdc14 release without nucleolar division
29%
27%
Extra budding
13%
12%
Extra nucleolar division
6%
10%
Absence of Cdc14 release
16%
6%
Budding
Cytokinesis
Nucleolar Separation
Cdk activity
sic1Δ cdh1Δ
wild type
GAL-SIC1
Cell cycle progression
C
Nucleolar Cdc14
Clb-Cdk
10/7π
A. U.
phase (φ)
SPB duplication
0.91π
Clb-Cdk
Licensing period

I tried two strategies to test this prediction, that lowering the amplitude of cyclin-Cdk oscillation should perturb the order of cell cycle events. I first used strong constitutive overexpression of the Sic1 inhibitor of Clb-Cdk activity from the *GAL1* promoter (Mendenhall and Hodge, 1998). Wild-type cells already have a very low trough (G1) level of Clb-Cdk activity due to high endogenous Sic1 accumulation and other mechanisms (Mendenhall and Hodge, 1998) ; Sic1 overexpression therefore seems unlikely to lower the trough level further, but could lower the peak level by constitutive inhibitor production, thus reducing the amplitude (Fig. 4.20B). *2XGAL1-SIC1* cells are fully viable on galactose medium, so this perturbation is, on the surface, not an extreme one. As a nearly opposite means to lower the amplitude, I used deletion of *CDH1* and *SIC1*, which results in a high trough level of Clb2-Cdk activity, probably not much lower than the peak level (Schwab et al., 1997; Visintin et al., 1997) (Fig. 4.20B). Although *cdh1Δ sic1Δ* cells are ultimately inviable (Schwab et al., 1997; Visintin et al., 1997), they undergo multiple cell cycles (Wäsch and Cross, 2002), allowing analysis of order of events by time-lapse microscopy. Note that these two mechanisms for reducing the amplitude may do so in one case by lowering the peak, and in the other case by raising the trough. A ratchet control model, in which specific Clb-Cdk levels are controlling sequential steps in a process, should predict very different results from these manipulations, since Clb-Cdk activity levels will be very different; for example, in *GAL-SIC1* cells, Clb-Cdk levels are extremely low during an extended G1, while in *cdh1Δ sic1Δ* cells there is probably no period with low Clb-Cdk levels (Wäsch and Cross, 2002). In contrast, the phase-locking

perspective can predict qualitatively similar outcomes of event disorder, and even obtaining identical outcomes is theoretically possible, depending on the nature and strength of coupling.

In these experiments, in order to focus specifically on reduction of amplitude of the Clb-Cdk oscillation, I also knocked out the spindle orientation checkpoint component *BUB2*, which should relieve dependence of Cdc14 release on spindle positioning (Bardin et al., 2000). (This genetic manipulation was indeed necessary for the full effects described below, although qualitatively similar effects on budding, cytokinesis, and anaphase were observed in a *BUB2* background; *bub2* deletion alone had no effect [data not shown]).

GAL1-SIC1 expression in *bub2Δ* cells resulted in 64% abnormal first cell cycles after Sic1 expression on galactose medium (supernumerary Cdc14 release without nucleolar separation; extra budding without Cdc14 release or cell division; or cytokinesis without Cdc14 release or nucleolar separation (Fig. 4.20B), resulting in a supernumerary bud following cytokinesis, which then fails to grow, presumably due to being anucleate). Remarkably, similar cell cycle anomalies with roughly similar frequencies were also observed in cycling *cdh1Δ sic1Δ bub2Δ* cells.

The conceptual phase-locking model qualitatively reproduced the loss-of-order phenotypes resulting from lowering the amplitude of Cdk oscillation (Fig. 4.20A).

Those anomalies are not likely due to nonspecific growth defects since *GAL1-SIC1 bub2* cells grow well both in bulk culture and when monitored as single cells. *cdh1Δ sic1Δ* occasionally causes permanent cell cycle block with large budded cells; such cells were excluded from analysis. In contrast, any Cdk-ratchet model would predict that reducing the Cdk oscillation amplitude will lead to elongation of cell cycle period or complete block of cell cycle progression; in either case, the normal orders of cell cycle events would be predicted to remain the same. Further, near-opposite phenotypes would be predicted for lowering the peak vs. raising the trough. Therefore, these results support phase-locking over ratchet control.

The phase-locking model describes how Cdk oscillation entrains autonomous peripheral oscillators to form a coherent cell cycle. This model coherently associates the cycling of an event (e.g. Cdc14 release, SPB duplication) in normal cell cycles with its capacity to operate in endocycles in blocked cells. The phase-locking model implies that these two phenotypes are driven by the same inherently oscillatory module, which is entrained to the cyclin-Cdk oscillation in normally cycling cells. In contrast, these two phenotypes are essentially uncoupled and independent of each other in any ratchet model that somehow incorporates the possibility of endocycles as a (pathological) consequence of cell cycle blockage. Therefore, an empirical test of the phase-locking vs. the ratchet perspective is to ask whether the response of the oscillatory module to fixed Clb-Cdk levels is predictive of timing in the normal cell cycle. To carry out this test, I derived an equation to calculate the stable phase offset

(the difference between peak Clb2 and peak Cdc14 release), based on the phase-locking model. This model contained only three parameters, all of which were extracted directly from the empirical observations (importantly, derived solely from Clb2kd-blocked cells) in Fig. 4.10B (Materials and Methods). A key parameter is the strength of coupling of Clb2 to the frequency of the Cdc14 cycles (as noted above, such coupling is indispensable for a phase-locking mechanism); this is simply determined as the slope of the straight-line fit in Fig. 4.10B. I solved the model analytically to determine the phase-offset. This calculation placed Cdc14 release late in the cell cycle, as Clb-Cdk levels decreased, consistent with experiment (Stegmeier and Amon, 2004). This conclusion is not especially sensitive to uncertainties in estimating the parameters, since a similar result is obtained increasing or decreasing the parameter estimates by one standard deviation of measurement error, alone or in combination (Fig. 4.20C). A ratchet model can accommodate the observations of Cdc14 endocycles in Clb2kd cells only by asserting that these endocycles are due to pathological conditions of Clb2kd accumulation; in this case, parameters derived from experiments with Clb2kd-blocked cells will be irrelevant to timing in cycling cells.

The phase-locking model can be applied to any oscillating module under the control of Cdk activity. I performed the same test on the hypothesized SPB duplication module to see if this model can 'predict' the timing of SPB duplication in normal cell cycles. Published data are insufficient to obtain empirical estimates of

parameters to calculate the timing of SPB duplications. Still, I could estimate predicted timing using my model and plausible parameter choices (Materials and Methods). SPB duplication was predicted to occur early in the cell cycle, before the rise in Clb-Cdk, as observed experimentally (Fig. 4.20C). This result shows consistency of timing of SPB duplication with a phase-locking model.

The severe disruptions in normal Cdc14 release by manipulations specifically predicted to perturb the autonomous Cdc14 release module, even in free-running cell cycles, imply that oscillatory function of this module and its coupling to Clb-Cdk oscillations is required for normal Cdc14 release timing. It is likely that any phase-locking control system could transit evolutionarily to a pure ratchet-control system; indeed, this is formally the result of increasing coupling strength to arbitrarily high values, such that the peripheral oscillator will not move within a physiological timescale without a 'kick' from the entraining oscillator. Different cell cycle systems, even if initially independently oscillatory, may vary in the degree to which they are at present under ratchet control; for example, DNA replication may be entirely under cyclin-Cdk ratchet control in modern eukaryotes, despite its intrinsically oscillatory character. This may represent a tradeoff between the robustness and simplicity of the PL mechanism, and the cost in some systems of occasional uncoupling (aneuploidy in the case of DNA replication).

9. Implications for the evolution of the cell cycle

Modularity in biology has been argued to create functional robustness and evolvability (Bhattacharyya et al., 2006; Hartwell et al., 1999). My study suggests that certain modules in cell cycle are intrinsically oscillatory; coupling of these oscillators to the central Cdk oscillator can nevertheless readily ensure once-per-cell-cycle events (Fig. 4.19A).

The eukaryotic cell cycle evolved from Cdk-free precursor(s), since Cdk is a eukaryotic-specific kinase (Nasmyth, 1995). Critical biological processes such as DNA replication and cell division obviously predated Cdk, and may be intrinsically cyclical processes ultimately brought under control of a Cdk oscillator by phase-locking. Consistent with this idea, Cdks may have evolved late, after other eukaryotic cell-cycle-regulatory protein kinases (Krylov et al., 2003). If cell cycle processes were intrinsically oscillatory before the emergence of Cdk, then Cdk would only need to gain the ability to modulate these oscillators to gradually become a master regulator. This provides a clear evolutionary case with plausible selection for utility of intermediate forms (Darwin, 1859). In contrast, direct evolution of ratchet control appears to require much more 'forceful' evolutionary change.

I speculate that in primordial eukaryotes, multiple autonomous biochemical oscillators entrained each other to an approximate aggregate rhythm. Cyclin-Cdk

oscillation could then have emerged as a central cell cycle controller to stabilize the phase-locking structure. In computer simulations, selection for entrainment in large oscillator populations efficiently yielded central pacemaker oscillators (Brede, 2008; Sendina-Nadal et al., 2008). These evolved pacemaker systems exhibited high stability to weakening of oscillator coupling as an unselected 'phenotype' (Brede, 2008). To understand the advantage of having a central oscillatory controller like Cdk, I constructed random networks of coupled Kuramoto oscillators (Kuramoto, 1975) in computer simulation. Increasing centralization of control by gradually changing network connections increased the stability of spontaneous entrainment (Fig. 4.21). This result could potentially justify the evolution of cyclin-Cdk oscillator system.

Figure 4.21. **Simulation showing that centralization of control enhances global entrainment in an oscillator network.** For a range of coupling strengths (equivalent to magnitude of the Z response curve; see Materials and Methods) on the x-axis, we randomly generated Kuramoto oscillator networks containing 100 independent oscillators, either connected randomly (black), or with preference for in-connection from an oscillator that already has multiple out-connections (preferential exponent=1.0 in green, or 2.0 in blue, see Materials and Methods). For all networks, the average number of 'in' and 'out' connections was constrained to be the same (<k>=2). Inset: the out-degree distribution (kout) for each connection scheme: increasing preferential connection resulted in networks with a small number of highly out-connected nodes (cluster of low frequency green and blue points with high kout). The networks were run from random initial conditions and random intrinsic frequencies for each of the 100 nodes. An order parameter R was calculated for each network to determine the degree of entrainment $R = \frac{1}{N \cdot T}\int_0^T \left| \sum_{i=0}^{N} e^{i\varphi_i} \right| dt$ (φ_i is the phase of the ith oscillator; T=100, N=100; R=1 represents complete entrainments, see Materials and Methods). 1000 networks were sampled randomly for each coupling strength. Shaded areas: standard deviations. At all coupling strengths, increasing centralization of oscillator coupling enhanced entrainment (blue curve > green curve > black curve)

Figure 4.21

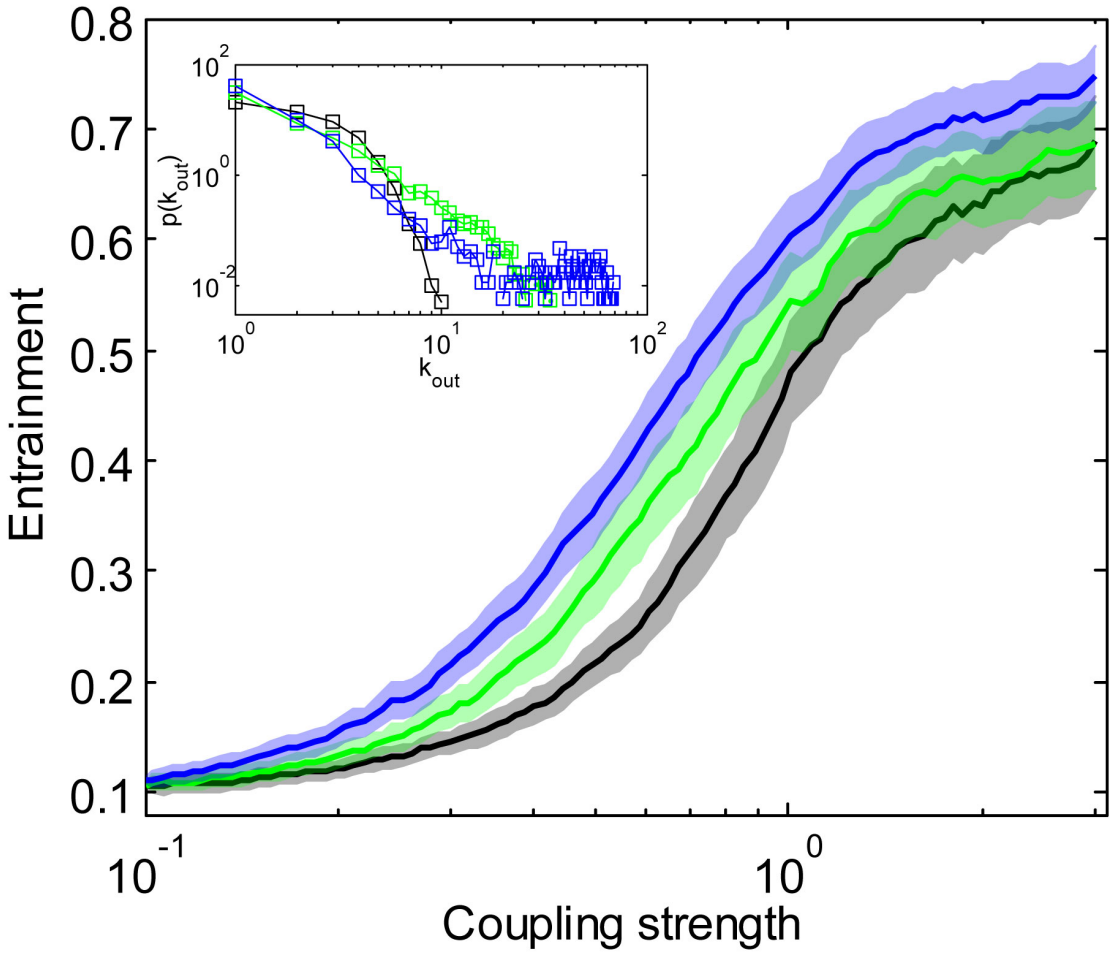
Entrainment
Coupling strength
0.8
0.7
0.6
0.5
0.4
0.3
0.2
0.1
10^-1
10^0
p(k_out)
k_out
10^2
10^0
10^-2
10^0
10^1
10^2

10. Mob1-GFP localizes to SPB in phase with Cdc14 release during Cdc14 endocycles.

Mob1 is an essential component of the mitotic exit network (MEN) (Stegmeier and Amon, 2004). Mob1-GFP localizes to both daughter- and mother-orientated SPB during ME, coinciding with Cdc14 release (Yoshida and Toh-e, 2001). It has been suggested that Mob1's SPB localization is important for its activation, although a direct causal relationship has not been shown (Stegmeier and Amon, 2004).

Cdc14 can dephosphorylate Cdc15, another essential MEN component upstream of Mob1, probably leading to full activation of the MEN (Jaspersen and Morgan, 2000; Stegmeier et al., 2002). In order to study whether MEN activity also oscillates during the Cdc14 endocycles, I examined the localization of Mob1-GFP in the Clb2kd pulse experiment. In 9/10 cells showing Cdc14 endocycles, Mob1-GFP localization also changed periodically, and its SPB localization coincided with Cdc14 release (Fig. 4.22). This observation suggests that the MEN activity may also oscillate during the Cdc14 endocycles, although I lack a technical means to directly measure Dbf2 kinase activity, the likely final effector of the MEN pathway, in single-cell analysis.

Figure 4.22

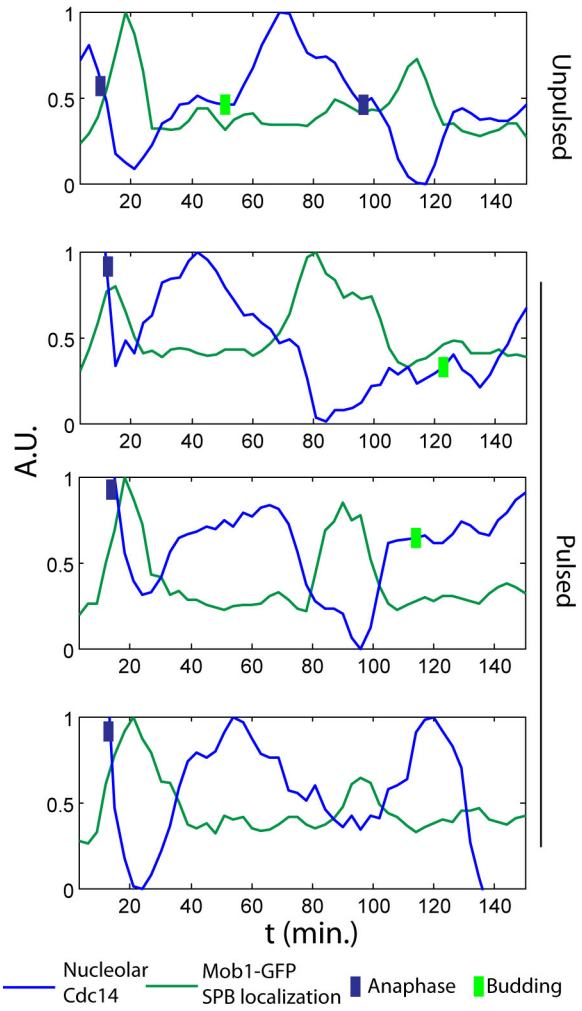

Figure 4.22. **Mob1-GFP localization during the Cdc14 endocycles.**

MET-CDC20 MOB1-GFP CDC14-YFP NET1-mCherry cells were pulsed with Clb2kd for 30 minutes as in Fig. 4.1D, and released into cell cycle. The maximum GFP intensity was used a proxy for Mob1-GFP SPB localization (higher value indicates stronger SPB localization). In 9/10 cell showing Cdc14 endocycles, Mcm2-GFP SPB localization appeared to oscillate in-phase with Cdc14 release.

11. Bypassing the lethality of *cdc14Δ* and the role of Cdc14 phosphatase activity in its resequestration

Cdc14 is normally essential for cell viability. It has been shown that shortening the length of rDNA allows *GAL1-SIC1* overexpression to rescue the *cdc14-1* temperature sensitive allele at restrictive temperatures (Machin et al., 2006). I created a *cdc14Δ* strain with shortened rDNA and *GAL1-SIC1* overexpression. This strain was viable and slow-growing on galactose medium, but totally inviable on glucose medium (without Sic1 overexpression).

The existence of this strain strongly suggests that the cyclin-Cdk cycle is intrinsically more important and primary in cell cycle regulation than the Cdc14 cycle; this idea is consistent with the universal conserved role of cyclin-Cdk in regulating the eukaryotic cell cycle, as compared to the more variable and less central role of Cdc14 in other eukaryotes (Morgan, 2007). A similar strain construction demonstrated that the anaphase-promoting complex is dispensable provided that periodic cyclin-Cdk regulation is allowed (Thornton and Toczyski, 2003). These results suggest that cyclin-Cdk is truly the ultimate driver of cell cycle regulation.

In addition, the *cdc14Δ* strain can be employed to study an important question: whether Cdc14 resequestration into nucleolus requires Cdc14 phosphatase activity. Cdc14 has been proposed to promote its return to the nucleolus after release by

dephosphorylating several targets including Bub2, Lte1, Cdh1, and Net1 (Stegmeier and Amon, 2004). However, inactivating Cdc14 phosphatase activity usually leads to mitotic cyclin stabilization and ME block. Mitotic cyclin-Cdk activity also controls Cdc14 localization, which complicates the explanation of results as to whether the Cdc14 requirement for its nucleolar resequestration it is due to lack of Cdc14 phosphatase activity *per se* or due to high mitotic cyclin-Cdk activity. (These activities are further intertwined by the likely direct dephosphorylation of multiple cyclin-Cdk targets by Cdc14).

I employed the *cdc14Δ* strain to address this problem. I introduced a phosphatase-inactive *cdc14C283S/R289A-GFP* construct into the *cdc14Δ* background (with shortened rDNA and *GAL-SIC1* expression). The catalytically inactive *cdc14C283S/R289A-GFP* had essentially no effect on the strain's phenotype, which included massive cytokinetic defects and frequent cell cycle arrest. I used time-lapse microscope to specifically examine cycling cells, to observe localization changes of catalytically inactive Cdc14. Within this population, 17/21 cells under investigation demonstrated a clear release/resequestration pattern comparable to that of wild type cells (Fig. 4.23). Occasionally, Cdc14 release lasted longer than the 20 minutes characteristic of wild-type. The amplitude of Cdc14 release appeared to be smaller than wild type, but due to the elongated cell morphology in *cdc14C283S/R289A-GFP GAL1-SIC1* cells, direct quantitative comparison with wild type cells is difficult. Therefore, I conclude that Cdc14 phosphatase activity may contribute to, but is not

strongly required for Cdc14 resequestration. In the absence of Cdc14 phosphatase activity, other phosphatases may also dephosphorylate relevant targets after mitotic cyclin inactivation to promote Cdc14 resequestration, especially with strong overexpression of the Sic1 cyclin-Cdk inhibitor.

Figure 4.23

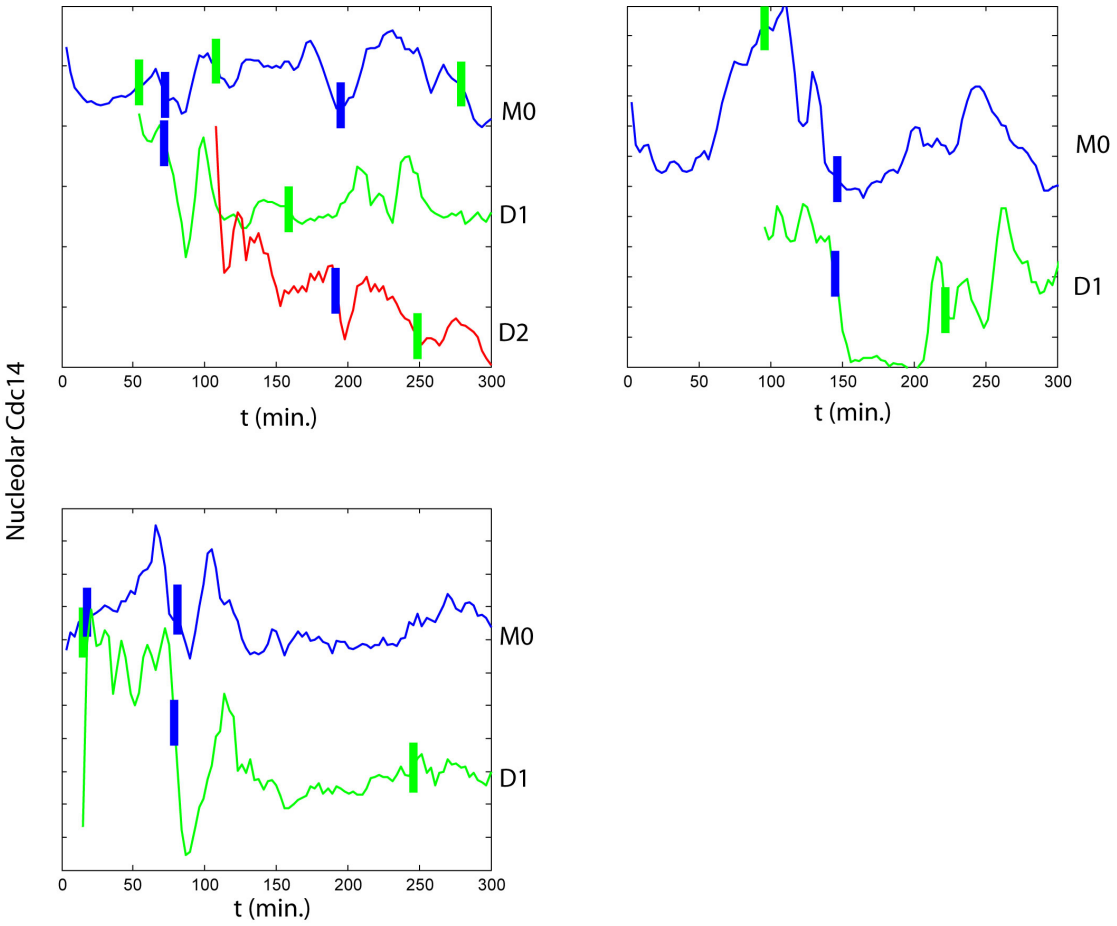

Figure 4.23. **The phosphatase activity of Cdc14 is not absolutely required for its nuclear sequestration.** *cdc14::cdc14C283S/R289A-GFP NET1-mcherry GAL1-SIC1 short-rDNA* was grown in galactose medium and analyzed using time-lapse microscopy. Due to massive growth defects, only cycling cells were picked up. 3 cell lineages show that Cdc14 nucleolar localization is still cell cycle regulated in dividing cells (n=15). Traces are shifted along Y-axis for presentation. Blue bars: anaphase; green bars: budding.

12. Discussion

Here, I propose that an intrinsic oscillatory module controls Cdc14 release, and that cyclin-Cdk oscillation could order Cdc14 release, and likely other cell cycle events under independent oscillator control, by phase-locking these modules to the frequency of the cyclin-Cdk cycle.

I describe the capacity of Cdc14 release and resequestration to oscillate spontaneously, independent of Clb-Cdk oscillations and thus independent of the main cell cycle driver. This oscillatory module functioned at varying fixed Clb2-Cdk levels; importantly, though, Clb-Cdk levels nevertheless regulated the Cdc14 oscillator, with higher Clb-Cdk increasing Cdc14 release frequency.

The canonical model for once-per-cell-cycle regulation by cyclin-Cdk oscillations proposes that high and low cyclin-Cdk levels promote alternating steps of a process; I refer to this as a 'ratchet' model (see Introduction). Such a model rather clearly predicts that any given fixed level of cyclin-Cdk should result in a terminal arrest with one or the other steps of each cell cycle process completed and the next never occurring. Cdc14 endocycles at fixed Clb2 levels are hard to reconcile with this idea; further, there are at least three other once-per-cell-cycle events that are now known to have the potential to occur in a cyclical fashion independent of cyclin-Cdk oscillations: budding, cell-cycle-regulated transcription, and SPB duplication. As an alternative to ratchet models, to account for existence and entrainment of these endocycles at a

common frequency, I propose here a phase-locking model by Cdk oscillation to order cell cycle events.

It is important to note that such a phase-locking model is consistent with mechanistic regulatory details that are frequently interpreted as support for ratchet models; for example, the documented ability of high mitotic cyclin-Cdk activity to prevent SPB 'licensing' for duplication is not somehow 'eliminated' by a phase-locking model – it is considered as a mechanism of oscillator coupling. The phase-locking model may provide deeper insight into cell cycle regulation since it incorporates the endocycle phenotypes, which despite the accumulation of an increasing number of examples, must be regarded as 'outliers' or artifacts in order to maintain the generality of ratchet-type models. I generated and tested qualitative predictions of phase-locking models that clearly differ from the predictions of ratchet models, and the phase-locking model appeared to give a better fit.

Further, I generated a simple but quantitative phase-locking model with parameters estimated solely from experiments on cells blocked in the cell cycle by undegradable mitotic cyclin. This model then predicted Cdc14 release from the nucleolus late in the cell cycle, as the Clb-Cdk level is declining, as is observed experimentally. This result is empirically meaningful since estimates from blocked cells, placed in the phase-locking model, yielded a correct answer for freely cycling cells, suggesting that the normal Cdc14 release cycles and endocycles are closely

related phenotypes, likely driven by the same oscillatory module.

The predominant model for cell cycle control involves direct cyclin-Cdk control of cell cycle events, with surveillance checkpoints to ensure order. An earlier model, derived from the study of *cdc* mutants (Morgan, 2007), considered cell cycle control to be due to parallel, interlocking but unidirectional morphogenetic pathways arranged in a functional sequence map. My phase-locking model combines aspects of both models: a central cyclin-Cdk oscillator drives the cell cycle as in the first model; functional sequences emerge in the phase-locking model as independent oscillatory modules controlling specific cell cycle events. Such independent cyclical processes are highly analogous to 'independent functional sequences' in the original *cdc* formulation – processes that can operate freely in parallel, such as DNA replication and spindle morphogenesis (Hartwell, 1974). Such an arrangement gives great flexibility and resistance to deleterious effects of delays, once surveillance 'checkpoint' mechanisms are in place. Phase-locking of these autonomous oscillators by a central Cdk pacemaker could have been an important early event in cell cycle evolution, and this mechanism may control multiple autonomous cell cycle oscillators, even in modern eukaryotes.

13. Unsolved issues

1. What is the nature of the small amplitude oscillation of Cdc14 release in *cdh1Δ* cells with >2x peak Clb2kd? I did not observe this small amplitude oscillation in the presence of CHX, indicating that transcriptional regulation may also drive this phenotype. I have shown that Cdc14 release induced by Esp1 overexpression is more nuclear-concentrated in *cdh1Δ* cells than *CDH1+* (Fig. 3.15). Therefore, the reduced amplitude may reflect the fact that Cdc14 can still concentrates in the nucleus after nucleolar release; assuming microscopic colocalization of some of the nuclear-concentrated Cdc14 with nucleolar Net1 (a reasonable assumption given imperfect geometry and the close contact between nucleus and nucleolus), the quantitative measure of Cdc14 release would necessarily adopt a lower amplitude even if fully released from the nucleolus. High levels of mitotic cyclin-Cdk may block Cdc14 nuclear export (Fig. 3.15), which is also consistent with this observation.

2. Does oscillation of MEN activity drive the Cdc14 endocycle in *cdh1 sic1 bub2* cells? and what is role of MEN in promoting Cdc14 endocycles in Clb2kd cells, if any? Using Mob1-GFP construct to observe its SPB localization may answer this question.

3. What is the threshold of Cdc5 for Cdc14 release? I observed that Cdc14 release amplitude is not controlled by Clb2kd levels. The digital behavior of Cdc14 release can be explained by either positive feedbacks in Cdc14 control network or a sharp threshold for the Cdc5 level. To determine the Cdc5 threshold, cells should be blocked in telophase by depleting Cdc5 using *cdc5::MET3-CDC5*. Then various concentrations of stable Cdc5-ΔNT-GFP could be expressed in the cell to correlate Cdc14 localization changes with Cdc5 level, as I did for Clb2kd-GFP.

4. If Cdc14 release controlled by Cdk oscillation through phase-locking, why is DNA replication much more likely controlled through a ratchet mechanism? Besides the possibility that those two events followed different evolutionary routes, it is possible that phase-locking and ratchet mechanisms may have specific advantages that make them suitable for different circumstances. Cdc14 endocycles may be utilized by the cells under certain physiological conditions. The likely ability of Cdc14 to inactivate the spindle checkpoint (see above) combined with potential Cdc14 oscillations under some conditions marginally activating the checkpoint, could periodically provide an escape 'opportunity' for checkpoint-arrested cells, i.e., a recovery mechanism. In this context, it is interesting that adaptation to some forms of checkpoint arrest has been linked to Cdc5 (Toczyski et al., 1997), which is essential for Cdc14 release, including in endocycles (see above). Periodic chromosome decondensation/recondensation

in animal cells blocked in mitosis with colcemid is a classical observation that comes to mind. Formally similar proposals have been made to rationalize the physiological significance of the Mdm2-p53 oscillation in mammalian cells after DNA damage, where the oscillatory phenotype could be important for DNA damage repair.

5. Can the cell cycle be driven by oscillation of phosphates activity alone? Free control of Cdc14 localization or activity may be important for answering this question. Besides deleting *NET1,* constitutive Cdc14 release throughout the cell cycle has not been achieved (and *net1* deletion in fact does not result in full release of Cdc14, as I showed in Chapter 3, since Cdc14 is largely nuclear-restricted in the absence of Net1). Using *GAL/MET-URL-CDC14-YFP* construct, and periodically controlling promoter activities with a microfluidic system could be feasible, to see if normal cell cycle progression can be achieved in the presence of constitutive mitotic cyclin-Cdk activity (*CLB2kd sic1Δ*).

References:

Alexandru, G., Zachariae, W., Schleiffer, A., and Nasmyth, K. (1999). Sister chromatid separation and chromosome re-duplication are regulated by different mechanisms in response to spindle damage. The EMBO journal *18*, 2707-2721.

Azzam, R., Chen, S.L., Shou, W., Mah, A.S., Alexandru, G., Nasmyth, K., Annan, R.S., Carr, S.A., and Deshaies, R.J. (2004). Phosphorylation by cyclin B-Cdk underlies release of mitotic exit activator Cdc14 from the nucleolus. Science (New York, NY *305*, 516-519.

Bachant, J., Jessen, S.R., Kavanaugh, S.E., and Fielding, C.S. (2005). The yeast S phase checkpoint enables replicating chromosomes to bi-orient and restrain spindle extension during S phase distress. The Journal of cell biology *168*, 999-1012.

Barabasi, A.L., and Albert, R. (1999). Emergence of scaling in random networks. Science (New York, NY *286*, 509-512.

Bardin, A.J., Visintin, R., and Amon, A. (2000). A mechanism for coupling exit from mitosis to partitioning of the nucleus. Cell *102*, 21-31.

Bean, J.M., Siggia, E.D., and Cross, F.R. (2006). Coherence and timing of cell cycle start examined at single-cell resolution. Molecular cell *21*, 3-14.

Bembenek, J., Kang, J., Kurischko, C., Li, B., Raab, J.R., Belanger, K.D., Luca, F.C., and Yu, H. (2005). Crm1-mediated nuclear export of Cdc14 is required for the completion of cytokinesis in budding yeast. Cell cycle (Georgetown, Tex *4*, 961-971.

Bhattacharyya, R.P., Remenyi, A., Yeh, B.J., and Lim, W.A. (2006). Domains, motifs, and scaffolds: the role of modular interactions in the evolution and wiring of cell signaling circuits. Annual review of biochemistry *75*, 655-680.

Bi, E., Maddox, P., Lew, D.J., Salmon, E.D., McMillan, J.N., Yeh, E., and Pringle, J.R. (1998). Involvement of an actomyosin contractile ring in Saccharomyces cerevisiae cytokinesis. The Journal of cell biology *142*, 1301-1312.

Bloom, J., and Cross, F.R. (2007). Multiple levels of cyclin specificity in cell-cycle control. Nature reviews *8*, 149-160.

Brede, M. (2008). Construction principles for highly synchronizable sparse directed networks. Physics Letters A *372*, 5305-5308.

Charles, J.F., Jaspersen, S.L., Tinker-Kulberg, R.L., Hwang, L., Szidon, A., and Morgan, D.O. (1998). The Polo-related kinase Cdc5 activates and is destroyed by the mitotic cyclin destruction machinery in S. cerevisiae. Curr Biol *8*, 497-507.

Charvin, G., Cross, F.R., and Siggia, E.D. (2008). A microfluidic device for temporally controlled gene expression and long-term fluorescent imaging in unperturbed dividing yeast cells. PLoS ONE *3*, e1468.

Charvin, G., Cross, F.R., and Siggia, E.D. (2009). Forced periodic expression of G1 cyclins phase-locks the budding yeast cell cycle. Proceedings of the National Academy of Sciences of the United States of America *106*, 6632-6637.

Cohen-Fix, O., Peters, J.M., Kirschner, M.W., and Koshland, D. (1996). Anaphase initiation in Saccharomyces cerevisiae is controlled by the APC-dependent degradation of the anaphase inhibitor Pds1p. Genes & development *10*, 3081-3093.

Cross, F.R. (2003). Two redundant oscillatory mechanisms in the yeast cell cycle. Developmental cell *4*, 741-752.

D'Amours, D., Stegmeier, F., and Amon, A. (2004). Cdc14 and condensin control the dissolution of cohesin-independent chromosome linkages at repeated DNA. Cell *117*, 455-469.

Darwin, C.R. (1859). The origin of species by means of natural selection, or the preservation of favoured races in the struggle for life. (EZreads Publications, LLC (March 4, 2009)).

Di Talia, S., Skotheim, J.M., Bean, J.M., Siggia, E.D., and Cross, F.R. (2007). The effects of molecular noise and size control on variability in the budding yeast cell cycle. Nature *448*, 947-951.

Elledge, S.J. (1996). Cell cycle checkpoints: preventing an identity crisis. Science (New York, NY *274*, 1664-1672.

Eluere, R., Offner, N., Varlet, I., Motteux, O., Signon, L., Picard, A., Bailly, E., and Simon, M.N. (2007). Compartmentalization of the functions and regulation of the mitotic cyclin Clb2 in S. cerevisiae. Journal of cell science *120*, 702-711.

Epstein, C.B., and Cross, F.R. (1992). CLB5: a novel B cyclin from budding yeast with a role in S phase. Genes & development *6*, 1695-1706.

Fesquet, D., Fitzpatrick, P.J., Johnson, A.L., Kramer, K.M., Toyn, J.H., and Johnston, L.H. (1999). A Bub2p-dependent spindle checkpoint pathway regulates the Dbf2p kinase in budding yeast. The EMBO journal *18*, 2424-2434.

Fisher, R.A. (1935). The Design of Experiments. Hafner Publishing Company, New York 1971. 96-106

Fitch, I., Dahmann, C., Surana, U., Amon, A., Nasmyth, K., Goetsch, L., Byers, B., and Futcher, B. (1992). Characterization of four B-type cyclin genes of the budding yeast Saccharomyces cerevisiae. Mol Biol Cell *3*, 805-818.

Gadal, O., Strauss, D., Kessl, J., Trumpower, B., Tollervey, D., and Hurt, E. (2001). Nuclear export of 60s ribosomal subunits depends on Xpo1p and requires a nuclear export sequence-containing factor, Nmd3p, that associates with the large subunit protein Rpl10p. Molecular and cellular biology *21*, 3405-3415.

Gard, D.L., Hafezi, S., Zhang, T., and Doxsey, S.J. (1990). Centrosome duplication continues in cycloheximide-treated Xenopus blastulae in the absence of a detectable cell cycle. The Journal of cell biology *110*, 2033-2042.

Glass, L. (2001). Synchronization and rhythmic processes in physiology. Nature *410*, 277-284.

Gray, C.H., Good, V.M., Tonks, N.K., and Barford, D. (2003). The structure of the cell cycle protein Cdc14 reveals a proline-directed protein phosphatase. The EMBO journal *22*, 3524-3535.

Haase, S.B., and Reed, S.I. (1999). Evidence that a free-running oscillator drives G1 events in the budding yeast cell cycle. Nature *401*, 394-397.

Haase, S.B., Winey, M., and Reed, S.I. (2001). Multi-step control of spindle pole body duplication by cyclin-dependent kinase. Nature cell biology *3*, 38-42.

Hartwell, L.H. (1974). Saccharomyces cerevisiae cell cycle. Bacteriological reviews *38*, 164-198.

Hartwell, L.H., Hopfield, J.J., Leibler, S., and Murray, A.W. (1999). From molecular to modular cell biology. Nature *402*, C47-52.

Higuchi, T., and Uhlmann, F. (2005). Stabilization of microtubule dynamics at anaphase onset promotes chromosome segregation. Nature *433*, 171-176.

Hirano, T., Funahashi, S.I., Uemura, T., and Yanagida, M. (1986). Isolation and characterization of Schizosaccharomyces pombe cutmutants that block nuclear division but not cytokinesis. The EMBO journal *5*, 2973-2979.

Hofken, T., and Schiebel, E. (2002). A role for cell polarity proteins in mitotic exit. The EMBO journal *21*, 4851-4862.

Holt, L.J., Krutchinsky, A.N., and Morgan, D.O. (2008). Positive feedback sharpens the anaphase switch. Nature *454*, 353-357.

Hu, F., Wang, Y., Liu, D., Li, Y., Qin, J., and Elledge, S.J. (2001). Regulation of the Bub2/Bfa1 GAP complex by Cdc5 and cell cycle checkpoints. Cell *107*, 655-665.

Hwang, L.H., Lau, L.F., Smith, D.L., Mistrot, C.A., Hardwick, K.G., Hwang, E.S., Amon, A., and Murray, A.W. (1998). Budding yeast Cdc20: a target of the spindle checkpoint. Science (New York, NY *279*, 1041-1044.

Inze, D., and De Veylder, L. (2006). Cell cycle regulation in plant development. Annual review of genetics *40*, 77-105.

Jaspersen, S.L., Charles, J.F., and Morgan, D.O. (1999). Inhibitory phosphorylation of the APC regulator Hct1 is controlled by the kinase Cdc28 and the phosphatase Cdc14. Curr Biol *9*, 227-236.

Jaspersen, S.L., and Morgan, D.O. (2000). Cdc14 activates cdc15 to promote mitotic exit in budding yeast. Curr Biol *10*, 615-618.

Jensen, S., Geymonat, M., Johnson, A.L., Segal, M., and Johnston, L.H. (2002). Spatial regulation of the guanine nucleotide exchange factor Lte1 in Saccharomyces cerevisiae. Journal of cell science *115*, 4977-4991.

Jensen, S., Segal, M., Clarke, D.J., and Reed, S.I. (2001). A novel role of the budding yeast separin Esp1 in anaphase spindle elongation: evidence that proper spindle association of Esp1 is regulated by Pds1. The Journal of cell biology *152*, 27-40.

Jimenez, J., Castelao, B.A., Gonzalez-Novo, A., and Sanchez-Perez, M. (2005). The role of MEN (mitosis exit network) proteins in the cytokinesis of Saccharomyces cerevisiae. Int Microbiol *8*, 33-42.

Kearsey, S.E., and Cotterill, S. (2003). Enigmatic variations: divergent modes of regulating eukaryotic DNA replication. Molecular cell *12*, 1067-1075.

Kim, S.H., Lin, D.P., Matsumoto, S., Kitazono, A., and Matsumoto, T. (1998). Fission yeast Slp1: an effector of the Mad2-dependent spindle checkpoint. Science (New York, NY *279*, 1045-1047.

King, R.W., Jackson, P.K., and Kirschner, M.W. (1994). Mitosis in transition. Cell *79*, 563-571.

Krylov, D.M., Nasmyth, K., and Koonin, E.V. (2003). Evolution of eukaryotic cell cycle regulation: stepwise addition of regulatory kinases and late advent of the CDKs. Curr Biol *13*, 173-177.

Kuramoto, Y. (1975). Int. Symp. on Mathematical problems in theoretical physics. In Lect N Phys, H. Araki, ed. (New York, Springer), pp. 420-422.

Lew, D.J., and Reed, S.I. (1993). Morphogenesis in the yeast cell cycle: regulation by Cdc28 and cyclins. The Journal of cell biology *120*, 1305-1320.

Lu, Y., and Cross, F. (2009). Mitotic exit in the absence of separase activity. Mol Biol Cell *20*, 1576-1591.

Machin, F., Torres-Rosell, J., De Piccoli, G., Carballo, J.A., Cha, R.S., Jarmuz, A., and Aragon, L. (2006). Transcription of ribosomal genes can cause nondisjunction. The Journal of cell biology *173*, 893-903.

Mateus, C., and Avery, S.V. (2000). Destabilized green fluorescent protein for monitoring dynamic changes in yeast gene expression with flow cytometry. Yeast (Chichester, England) *16*, 1313-1323.

McCleland, M.L., and O'Farrell, P.H. (2008). RNAi of mitotic cyclins in Drosophila uncouples the nuclear and centrosome cycle. Curr Biol *18*, 245-254.

Mendenhall, M.D., and Hodge, A.E. (1998). Regulation of Cdc28 cyclin-dependent protein kinase activity during the cell cycle of the yeast Saccharomyces cerevisiae. Microbiol Mol Biol Rev *62*, 1191-1243.

Menssen, R., Neutzner, A., and Seufert, W. (2001). Asymmetric spindle pole localization of yeast Cdc15 kinase links mitotic exit and cytokinesis. Curr Biol *11*, 345-350.

Michaelis, C., Ciosk, R., and Nasmyth, K. (1997). Cohesins: chromosomal proteins that prevent premature separation of sister chromatids. Cell *91*, 35-45.

Mohl, D.A., Huddleston, M.J., Collingwood, T.S., Annan, R.S., and Deshaies, R.J. (2009). Dbf2-Mob1 drives relocalization of protein phosphatase Cdc14 to the cytoplasm during exit from mitosis. The Journal of cell biology *184*, 527-539.

Morgan, D.O. (2007). The cell cycle : principles of control (London Sunderland, MA, Published by New Science Press in association with Oxford University Press).

Mumberg, D., Muller, R., and Funk, M. (1994). Regulatable promoters of Saccharomyces cerevisiae: comparison of transcriptional activity and their use for heterologous expression. Nucleic acids research *22*, 5767-5768.

Murray, A.W., and Kirschner, M.W. (1989). Dominoes and clocks: the union of two views of the cell cycle. Science (New York, NY *246*, 614-621.

Nasmyth, K. (1995). Evolution of the cell cycle. Philosophical transactions of the Royal Society of London *349*, 271-281.

Nasmyth, K. (1996). At the heart of the budding yeast cell cycle. Trends Genet *12*, 405-412.

Norden, C., Mendoza, M., Dobbelaere, J., Kotwaliwale, C.V., Biggins, S., and Barral, Y. (2006). The NoCut pathway links completion of cytokinesis to spindle midzone function to prevent chromosome breakage. Cell *125*, 85-98.

Orlando, D.A., Lin, C.Y., Bernard, A., Wang, J.Y., Socolar, J.E., Iversen, E.S., Hartemink, A.J., and Haase, S.B. (2008). Global control of cell-cycle transcription by coupled CDK and network oscillators. Nature *453*, 944-947.

Padmashree, C.G., and Surana, U. (2001). Cdc28-Clb mitotic kinase negatively regulates bud site assembly in the budding yeast. Journal of cell science *114*, 207-218.

Palmer, R.E., Koval, M., and Koshland, D. (1989). The dynamics of chromosome movement in the budding yeast Saccharomyces cerevisiae. The Journal of cell biology *109*, 3355-3366.

Pereira, G., Hofken, T., Grindlay, J., Manson, C., and Schiebel, E. (2000). The Bub2p spindle checkpoint links nuclear migration with mitotic exit. Molecular cell *6*, 1-10.

Pereira, G., Manson, C., Grindlay, J., and Schiebel, E. (2002). Regulation of the Bfa1p-Bub2p complex at spindle pole bodies by the cell cycle phosphatase Cdc14p. The Journal of cell biology *157*, 367-379.

Queralt, E., Lehane, C., Novak, B., and Uhlmann, F. (2006). Downregulation of PP2A(Cdc55) phosphatase by separase initiates mitotic exit in budding yeast. Cell *125*, 719-732.

Rodrigues, F., van Hemert, M., Steensma, H.Y., Corte-Real, M., and Leao, C. (2001). Red fluorescent protein (DsRed) as a reporter in Saccharomyces cerevisiae. Journal of bacteriology *183*, 3791-3794.

Ross, K.E., and Cohen-Fix, O. (2004). A role for the FEAR pathway in nuclear positioning during anaphase. Developmental cell *6*, 729-735.

Schwab, M., Lutum, A.S., and Seufert, W. (1997). Yeast Hct1 is a regulator of Clb2 cyclin proteolysis. Cell *90*, 683-693.

Sendina-Nadal, I., Buldu, J.M., Leyva, I., and Boccaletti, S. (2008). Phase locking induces scale-free topologies in networks of coupled oscillators. PLoS ONE *3*, e2644.

Severin, F., Hyman, A.A., and Piatti, S. (2001). Correct spindle elongation at the metaphase/anaphase transition is an APC-dependent event in budding yeast. The Journal of cell biology *155*, 711-718.

Shirayama, M., Toth, A., Galova, M., and Nasmyth, K. (1999). APC(Cdc20) promotes exit from mitosis by destroying the anaphase inhibitor Pds1 and cyclin Clb5. Nature *402*, 203-207.

Shirayama, M., Zachariae, W., Ciosk, R., and Nasmyth, K. (1998). The Polo-like kinase Cdc5p and the WD-repeat protein Cdc20p/fizzy are regulators and substrates of the anaphase promoting complex in Saccharomyces cerevisiae. The EMBO journal *17*, 1336-1349.

Shou, W., Seol, J.H., Shevchenko, A., Baskerville, C., Moazed, D., Chen, Z.W., Jang, J., Shevchenko, A., Charbonneau, H., and Deshaies, R.J. (1999). Exit from mitosis is triggered by Tem1-dependent release of the protein phosphatase Cdc14 from nucleolar RENT complex. Cell *97*, 233-244.

Sluder, G., Miller, F.J., Cole, R., and Rieder, C.L. (1990). Protein synthesis and the cell cycle: centrosome reproduction in sea urchin eggs is not under translational control. The Journal of cell biology *110*, 2025-2032.

Stegmeier, F., and Amon, A. (2004). Closing mitosis: the functions of the Cdc14 phosphatase and its regulation. Annual review of genetics *38*, 203-232.

Stegmeier, F., Visintin, R., and Amon, A. (2002). Separase, polo kinase, the kinetochore protein Slk19, and Spo12 function in a network that controls Cdc14 localization during early anaphase. Cell *108*, 207-220.

Stern, B., and Nurse, P. (1996). A quantitative model for the cdc2 control of S phase and mitosis in fission yeast. Trends Genet *12*, 345-350.

Sullivan, M., Higuchi, T., Katis, V.L., and Uhlmann, F. (2004). Cdc14 phosphatase induces rDNA condensation and resolves cohesin-independent cohesion during budding yeast anaphase. Cell *117*, 471-482.

Sullivan, M., Lehane, C., and Uhlmann, F. (2001). Orchestrating anaphase and mitotic exit: separase cleavage and localization of Slk19. Nature cell biology *3*, 771-777.

Sullivan, M., and Uhlmann, F. (2003). A non-proteolytic function of separase links the onset of anaphase to mitotic exit. Nature cell biology *5*, 249-254.

Surana, U., Amon, A., Dowzer, C., McGrew, J., Byers, B., and Nasmyth, K. (1993). Destruction of the CDC28/CLB mitotic kinase is not required for the metaphase to anaphase transition in budding yeast. The EMBO journal *12*, 1969-1978.

Thornton, B.R., and Toczyski, D.P. (2003). Securin and B-cyclin/CDK are the only essential targets of the APC. Nature cell biology *5*, 1090-1094.

Tinker-Kulberg, R.L., and Morgan, D.O. (1999). Pds1 and Esp1 control both anaphase and mitotic exit in normal cells and after DNA damage. Genes & development *13*, 1936-1949.

Toczyski, D.P., Galgoczy, D.J., and Hartwell, L.H. (1997). CDC5 and CKII control adaptation to the yeast DNA damage checkpoint. Cell *90*, 1097-1106.

Toyn, J.H., Johnson, A.L., Donovan, J.D., Toone, W.M., and Johnston, L.H. (1997). The Swi5 transcription factor of Saccharomyces cerevisiae has a role in exit from mitosis through induction of the cdk-inhibitor Sic1 in telophase. Genetics *145*, 85-96.

Uhlmann, F., Lottspeich, F., and Nasmyth, K. (1999). Sister-chromatid separation at anaphase onset is promoted by cleavage of the cohesin subunit Scc1. Nature *400*, 37-42.

Uhlmann, F., Wernic, D., Poupart, M.A., Koonin, E.V., and Nasmyth, K. (2000). Cleavage of cohesin by the CD clan protease separin triggers anaphase in yeast. Cell *103*, 375-386.

Verma, R., Annan, R.S., Huddleston, M.J., Carr, S.A., Reynard, G., and Deshaies, R.J. (1997). Phosphorylation of Sic1p by G1 Cdk required for its degradation and entry into S phase. Science (New York, NY *278*, 455-460.

Visintin, C., Tomson, B.N., Rahal, R., Paulson, J., Cohen, M., Taunton, J., Amon, A., and Visintin, R. (2008). APC/C-Cdh1-mediated degradation of the Polo kinase Cdc5 promotes the return of Cdc14 into the nucleolus. Genes & development *22*, 79-90.

Visintin, R., Craig, K., Hwang, E.S., Prinz, S., Tyers, M., and Amon, A. (1998). The phosphatase Cdc14 triggers mitotic exit by reversal of Cdk-dependent phosphorylation. Molecular cell *2*, 709-718.

Visintin, R., Hwang, E.S., and Amon, A. (1999). Cfi1 prevents premature exit from mitosis by anchoring Cdc14 phosphatase in the nucleolus. Nature *398*, 818-823.

Visintin, R., Prinz, S., and Amon, A. (1997). CDC20 and CDH1: a family of substrate-specific activators of APC-dependent proteolysis. Science (New York, NY *278*, 460-463.

Visintin, R., Stegmeier, F., and Amon, A. (2003). The role of the polo kinase Cdc5 in controlling Cdc14 localization. Mol Biol Cell *14*, 4486-4498.

Wang, B.D., Yong-Gonzalez, V., and Strunnikov, A.V. (2004). Cdc14p/FEAR pathway controls segregation of nucleolus in S. cerevisiae by facilitating condensin targeting to rDNA chromatin in anaphase. Cell cycle (Georgetown, Tex *3*, 960-967.

Wasch, R., and Cross, F.R. (2002). APC-dependent proteolysis of the mitotic cyclin Clb2 is essential for mitotic exit. Nature *418*, 556-562.

Wäsch, R., and Cross, F.R. (2002). APC-dependent proteolysis of the mitotic cyclin Clb2 is essential for mitotic exit. Nature *418*, 556-562.

Weinert, T.A., Kiser, G.L., and Hartwell, L.H. (1994). Mitotic checkpoint genes in budding yeast and the dependence of mitosis on DNA replication and repair. Genes & development *8*, 652-665.

Weiss, A., Herzig, A., Jacobs, H., and Lehner, C.F. (1998). Continuous Cyclin E expression inhibits progression through endoreduplication cycles in Drosophila. Curr Biol *8*, 239-242.

Winfree, A.T. (1967). Biological rhythms and the behavior of populations of coupled oscillators. J Theor Biol *16*, 15-42.

Wirth, K.G., Wutz, G., Kudo, N.R., Desdouets, C., Zetterberg, A., Taghybeeglu, S., Seznec, J., Ducos, G.M., Ricci, R., Firnberg, N.*, et al.* (2006). Separase: a universal trigger for sister chromatid disjunction but not chromosome cycle progression. The Journal of cell biology *172*, 847-860.

Wittenberg, C., and Reed, S.I. (2005). Cell cycle-dependent transcription in yeast: promoters, transcription factors, and transcriptomes. Oncogene *24*, 2746-2755.

Wittenberg, C., Sugimoto, K., and Reed, S.I. (1990). G1-specific cyclins of S. cerevisiae: cell cycle periodicity, regulation by mating pheromone, and association with the p34CDC28 protein kinase. Cell *62*, 225-237.

Xu, S., Huang, H.K., Kaiser, P., Latterich, M., and Hunter, T. (2000). Phosphorylation and spindle pole body localization of the Cdc15p mitotic regulatory protein kinase in budding yeast. Curr Biol *10*, 329-332.

Yeh, E., Skibbens, R.V., Cheng, J.W., Salmon, E.D., and Bloom, K. (1995). Spindle dynamics and cell cycle regulation of dynein in the budding yeast, Saccharomyces cerevisiae. The Journal of cell biology *130*, 687-700.

Yeong, F.M., Lim, H.H., Padmashree, C.G., and Surana, U. (2000). Exit from mitosis in budding yeast: biphasic inactivation of the Cdc28-Clb2 mitotic kinase and the role of Cdc20. Molecular cell *5*, 501-511.

Yoshida, S., and Toh-e, A. (2001). Regulation of the localization of Dbf2 and mob1 during cell division of saccharomyces cerevisiae. Genes & genetic systems *76*, 141-147.

Zachariae, W., Schwab, M., Nasmyth, K., and Seufert, W. (1998). Control of cyclin ubiquitination by CDK-regulated binding of Hct1 to the anaphase promoting complex. Science (New York, NY *282*, 1721-1724.

Epilogue

Theory and complexity

One familiar with images of fractals may be amazed by the great details of their fine structures. However, a fractal image is usually generated by a rather short computer program, typically less than 100 letters. Does the short program contain the same amount of information as the fractal images it generates? What if the generation involves uncertainty or noise?

The organic world contains unlimited possibility and complexity, which traditional methodology, namely reductionism, appears rather inefficient in dealing with. There must be at least two reasons: 1. Complexity is an inherent property of any biological system that emerges from myriads of 'frozen incidences' during billon years of evolution. Meanwhile, its evolvability depends on the ability to generate enough phenotypic variations. 2. Partially due to the first reason, biologists are usually satisfied with qualitative results on their questions, which creates ambiguity and even leads to wrong conclusions. Just like looking at ultra-low resolution images. The same object could appear quite differently, and different objects could appear the same.

The contribution of theories to understanding biology is subtle, most successfully

in summarizing experimental results. Better ones could reflect dynamic modes common in different systems. To me, a good theory should provide a novel way of reasoning, even about old things. Information theory and game theory, for example, do not solve previously forbidden questions, but provide a natural and concise way to re-analyze them, thus increase the efficiency of human brains at working on questions which they are not evolved to be good at. Therefore, 'concepts' may be what we really need.

We can not consider that there is a simple common principle underlying each phenomenon within different systems, more than a wish. Due to the complexity of its nature, it's often necessary to neglect some facts when trying to summary a theoretical model. The mind primed by any particular model or paradigm tends to discriminate among experimental approaches and results, intentionally or unintentionally, merely for the simplicity and beauty of its proof. 'It's a tragedy when a beautiful theory in physics is disproved by ugly experiments.' In biology, it only means the theory is not beautiful enough.

To understand or apply any theoretical model, it is very important to distinguish between what should happen and what actually happened. Models of any kinds are merely ways to describe and justify observations, for our own convenience. This straightforward notion tends to be ignored by many, mostly because, I think, blurring the distinction between theory and reality is important for cultivating intuitions,

although sometimes, quite misleading.

Efficiency and curiosity

When you lose something, do you immediately search all possible places, or take some time first to think carefully where it could be? Conducting biological research sometimes is like looking for lost things, except that what you find may not be what you expected.

Biologists are accumulating information at an amazing speed. Eventually, any particular question will be answered, slowly but surely (physicists are less lucky in this aspect). The real question is how to get there most efficiently. After the goal is enlightened by curiosity, collecting all available information and analyzing it is the first step. That allows distinguishing promising way(s) to go. It is also important to wander around occasionally to avoid or escape traps on the path. A similar idea is called 'simulated annealing', and has been quite useful to me.

The progression of science seldom follows people's expectation. Intellectual works of great brains shine only as time goes by. Certain attempts that will almost for sure not fall into that category, such as conducting biological experiments catering a well-established model to establish faked satisfaction to the lay, in that neither new information nor fresh ways of analysis is provided, shall be avoided in any cases.